Research Programme of the Research Fund for Coal and Steel

FIre and Seismic performances of Hybrid fire WALLs in case of single-storey industrial and commercial steel buildings (FISHWALL)

Design guidance and constructional details for the investigated fire wall solution

Christophe RENAUD – CTICM

WP5: Development of design rules, recommendations and innovative solutions

Deliverable: D5.2

Contributing partners		
	UNITN	Italy
	CVUT	Czech Republic
	JORIS	Belgium
	PAVUS	Czech Republic
	EMB	France
	EFR	France

Grant agreement No: 101034083

Version	Issue	Purpose	Author	Reviewer	Approved
A	D5.2	15/05/2025	C. Renaud	All partners	
B	D5.2	23/06/2025 (Comments from partners considered)	C. Renaud	B. Zhao	C. Renaud

TABLE OF CONTENTS

ABSTRACT

It is well known that the intrinsic fire resistance of single-storey unprotected steel-framed buildings is largely sufficient to guarantee the evacuation of occupants in the event of fire. In consequence, for this type of building, the main concern of national fire regulations in Europe is how to prevent the spread of fire to the whole building. To achieve this objective, two performances shall be usually satisfied, namely, the appropriateness of constructive systems to ensure that there is no progressive collapse between fire compartments, and the efficiency of fire walls to stop the fire inside the initial compartment regardless of the state of structures exposed to fire. In practice, many constructional solutions can be implemented in order to preserve the integrity of the fire walls, while accepting that the fire exposed part of the structure may collapse. One of the most common solutions is to place a non-load bearing wall between two independent steel structures and to connect it to them by means of "fusible" links. In fire situation, these fusible links have to allow the wall to be disconnected from the structure affected by fire without endangering the separating function of the wall, which shall remain fixed to the steel structure on the other side of the wall and therefore not exposed to fire. However, due to the lack of corresponding scientific evidence, questions are being very often raised about the real efficiency of such systems in fire situation, which, in certain cases, have also to provide an adequate seismic resistance, if they are used in seismic areas.

Today, concrete or masonry wall solutions are frequently used for the compartmentation of buildings, predominately for low-rise commercial and industrial steel buildings. However, as an alternative, lightweight sandwich panels (comprising two thin flat metal faces and an insulated core) could become an appropriate steel fire wall solution, offering numerous benefits in comparison to other solutions, including fire resistance, durability, flexibility, easy dismounting and fast construction times. But, there is an evident lack of technical information about the adequate fire performance of such type of wall solutions when they are implemented in single-storey buildings with unprotected steel structure, which constitutes a major obstacle for their large use.

In this context, the overall goal of the FISHWALL project is to develop a design guidance and recommendations for an innovative hybrid fire wall solution based on lightweight steel-faced sandwich panels associated with unprotected steel structure under both fire and seismic actions but considered individually. This will be achieved through the following specific tasks: i) Establishing of a full range of experimental evidence about the fire and seismic behaviour of the investigated hybrid fire wall solution by carrying out a number of tests; ii) Investigating intensively the fire and seismic performances of the above hybrid fire wall solution in combination with unprotected single-storey steel structures through a variety of parametric numerical studies by means of validated FE numerical models; iii) Developing both cost-effective and innovative "fusible" connection systems for fire walls to be used in combination with unprotected steel structures of single-storey buildings; and iv) Developing a design guidance and practical recommendations for the studied hybrid fire wall and fusible links solutions, on the basis of above studies, from which engineers can carry out very efficient design.

The present report aims at providing some background information on the design rules and construction details set out in the design guide produced as part of the project. The document's primary objective is to provide justification for the simplified calculation rules and construction details presented in the guide. This is often achieved through both outputs of tests and numerical investigations carried out within the FISHWALL project, as well as with research findings reported in the technical literature.

1 INTRODUCTION

The purpose of this document is to provide an overview of the design calculation rules and construction details proposed in the Fishwall project, ensuring the adequate performance of the investigated fire wall solution made of sandwich panels, as well as that of the developed fusible link systems in single-storey steel buildings with unprotected steel structure, in the event of a fire or seismic activity. The document also provides background information based on the results of tests and numerical investigations carried out within the FISHWALL project, as well as research findings reported in the technical literature.

The design of the sandwich panels forming the fire walls can be easily carried out by complying with the current rules of good practice. Therefore this document therefore does not cover this topic, but information is provided in the design guide produced as part of the Fishwall project.

It should be noted that the proposed simplified design rules and construction provisions are intended to ensure that:

- In the event of a fire in one of the fire compartments of the building:
    - The collapse of the part of the building exposed to the fire does not lead to progressive collapse of the building structure, including the fire walls installed in the building.
    - The structure of the building (including the façade elements) does not collapse outwards.
- In the event of an earthquake a seismic intensity characterised by a peak ground acceleration of up to 0.12g, partition fire walls can resist seismic actions, by preventing complete collapse.

2 INVESTIGATED FIRE WALL AND FUSIBLE LINK SOLUTIONS

2.1 Fire walls

The fire wall solution investigated with the fish wall project is illustrated in Figure 2.1, consisting of lightweight insulated sandwich panels spanning horizontally between fire-protected supporting steel columns (by means of sandwich panels or any other fire protection product), located on one side of the wall only. The sandwich panels are no structural (no participation in local and global maintenance of the cladding rail, no diaphragm effect). They are fixed either horizontally or vertically and the steel columns can also be encased in sandwich panels laid down either horizontally or vertically.

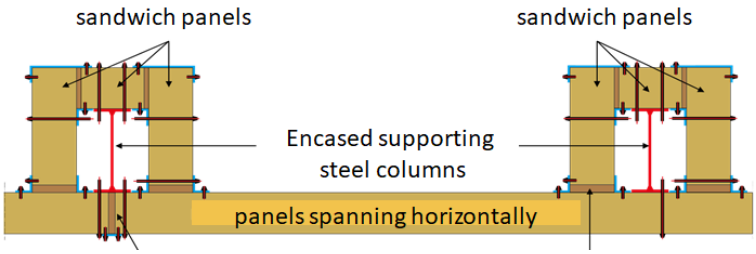

Figure 2.1: Fire wall solution considered in the project

The fire wall can be solidly attached to the steel structure or inserted between two steel structures and attached to these structures with "fusible" links, as illustrated Figure 2.2. The fire wall can be inserted into a row of columns of the steel portal frames, or it can be mounted away from the columns, depending on the wall solution used.

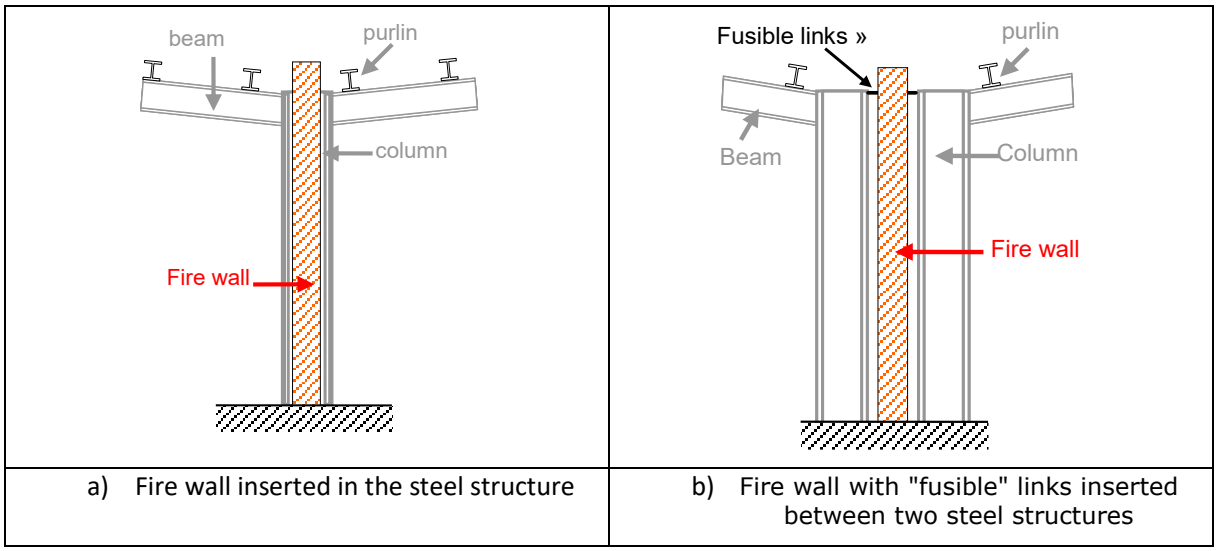

a) Fire wall inserted in the steel structure

b) Fire wall with "fusible" links inserted between two steel structures

Figure 2.2: Fire wall configurations

2.2 Fusible links

The investigated fusible link solutions consist of common steel joints with aluminium bolts acting as the fusible component. It should be mentioned that aluminium bolts have a relatively low melting temperature (below 500°C) and their resistance decreases significantly with the temperature increase.

The fusible links can be any of the following solutions:

- Links composed of Z-shaped steel profiles and U-shaped steel profiles arranged back-to-back and assembled with aluminium bolts (see Figure 2.3). Each Z-profile may be welded or bolted to the column of the building steel structure, while the U-profiles are bolted to the column

supporting the sandwich panels, using four threaded steel rods passing through the fire wall on the wall side and four steel bolts on the other side.

- Links composed of L-shaped folded plates welded to a gusset plate placed between the column flanges and U-shaped steel profiles, assembled with aluminium bolts (see Figure 2.5). The U-profiles are bolted to the column supporting the sandwich panels, using four threaded steel rods passing through the fire wall on the wall side and four steel bolts on the other side.
- Links consisting of an L or T-shaped steel profile assembled with aluminium bolts to a steel channel that extends horizontally between the columns of the building steel structure (see Figure 2.5). The L-shaped profiles are attached to the wall steel column by means of four threaded steel rods passing through the fire wall on the wall side and four steel bolts on the other side.

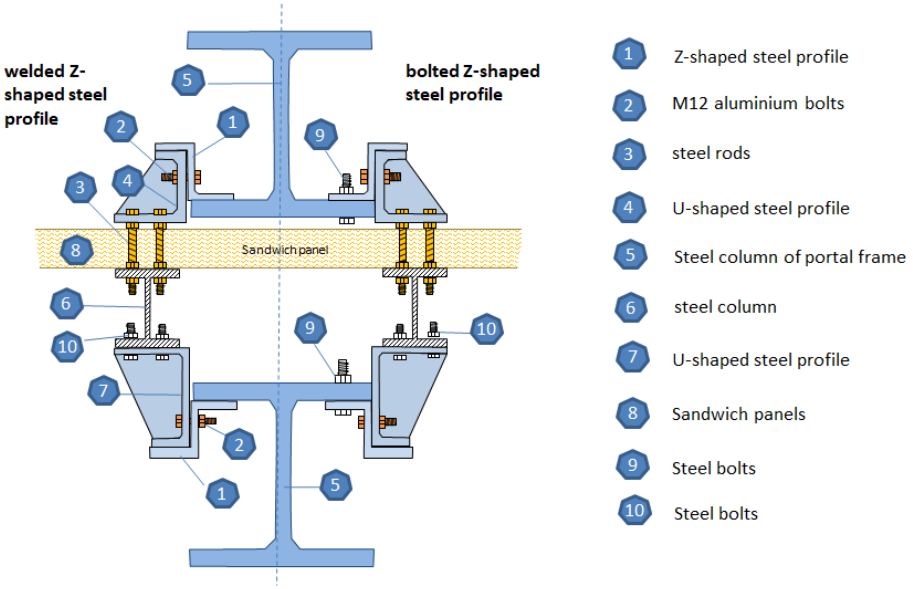

Figure 2.3: Schematic of the first link solution – sectional view

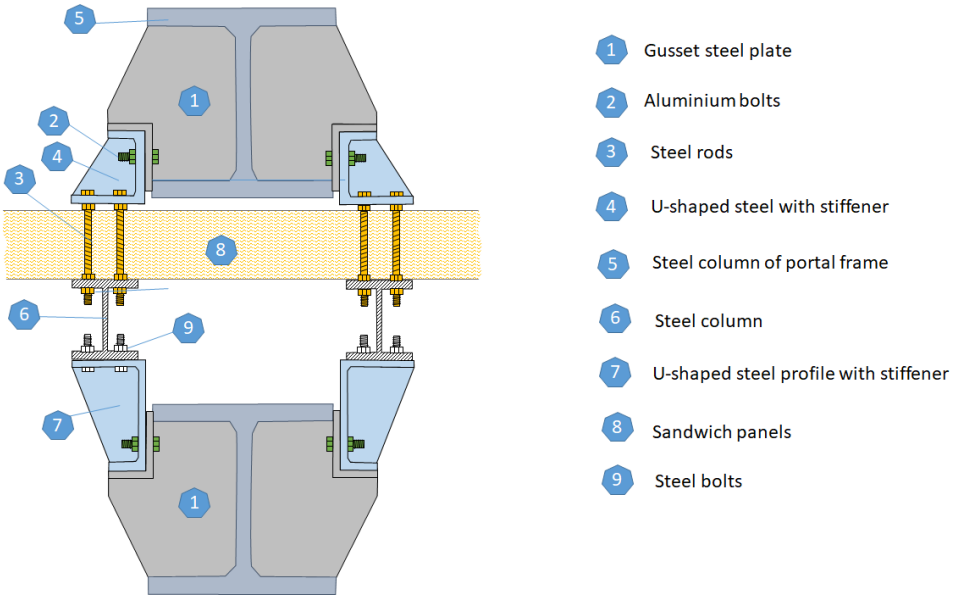

Figure 2.4: Schematic of the second link solution – sectional view

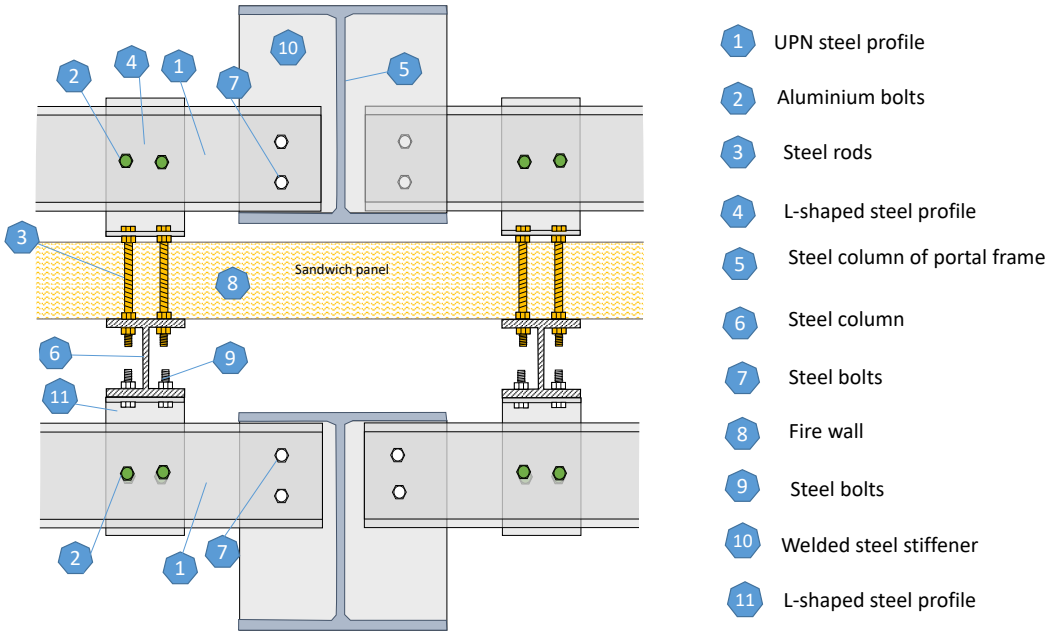

Figure 2.5: Schematic of the third link solution with L-shaped profiles– sectional view

3 DESIGN CALCULATION RULES FOR FUSIBLE LINKS

Where used, the fusible link systems must be designed to:

- Withstand all combinations of loads commonly checked for conditions of normal use.
- Resist the compressive forces due to the thermal expansion of the steel structure exposed to fire but break under tensile forces if the steel structure collapses.
- Resist the seismic actions, if relevant.

3.1 Fire design

Although it appears feasible to use the calculation rules already employed for more common steel connections to calculate the resistance of fusible links in conditions of normal use and seismic situation, EN 1993-1-2 contains no recommendations or simple, well-developed calculation rules to check the resistance of these links at elevated temperatures. Advanced finite element analyses (thermal and mechanical) can be used to evaluate the fire resistance of fusible links. However, these analyses can be complex and time-consuming, and engineers and designers require proper training in how to use them and understand their limitations. Consequently, important development work was undertaken to provide simple rules for easily designing the investigated fusible link solutions at elevated temperatures. This was achieved by analysing the set of results (failure loads, failure modes and temperature rise) obtained from the parametric numerical studies summarised in Deliverable 3.4 [12].

The design rules proposed at elevated temperatures are based on common practices in cold design. These rules are based on the simplified design rules provided in EN 1993-1-1 and EN 1993-1-8, which were adapted to account for temperature-related changes in material resistance where necessary.

3.1.1 Design procedure

According to EN 1993-1-2, the load-bearing function of fusible links should be assumed to be maintained at a time *t* if:

$$E_{\mathrm{fi,d}} < R_{\mathrm{d,fi,t}} \tag{3.1}$$

where:

$E_{\mathrm{fi,d}}$ is the design effect of actions for the fire design situation

$R_{\mathrm{d,fi,t}}$ is the design resistance of the fusible link, for the fire design situation

The calculation of the design resistance of the fusible links requires a two-step calculation process:

- Firstly, the temperatures in the fusible link under consideration (temperature in different components) at the required time must be calculated, and
- Then, the load-bearing capacity of the fusible link is calculated, considering the changes in material properties at elevated temperatures.

3.1.2 Calculation of the fusible link temperatures

To calculate the resistance of the fusible links, the temperature field within the link at elevated temperatures must first be determined. Although there are sometimes steep temperature gradients (as for rods), to simplify the method, a single mean or equivalent temperature is calculated for each component to be checked (see Figure 3.1):

- Temperature in steel profiles:
    - Temperature in the bottom flange of the U-shaped profile: $\theta_{BF,U}$
    - Temperature in the bottom flange of the Z-shaped profile, $\theta_{BF,Z}$

- Temperature in the web of the Z-shaped profile, $\theta_{W,Z}$
- Temperature in the top flange of the Z-shaped profile, $\theta_{TF,Z}$
- Temperature in the L-shaped steel profile: θ_L
- Temperature in the steel channel that extends horizontally between the columns of the building steel structure: θ_{SC}

- Temperatures in web profile stiffeners.
  - Temperature in the web stiffener of the U-shaped profile: $\theta_{WS,U}$
  - Temperature in the web stiffener of the steel column: $\theta_{WS,C}$
- Temperature in steel rods: $\theta_{R,1}$ and $\theta_{R,2}$
- Temperatures in steel bolts: $\theta_{SB,Z}$

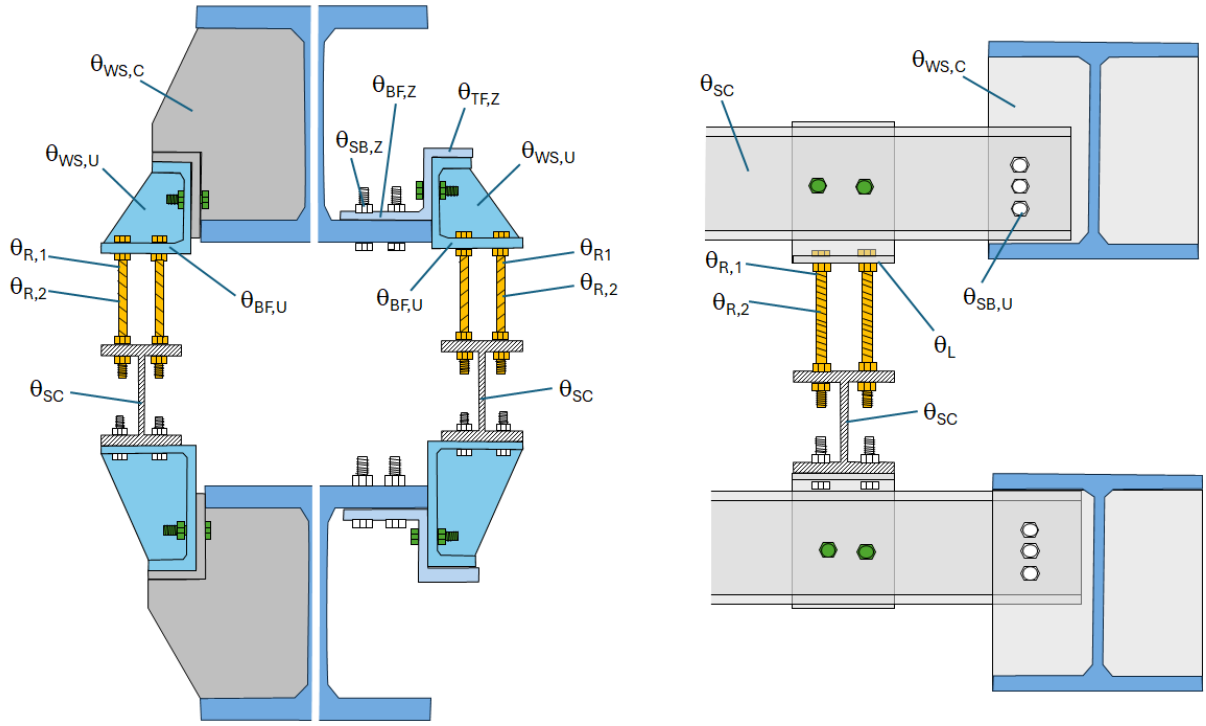

Figure 3.1: Temperatures for fire design check of fusible links

Temperatures of steel profiles can be easily calculated based on the simple analytical approach given in EN 1993-1-2 using an appropriate value of the section factor A_m/V for the considered part forming the fusible link. The increase of temperature $\Delta\theta_{a,t}$ in the considered link part during a time interval Δt should be determined from:

$$\Delta\theta_{a,t} = \frac{A_m/V}{c_a \rho_a} \dot{h}_{\mathrm{net},d} \Delta t \qquad (3.2)$$

Where:

$\dot{h}_{\mathrm{net,d}}$	is the design value of the net heat flux per unit area [W/m^2]
Δt	is the time interval [s]
c_a, ρ_a	are the specific heat [J/(kgK)] and the density of steel [kg/m^3] according to EN 1993-1-2

Formulae for calculating the section factors to be used according to the wanted temperature may be taken from Table 1. The geometrical dimensions characterising the size of fusible link components are illustrated from Figure 3.2 to Figure 3.4.

Table 1: Design values of the section factors for the different components of fusible links

Parts forming the link	Asked temperature	Section factor A_m/V [m^{-1}]
U-shaped steel profile	$\theta_{BF,U}$	$\frac{A_m}{V} = \frac{b_{BF,U} + h_U + 2t_{F,L} + t_{W,L} + b_L + t_{TF,U} + t_{BF,U} + L)}{A_{S,U} + A_{S,L}}$ With: $L = \sqrt{\left(h_U - t_{BF,U} - t_{TF,U}\right)^2 + \left(b_{BF,U} - (b_L - t_{W,L})\right)^2}$ $A_{S,U} = b_{BF,U} \times t_{BF,U} + b_{TF,U} \times t_{TF,U} + \left(h_U - t_{BF,U} - t_{TF,U}\right) \times t_{BF,U}$ $A_{S,L} = b_L \times t_{B,L} + (h_L - t_{F,L}) \times t_{W,L}$
Z-shaped steel profile	$\theta_{BF,Z}$	$\frac{A_m}{V} = \frac{2(b_{BF,Z} + t_{BF,Z} + t_{F,C})}{b_{BF,Z} \times t_{BF,Z} + b_{BF,Z} \times t_{F,C}}$
Z-shaped steel profile	$\theta_{TF,Z}$ $\theta_{W,Z}$	$\frac{A_m}{V} = \frac{b_{BF,U} + h_U + 2t_{w,Z} + 2t_{TF,Z} + b_{TF,U} + t_{TF,U} + t_{BF,U} + L)}{A_{S,U} + A_{S,L}}$ With: $L = \sqrt{\left(h_U - t_{BF,U} - t_{TF,U}\right)^2 + \left(b_{BF,U} - (b_{TF,Z} - t_{W,Z})\right)^2}$ $A_{S,U} = b_{BF,U} \times t_{BF,U} + b_{TF,U} \times t_{TF,U} + \left(h_U - t_{BF,U} - t_{TF,U}\right) \times t_{BF,U}$ $A_{S,L} = b_{TF,Z} \times t_{TF,Z} + (h_{W,Z} - t_{TF,Z}) \times t_{W,Z}$
L-shaped steel profile	θ_L	$\frac{A_m}{V} \cong \frac{2}{t_L}$
web profile stiffeners	$\theta_{WS,U}$	$\frac{A_m}{V} \cong \frac{2}{t_{S,U}}$
web profile stiffeners	$\theta_{WS,C}$	$\frac{A_m}{V} \cong \frac{2}{t_{S,C}}$
steel channel	θ_{SC}	$\frac{A_m}{V} = \frac{2(b_{F,SC} + h_{W,SC})}{2b_{F,SC} \times t_{F,SC} + (h_{W,SC} - 2t_{F,SC}) \times t_{W,SC}}$

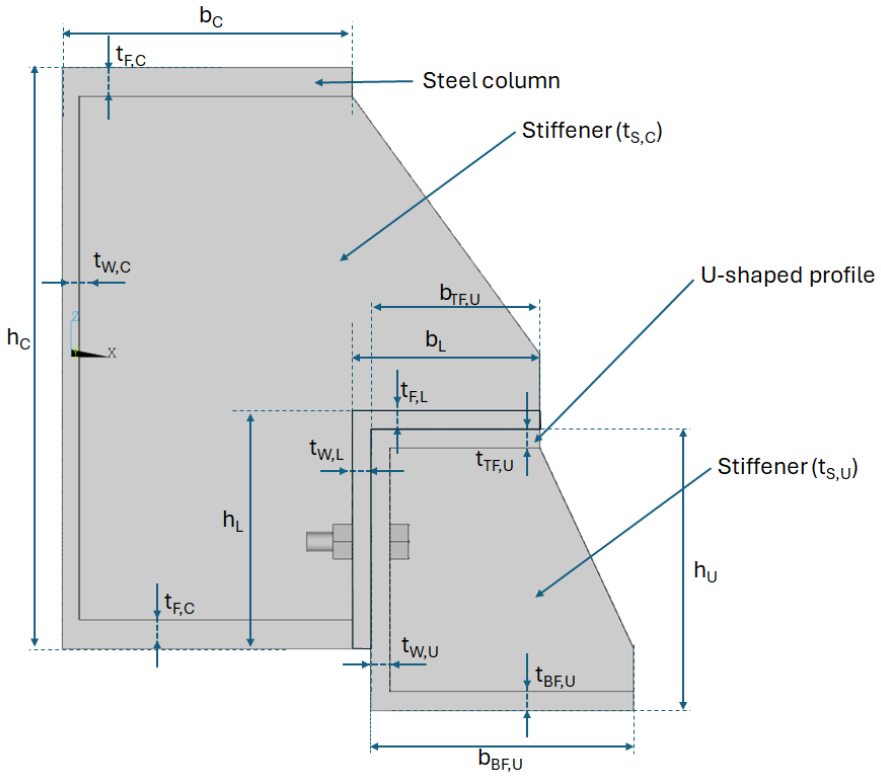

Figure 3.2: Definition of geometrical dimensions for the fusible link n°1

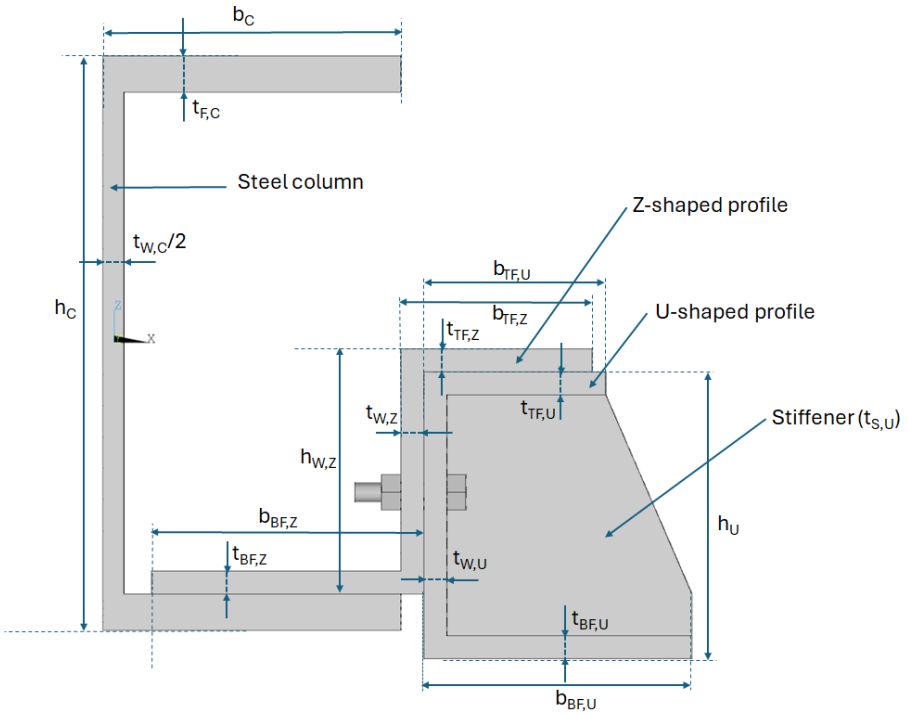

Figure 3.3: Definition of geometrical dimensions for the fusible link n°2

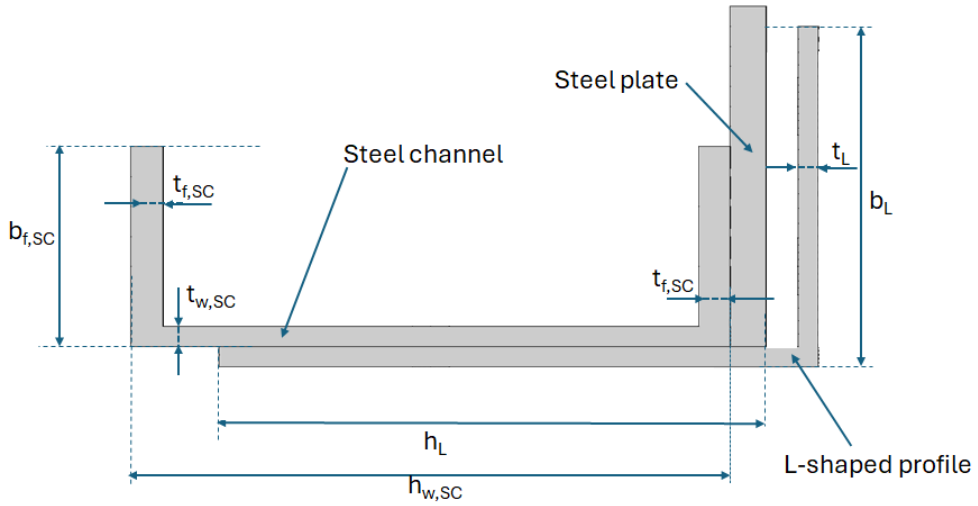

Figure 3.4: Definition of geometrical dimensions for the fusible link n°3

Regarding the steel rods, their temperatures can be calculated from the temperatures calculated in steel parts, using correction factors as follows:

$\theta_{R,1} = 0.9\theta_S$ but $\theta_{R,1} \geq 20.0°C$ (3.3)

$\theta_{R,2} = \alpha_T\theta_S$ but $\theta_{R,2} \geq 20.0°C$

Where

α_T is a reduction factor (dependent on the panel thickness) according to Table 2. For intermediate values of the slope, linear interpolation may be used.

θ_S is the temperature in the relevant steel part: θ_L or $\theta_{BF,U}$

Table 2: Reduction factors α_T

Panel thickness e (mm)	100	175	240
α_T	0.6	0.5	0.42

It can be noted that the rod temperatures predicted by the proposed simplified rules do not accurately reflect the thermal gradient that occurs along the rods during exposure to fire. This undoubtedly affects their fire resistance, particularly their buckling resistance, but it is difficult to take this into account in a simple way. Therefore, only one temperature pair is provided for use in the simple calculation model, which proved to be sufficient for calculating the resistance in compression of rods at elevated temperatures.

Regarding steel and aluminium bolts, their temperature can be taken as the maximum value of temperatures calculated for the steel parts they are bolting together.

3.1.3 Calculation of the resistance to compression

The fusible links' resistance at elevated temperatures is mainly provided by the steel components that make up the links. This can be determined based on the resistance of the weakest compression component. Depending on the fusible link solution being considered, it may be limited by one of the following components:

- The resistance of the bottom flange of the U-shaped profile in transverse bending.
- The resistance of the Z-shaped profile.
- The resistance of steel rods in compression.
- The shear resistance of steel bolts.

- The tension resistance of steel bolts.
- The bearing resistance of steel stiffeners.
- The lateral-torsional buckling of the steel channel that extends horizontally between the columns of the steel structure.

According to EN 1993-1-2, there is no requirement to calculate the net section resistance in fire.

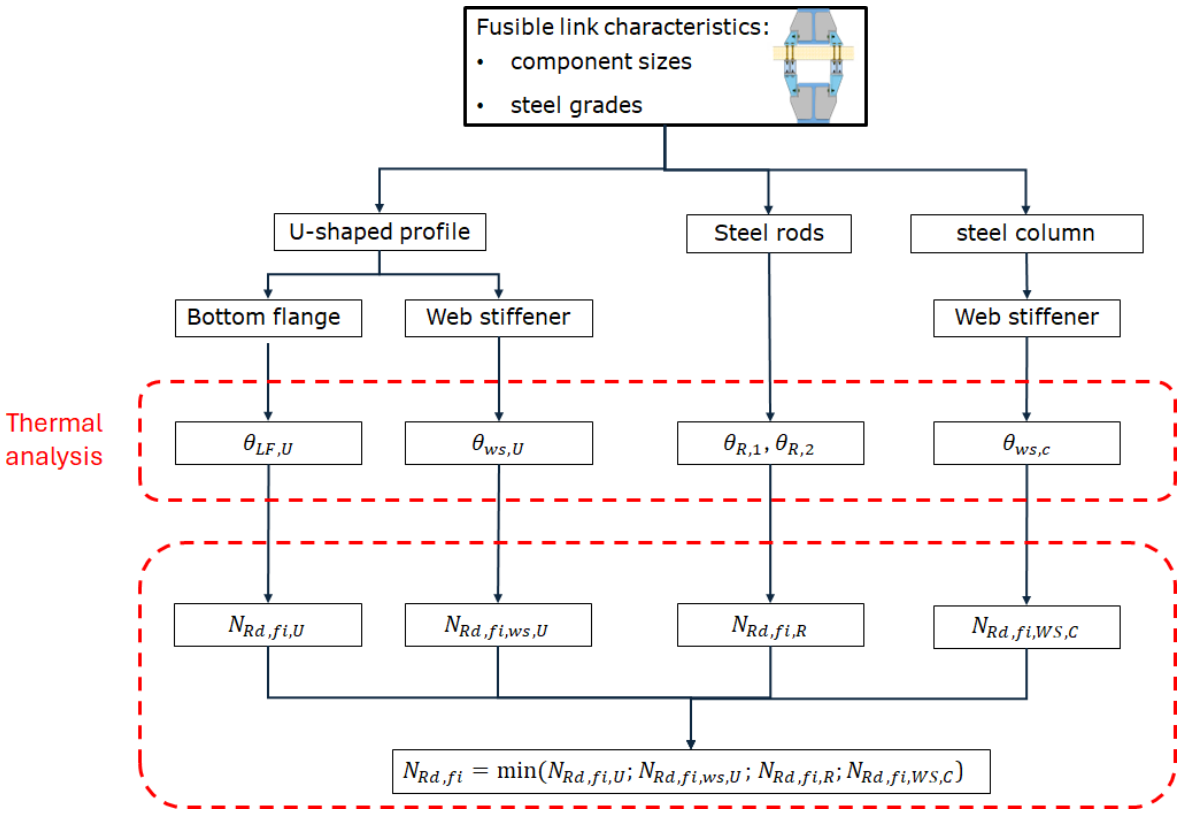

Figure 3.5: Flowchart to calculate the design resistance to compression of the first fusible link solution

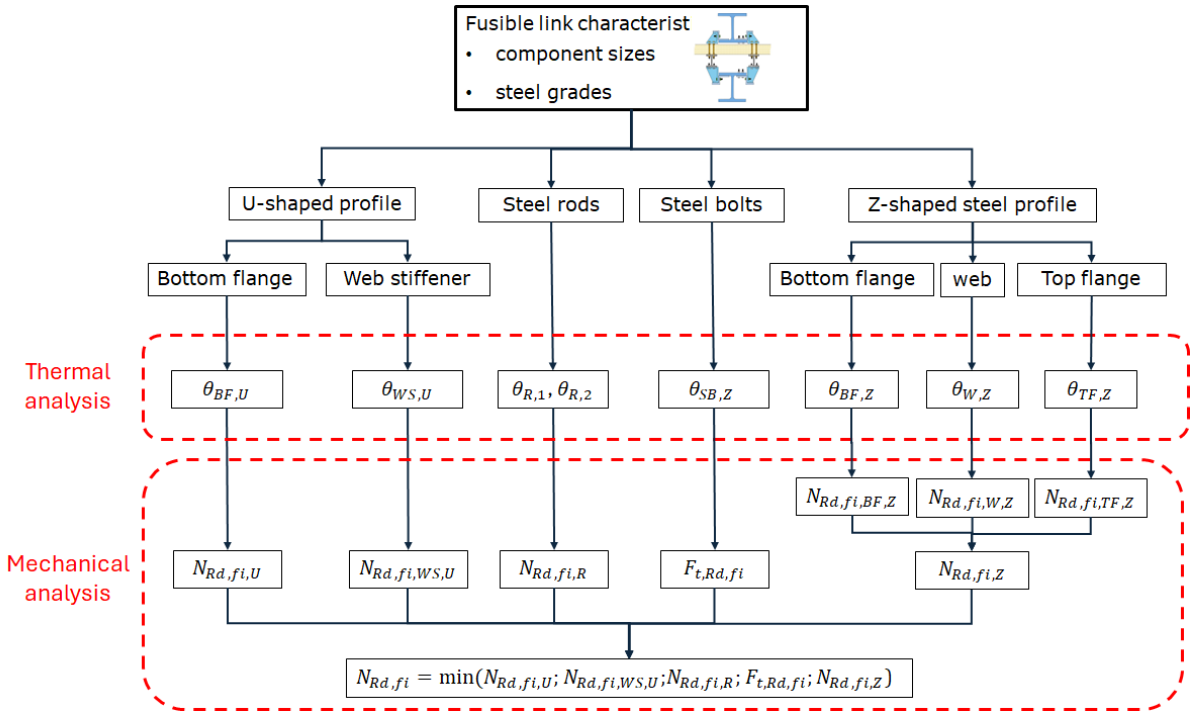

Figure 3.6: Flowchart to calculate the design resistance to compression of the second fusible link solution

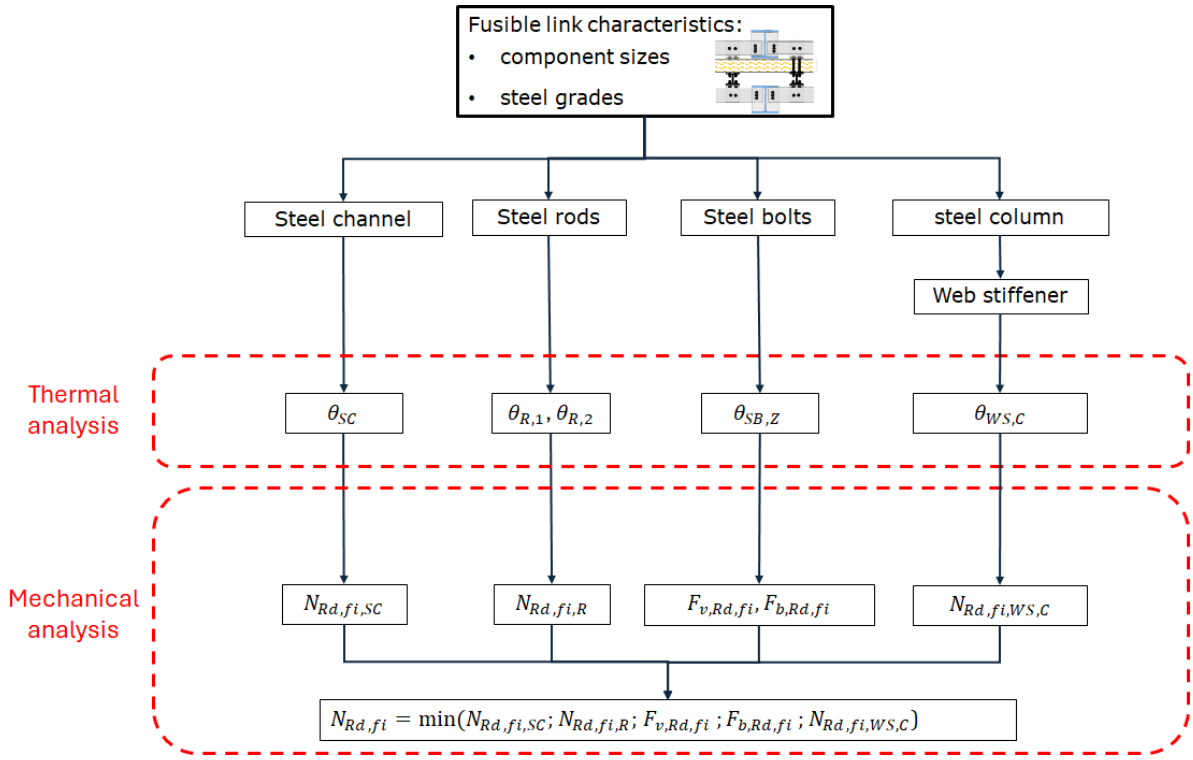

Figure 3.7: Flowchart to calculate the design resistance to compression of the third fusible link

3.1.3.1 Bottom flange of the U-shaped profile in transverse bending

The loading on the bottom flange of the U-shaped profile is a force perpendicular to the profile flange in steel rods, resulting in bending of the profile flange itself. The analysis of the numerical results showed that the response of the U-shaped profile can be idealised as a T-stub loaded in tension. Consequently, according to EN 1993-1-8, assuming on the other hand that the rod forces concentrate on the centreline of the rods and the rods are strong enough to allow the formation of two plastic hinges on either side of the profile web prior to bolt fracture, the design resistance $N_{Rd,fi,U}$ of the bottom flange of the U-shaped profile in transverse bending at elevated temperature can be determined as follows:

$$N_{Rd,fi,U} = \beta\, N_{Rd,fi,U,1+2} \tag{3.4}$$

Or

$$N_{Rd,fi,U} = \beta\, N_{Rd,fi,U,1}/\alpha_{LD} \quad \text{if} \quad N_{Rd,fi,R} \leq \beta\, N_{Rd,fi,U,1+2} \tag{3.5}$$

where

$N_{Rd,fi,U,1}$	is the design resistance of an individual equivalent T-stub involving the first rods-row only
$N_{Rd,fi,U,1+2}$	is the design resistance of the equivalent T-stub involving the two rods-rows
$N_{Rd,fi,R}$	is the design resistance of steel rods in compression according to §3.1.3.3
α_{LD}	is a correction factor that accounts for the distribution of the compression load between the rod rows in the fire situation (see Table 3)

and $\beta = 1.15$

Table 3: Correction factor α_{LD} according to the considered fusible link solution

Fusible link solution		
n°1	n°2	n°3
1.45	1	0.9

The design resistances $N_{Rd,fi,U,1}$ and $N_{Rd,fi,U,1+2}$ are defined as follows:

$$N_{Rd,fi,u,1} = \frac{4M_{pl,Rd,fi,1}}{m} \tag{3.6}$$

$$N_{Rd,fi,U,1+2} = \frac{4M_{pl,Rd,fi,1+2}}{m} \tag{3.7}$$

With

$$M_{pl,Rd,fi,1} = 0{,}25.\, l_{eff,1}.\, {t_{BF,u}}^2.\, k_{y,\theta_{BF,U}} \frac{f_y}{\gamma_{M,fi}} \tag{3.8}$$

$$M_{pl,Rd,fi,1+2} = 0{,}25.\, (l_{eff,1} + l_{eff,2)}.\, {t_{BF,u}}^2.\, k_{y,\theta_{BF,U}}\, \frac{f_y}{\gamma_{M,fi}} \tag{3.9}$$

where

f_y	is the yield strength of the steel profile
$t_{BF,u}$	is the thickness of the bottom flange of the steel profile
$l_{eff,1}$, $l_{eff,2}$	are the effective lengths of the yield lines for a plastic yield mechanism in the profile flange
$\theta_{BF,U}$	is the temperature in the bottom flange of the U-shaped profile

m is the distance from the centre of a fastener to a fillet weld or to the radius of a rolled section fillet (see Figure 3.8)

$\gamma_{M,fi}$ is the partial factor for fire conditions

The minimum effective lengths $l_{eff,1}$, $l_{eff,1}$should be as:

$$l_{eff,1} = min\{\pi m + p; 0.5p + \alpha m - (2m + 0.625e)\} \quad (3.10)$$

$$l_{eff,2} = min\{\pi m + p; 2e_1 + p; 2m + 0.625e + 0.5p\} \quad (3.11)$$

Where

$\alpha = 4 + 1{,}67\frac{e}{m}\left(\frac{m}{m_2}\right)^{0{,}67}$ but $\alpha \geq 4 + 1{,}25\frac{e}{m}$ and $\alpha \leq 8$

m, m_1, m_2, e, e_1, p are geometrical dimensions characterising the position of steel rods in relation to the flange and stiffener of the U-shaped profile (see Figure 3.8)

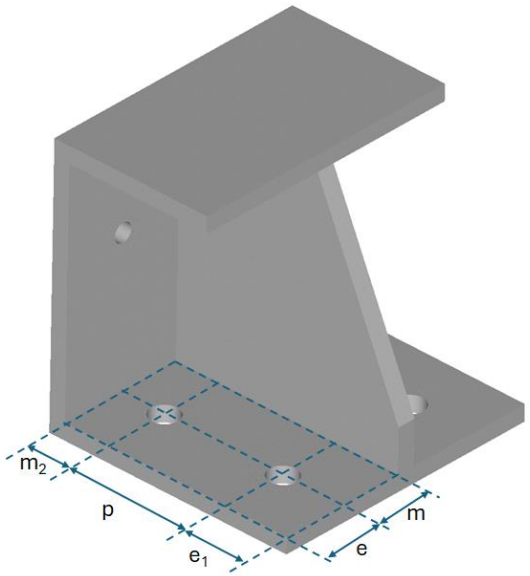

Figure 3.8: Definition of geometrical dimensions m, m_1 e, e_1 and p

3.1.3.2 Z-shaped profile

3.1.3.2.1 Bottom flange in transverse bending:

The loading of the bottom flange of the Z-shaped profile is a force perpendicular to the profile flange in steel bolts, resulting in bending of the profile flange itself. Like the U-shaped-profile, the analysis of the numerical results showed that the response of the Z-shaped profile (at least its lower part) can be idealised as a T-stub loaded in tension. Consequently, based on the provisions of EN 1993-1-8, the resistance $N_{Rd,fi,Z}$ of the bottom flange of the Z-shaped profile in transverse bending at elevated temperature can be determined from:

$$N_{Rd,fi,Z} = \frac{2M_{pl,Rd,fi,Z}}{m} \quad (3.12)$$

With

$$M_{pl,Rd,fi,Z} = 0{,}25.\, l_{eff,Z}.\, t_{BF,z}{}^2.\, k_{y,\theta_{BF,Z}} \frac{f_y}{\gamma_{M,fi}} \quad (3.13)$$

where

f_y is the yield strength of the steel profile

$t_{BF,z}$ is the thickness of the bottom flange of the steel profile

$l_{eff,Z}$ is the effective of the yield lines for a plastic yield mechanism in the profile flange

$\theta_{BF,Z}$ is the temperature in the bottom flange of the Z-shaped profile

m is the distance from the centre of a fastener to a fillet weld or to the radius of a rolled section fillet (see Figure 3.9)

$\gamma_{M,fi}$ is the partial factor for fire conditions

The minimum effective length $l_{eff,Z}$ should be as:

$$l_{eff,Z} = 2 \times min\{4(\pi m + p); 2(\pi m + p + 2e_1); 4m + 1.25(e_1 + e_2) + p\} \quad (3.14)$$

Where

m, m, e_1, e_2, p are geometrical dimensions characterising the position of steel bolts in relation to the flange Z-shaped profile (see Figure 3.9)

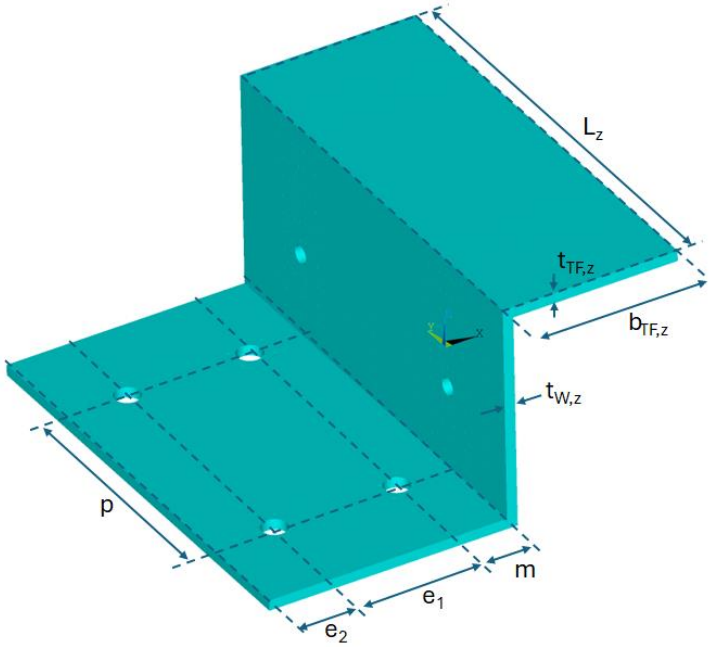

Figure 3.9: Definition of geometrical dimensions for the Z-shaped steel profile

3.1.3.2.2 Web in tension:

The resistance in tension $N_{\mathrm{Rd,fi,r}}$ of the web of the Z-shaped profile in tension at elevated temperature can be determined from:

$$N_{\mathrm{Rd,fi,W,Z}} = k_{y,\theta_{W,Z}}(L_z - n_b.d_o)t_{w,z}\frac{f_y}{\gamma_{M,fi}} \quad (3.15)$$

Where

f_y is the yield strength of the steel profile

$t_{w,z}, L_Z$ are geometrical dimensions characterising the size of the steel profile (see Figure 3.9)

n_b is the number of aluminium bolts

d_o is the diameter of bolt holes

$\theta_{W,Z}$ is the temperature in the web of the Z-shaped profile

$\gamma_{M,fi}$ is the partial factor for fire conditions

3.1.3.2.3 Bottom flange in transverse bending

The resistance $N_{\mathrm{Rd,fi,TF,Z}}$ of the top flange of the Z-shaped profile in transverse bending at elevated temperature can be determined from:

$$N_{\mathrm{Rd,fi,TF,Z}} = k_{\mathrm{y},\theta_{TF,Z}} \frac{L_Z {t_{TF,z}}^2}{2(b_{f,z}-2t_{w,z})} \frac{f_y}{\gamma_{M,fi}} \tag{3.16}$$

Where

f_y is the yield strength of the steel profile

$b_{TF,z}$, $t_{TF,z}$, $t_{w,z}$, L_Z are geometrical dimensions characterising the size of the steel profile (see Figure 3.9)

$\theta_{TF,Z}$ is the temperature in the top flange of the Z-shaped profile

$\gamma_{M,fi}$ is the partial factor for fire conditions

3.1.3.3 Steel rods in compression

The resistance in compression $N_{\mathrm{Rd,fi,r}}$ of steel rods at elevated temperature can be calculated from the simplified rules for cross-section resistance and buckling resistance given in EN 1993-1-2. It should be taken as the minimum value of the resistances obtained from the following equations:

$$N_{\mathrm{Rd,fi,r}} = n\ k_{\mathrm{b},\theta_{R,1}} A_s \frac{f_{ur}}{\gamma_{M,fi}} / \alpha_{LD} \tag{3.17}$$

$$N_{\mathrm{Rd,fi,r}} = n\ \chi_{fi}\left(\bar{\lambda}_{\theta_{R,2}}\right) k_{\mathrm{b},\theta_{r,2}} A_s \frac{f_{ur}}{\gamma_{M,fi}} / \alpha_{LD} \tag{3.18}$$

Where

f_{ur} is the ultimate tensile strength of the rods

A_s is the tensile stress area of the rods

n Is the number of steel rods to consider: n=1 for the second fusible link solution and n=2 for the two other solutions.

$k_{\mathrm{b},\theta_{r,2}}$ is the reduction factor determined for the temperature $\theta_{r,2}$ from

$\theta_{R,1}$, $\theta_{R,2}$ are the temperature in the rods

χ_{fi} is the reduction factor for flexural buckling in the fire design situation

α_{LD} is a correction factor that accounts for the distribution of the compression load between the rods in the fire situation (see Table 3)

$\gamma_{M,fi}$ is the partial factor for fire conditions

The reduction factor χ_{fi} for flexural buckling is obtained from the non-dimensional slenderness $\bar{\lambda}_{\theta_{r,2}}$ at temperature $\theta_{r,2}$ using:

$$\chi_{fi} = \frac{1}{\phi_\theta + \sqrt{{\phi_\theta}^2 - {\bar{\lambda}_{\theta_{r,2}}}^2}} \qquad \text{but} \quad \chi_{fi} \le 1 \tag{3.19}$$

with

$$\phi_\theta = \frac{1}{2}\left[1 + \alpha(\bar{\lambda}_{\theta_{r,2}} - 0.2) + {\bar{\lambda}_{\theta_{r,2}}}^2\right] \tag{3.20}$$

and $\alpha = 0.49$

The non dimensional slenderness at temperature θ is given by:

$$\bar{\lambda}_{\theta_{r,2}} = \bar{\lambda} \sqrt{k_{\mathrm{b},\theta_{r,2}} / k_{\mathrm{E},\theta_{r,2}}} \quad (3.21)$$

where:

$$\bar{\lambda} = \sqrt{\frac{A_s f_{ur}}{N_{\mathrm{cr}}}} \quad (3.22)$$

With:

$k_{\mathrm{E},\theta_{r,2}}$ is the reduction factor for the elastic modulus at the temperature $\theta_{r,2}$

N_{cr} is the elastic critical force based on the tensile stress area of the rods, using the buckling length L_{fi} under fire condition

For the second fusible link solution, the buckling length of steel rods L_{fi} can be determined as follows:

$$L_{fi} = 0.5\, L \quad (3.23)$$

Where:

L is the effective rod length between the steel profiles assembled, as indicated in Figure 3.10.

For the two other fusible link solutions, the buckling length of steel rods L_{fi} can be determined as follows:

$$L_{fi} = K_{cr} L \quad \text{with} \quad L_{fi} \leq 1.25L \quad (3.24)$$

Where

$k_{cr} = 0.5$ if $k_1 \leq 1$

$k_{cr} = 0.5 + 0.375(k_1 - 1)$ with $k_{cr} \leq 1.20$ if $k_1 > 1$

With

$$k_1 = \frac{N_{Rd,fi,r,0.5L}}{N_{Rd,fi,U,1}} \quad (3.25)$$

where

$N_{Rd,fi,U,1}$ is design resistance calculated according §3.1.3.1

$N_{Rdfi,r,0.5L}$ is the design resistance of the steel rods calculated according to (4.15) by considering a buckling length L_{fi} taken equal to 0.5×L

With

$$\bar{\lambda} = \frac{L_{\mathrm{fi}}}{i} \frac{1}{\pi} \sqrt{\frac{f_{ur}}{E}} \quad (3.26)$$

where

L_{fi} is the buckling length of the rods under fire condition

i is the radius of gyration determined using the tensile stress area of the rods

E is the modulus of elasticity of steel at normal temperature

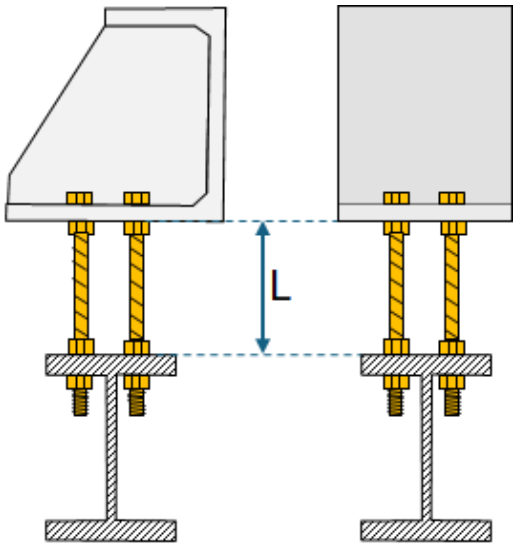

Figure 3.10: Effective length of steel rods L

3.1.3.4 Steel bolts

According to EN 1993-1-2, the shear resistance $F_{v,\text{Rd,fi}}$ of steel bolts at elevated temperature can be determined from:

$$F_{v,\text{Rd,fi}} = F_{v,\text{Rd}} k_{b,\theta} \frac{\gamma_{M2}}{\gamma_{M,\text{fi}}} \quad \text{but} \quad F_{v,\text{Rd,fi}} \leq F_{v,\text{Rd}} \tag{3.27}$$

Where

$k_{b,\theta}$ is the reduction factor determined for the appropriate bolt temperature from Table 5;

$F_{v,\text{Rd}}$ is the design shear resistance of the bolt per shear plane calculated according to EN 1993-1-8

γ_{M2} is the partial factor at normal temperature

$\gamma_{M,\text{fi}}$ is the partial factor for fire conditions

The bearing resistance $F_{b,\text{Rd,fi}}$ per bolt at elevated temperature can be determined from:

$$F_{b,\text{Rd,fi}} = F_{b,\text{Rd}} k_{b,\theta} \frac{\gamma_{M2}}{\gamma_{M,\text{fi}}} \quad \text{but} \quad F_{b,\text{Rd,fi}} \leq F_{b,\text{Rd}} \tag{3.28}$$

where

$F_{b,\text{Rd}}$ is the design bearing resistance per bolt determined from EN 1993-1-8

$k_{b,\theta}$ is the reduction factor determined for the appropriate bolt temperature from Table 5;

As an alternative to equation (3.28) the bearing resistance $F_{b,\text{Rd,fi}}$ per bolt at elevated temperature can be determined from:

$$F_{b,\text{Rd,fi}} = k_{y,\theta} \frac{k_1 \, \alpha_b \, f_u d \, t}{\gamma_{M,\text{fi}}} \tag{3.29}$$

with

$\alpha_b = \min(\alpha_{bd}; \frac{k_{u,\theta} f_{ub}}{k_{y,\theta} f_u}; 1)$ but $\alpha_b \leq 0.66$ for slotted holes

And

In the direction of load transfer:

$\alpha_d = \frac{e_1}{3d_0}$ for end bolts

$\alpha_d = \frac{p}{3d_0} - 0.25$ for inner bolts

perpendicular to the direction of load transfer:

$k_1 = \min\left(2.8\frac{e_2}{d_0} - 1.7;\ 2.5\right)$ for edge bolts

$k_1 = \min\left(1.4\frac{p_2}{d_0} - 1.7;\ 2.5\right)$ for inner bolts

Where

f_u	is the ultimate tensile strength of the steel profile/plate at normal temperature
$k_{y,\theta}$	is the reduction factor for the yield strength of steel at temperature θ from Table 4
f_{ub}	is the ultimate tensile strength of bolts at normal temperature
$k_{b,\theta}$	is the reduction factor determined for the appropriate bolt temperature θ from Table 5.
d	is the nominal bolt diameter
t	is the thickness of the considered cross-section part
d_0	is the bolt hole diameter
e_1	is the end distance from the centre of the bolt hole to the adjacent end of the considered steel part, measured in the direction of load transfer
e_2	is the edge distance from the centre of the bolt hole to the adjacent edge of the considered steel part, measured perpendicular to the direction of load transfer
p_1	is the spacing between centres of bolts in a line in the direction of load transfer
P_2	is the spacing measured perpendicular to the load transfer direction between adjacent lines of bolts
$\gamma_{M,fi}$	is the partial factor for fire conditions

The design tension resistance $F_{t,Rd,fi}$ of steel bolts ate elevated temperature should be determined from:

$$F_{t,Rd,fi} = F_{t,Rd} k_{b,\theta} \frac{\gamma_{M2}}{\gamma_{M,fi}} \quad \text{but} \quad F_{t,Rd,fi} \le F_{t,Rd} \tag{3.30}$$

where

$k_{b,\theta}$	is the reduction factor determined for the appropriate bolt temperature from Table 5.
$F_{t,Rd}$	is the design tension resistance of the bolt per shear plane calculated according to EN 1993-1-8

3.1.3.5 Web stiffeners (columns, U-shaped profile)

Avoiding class 4 cross-section, the design resistance of a web stiffener $N_{Rd,fi,ws}$ should be taken as the minimum value of its buckling or plastic resistances calculated according to EN 1993-1-2. For the calculation of these resistances, a maximum width of profile web equal to $12.75\sqrt{235 / f_y}\, e_w$ (where e_w is the web thickness and f_y is the yield strength of the steel profile) on each side of the stiffener may be added to the effective cross section of the stiffener (see Figure 11).

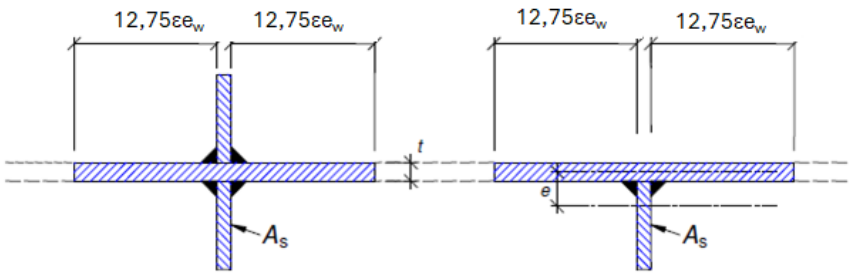

Figure 11 : Allowable area of profile web for the design resistance of web stiffeners in compression

3.1.3.6 Steel channel between columns

The loading on the steel channel extending between the columns of the steel structure is a force perpendicular to the profile web at the level of the fusible links location, resulting in bending of the channel.

The design resistance of the steel channel $N_{\mathrm{Rd,fi,SC}}$ in bending may be calculated from:

$$N_{\mathrm{Rd,fi,SC}} = M_{\mathrm{b,Rd,fi}} / \mathrm{d} \qquad (3.31)$$

Where

$M_{\mathrm{b,Rd,fi}}$ is the design lateral torsional buckling resistance moment of a laterally unrestrained member according to EN 1993-1-2

d is the distance between the fusible link and the bolt row of the beam connection with the column web stiffener as illustrated in

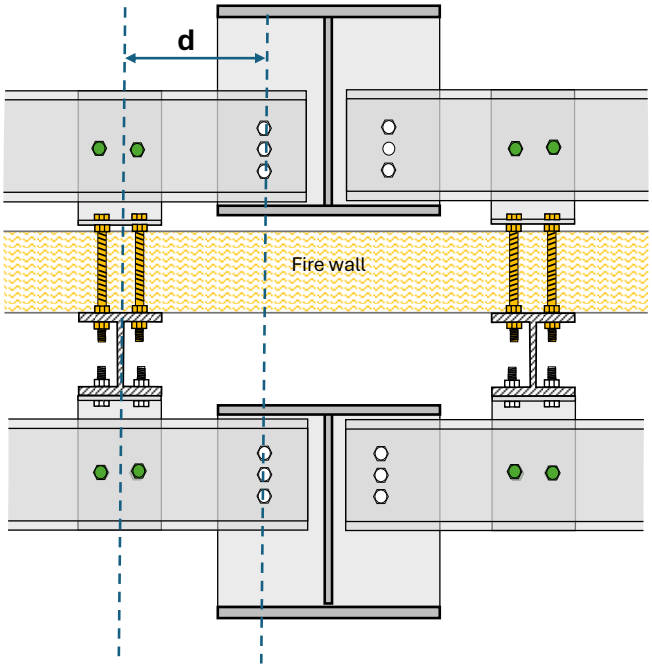

Figure 3.12: Definition of distance d

3.1.4 Resistance to traction

The overall resistance to traction of the fusible links exposed to fire is mainly provided by the aluminium bolts. Since the solutions studied involve loading the bolts in shear, the resistance to traction of the fusible links is equal to the shear resistance $F_{v,\mathrm{Rd,fi}}$ of the aluminium bolts, which can be determined from:

$$F_{v,\mathrm{Rd,fi}} = F_{v,\mathrm{Rd}} k_{b,\theta} \frac{\gamma_{M2}}{\gamma_{M,\mathrm{fi}}} \quad \text{but} \quad F_{v,\mathrm{Rd,fi}} \leq F_{v,\mathrm{Rd}} \qquad (3.32)$$

Where

$k_{b,\theta}$ is the reduction factor determined for the appropriate bolt temperature from Table 6

$F_{v,\mathrm{Rd}}$ is the design shear resistance of the bolt per shear plane calculated according to EN 1999-1-1

γ_{M2} is the partial factor at normal temperature

$\gamma_{M,\mathrm{fi}}$ is the partial factor for fire conditions

3.2 Design values of materials properties

All materials lose strength at elevated temperatures and to calculate the design member resistance with temperature, the strength reduction of material must be known.

3.2.1 Structural steel:

The strength and stiffness properties of steel decrease significantly with temperature. According to EN 1993-1-2, they can be obtained directly from the properties of steel at normal temperature by using reduction factors as follows:

$$k_{y,\theta} = f_{y,\theta} / f_y \quad (3.33)$$

$$k_{E,\theta} = E_{a,\theta} / E_a \quad (3.34)$$

where f_y and E_a are the yield strength and the elastic modulus at 20°C, respectively

The values of reduction factors are reported in Table 4.

Table 4: Reduction factors for structural steel at elevated temperatures

Temperature θ (°C)	$k_{y,\theta} = f_{y,\theta} / f_y$	$k_{E,\theta} = E_{a,\theta} / E_a$
20	1,000	1,000
100	1,000	1,000
200	1,000	0,900
300	1,000	0,800
400	1,000	0,700
500	0,780	0,600
600	0,470	0,310
700	0,230	0,130
800	0,110	0,090
900	0,060	0,0675
1000	0,040	0,0450
1100	0,020	0,0225
1200	0,000	0,0000
NOTE: For intermediate values of the steel temperature, linear interpolation can be used.		

3.2.2 Steel bolts and rods

The ultimate tensile strength at elevated temperatures of both steel bolts and rods can be obtained as follows:

$$f_{u,\theta} = k_{b,\theta} / f_u \quad (3.35)$$

where f_u is ultimate tensile strength at 20°C and $k_{b,\theta}$ is the reduction factor determined for the appropriate temperature from Table 5.

It should noted that there is no standard for the Young's modulus reduction of carbon steel bolts at elevated temperatures. Therefore, reduction factors of carbon steels from EN 1993-1-2 can be employed.

Table 5: Reduction factors for steel bolts and rods at elevated temperatures

Temperature θ (°C)	$k_{b,\theta}$
20	1,000
100	0,968
150	0,952
200	0,935
300	0,903
400	0,775
500	0,550
600	0,220
700	0,100
800	0,067
900	0,033
1000	0,000
NOTE: For intermediate values of the temperature, linear interpolation can be used.	

3.2.3 Aluminium bolts

The ultimate tensile strength at elevated temperatures of aluminium bolts be obtained as follows:

$$f_{u,\theta} = k_{b,\theta} / f_u \quad (3.36)$$

where f_u is ultimate tensile strength at 20°C and $k_{b,\theta}$ is the reduction factor determined for the appropriate temperature from Table 6.

Table 6: Reduction factors k_θ for aluminium bolts

Temperature θ (°C)	$k_{u,\theta}$
20	1.0
100	0.9
150	0.75
200	0.5
250	0.23
300	0.11
350	0.06
400	0.045
550	0
NOTE: For intermediate values of the temperature, linear interpolation can be used.	

It should be noted that, at present, EN 1999-1-2 [7]does not provide specific rules for determining the resistance of aluminium bolts at high temperatures. Only reduction factor values for yield strength (0.2% proof strength) and modulus of elasticity are given as a function of temperature for some aluminium alloys. Good agreement was obtained between the standard values of resistance degradation and the results of material tests performed on aluminium bolts [19].

3.3 Design loads in fire situation

As previously mentioned, the fusible links must be designed to withstand the compressive forces induced by the thermal expansion of the steel structure in the event of a fire, while also breaking under the tensile forces induced by the collapse of the structure if it occurs.

The corresponding design loads to be considered in the fire design of fusible links can be easily calculated using the simple rules developed in an earlier RFSC project [14] for checking the fire behaviour of single-storey steel buildings and easily designing steel structures that meet the structural behaviour requirements often defined in national fire regulations, which stipulate that

progressive collapse and collapse towards the outside should not occur in the case of compartmented buildings.

As demonstrated in the earlier project, the global structural analyses carried out as part of the FISHWALL project [12] showed that these rules provided a safe estimate of the forces generated by a steel structure exposed to a real fire.

3.4 Comparison of the proposed design rules with FE results

Comparisons have been carried out between the proposed design rules and the results of the parametric numerical studies presented in Deliverable D3.5 [12]. The comparison results are summarized in this section.

3.4.1 Heating calculations

Temperatures calculated according to the proposed simplified rules (see §3.1.2) were compared to the temperatures obtained in numerical analysis. First, the temperature rises of steel profiles were compared. Figure 3.13 and Figure 3.14 presents for the first fusible link solution the comparison of the U-profile temperatures obtained from numerical analysis (FEM) to the temperatures calculated using the equations of EN 1993-1-2 (SM), according to the profile thickness and the profile size respectively. Similarly, the analysis results for the U-shaped and the Z-shaped steel profile constituting fusible links as part of the second solution are presented in Figure 3.15 and Figure 3.16, respectively. Values of the section factors A_m/V used in calculation are reported in these figures. Moreover, the following abbreviations are used: FEM: finite element method, SM: simplified method, UF: upper flange of the U-shaped profile, W: web of the U-shaped profile, LF: lower flange of the U-shaped profile, eU: thickness of the U-shaped profile, eZ; thickness of the Z-shaped profile and eL: thickness of the L-shaped folded plate. In most cases, the analytically calculated temperature is systematically higher than the temperature calculated from FE models. In some cases, the simulated temperatures slightly exceed the analytical temperatures during the first stage of exposure to fire. However, the impact of this excess on the profile's resistance is minimal, as the corresponding temperatures do not exceed 400°C and there are no steel strength losses at this temperature level.

Figure 3.17 and Figure 3.18 show a temperatures comparison for the L-shaped steel profile and the UPN profile as part of the third link solution. The results indicate that the numerical temperatures are initially lower than the analytically predicted ones, but then progressively approach the same level. The analytical temperatures exceed the numerical values by a maximum of 10%.

For information purposes, the Figure 3.20 to Figure 3.23 show the evolution over time of the ratio between the temperature of the rod at points P1 or P2 (T_P1 and T_P2) and the temperature of the U-profile flange (T_U), as calculated from the FE models for the various rod lengths considered in the parametric study. The results are compared with the proposed fixed values (depicted as dashed lines). In Figure 3.23 to Figure 3.25, show a comparison of the rod temperatures obtained from numerical analysis and those obtained using simplified design rules, according to rod length. The rod temperatures are calculated as the mean value of the temperature just above the nut exposed to fire (point P1) and at three quarters of the rod's length (point P2). To avoid overloading the report, only the comparison for fusible fasteners consisting of a U-section is given (these are deemed representative results). The analytical temperatures are generally higher than the numerical temperatures. The difference is greater at point P1 than at point P2 and decreases as the thickness of the U-section increases. For point P2, the analytical temperatures slightly underestimate the numerical temperatures after a certain duration of fire exposure (ranging from 1300 to 1500 seconds in the present case). However, the impact of this underestimation on the rod's resistance is limited, as the corresponding temperature differences do not exceed 10%. Moreover, the maximum temperatures reached are lower than 500°C and there are limited losses in steel strength at this temperature level.

Finally, Figure 3.26 shows a temperature comparison for the steel bolts of the first fusible link solution. The simplified rules provide safe temperature predictions for the bolts, which are always higher than the numerical temperatures.

Based on these results, the mean temperature of the steel profiles, as determined using the EN 1993-1-2 equations and the design values proposed for the section factors, provides a reliable estimate of the heating of the steel components of the studied fusible links with different geometries.

The simplified rules proposed for both the steel rods and bolts also lead to a satisfactory prediction of their heating.

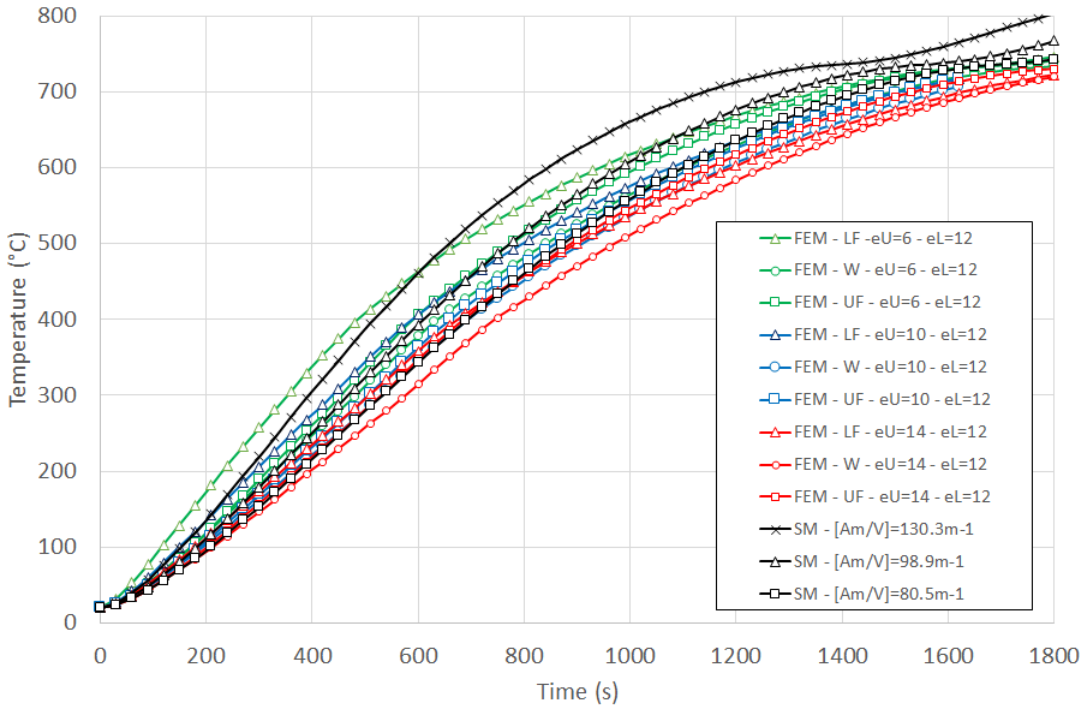

Figure 3.13: Temperature rises calculated for the U-shaped steel profiles according to their thicknesses – first fusible link solution

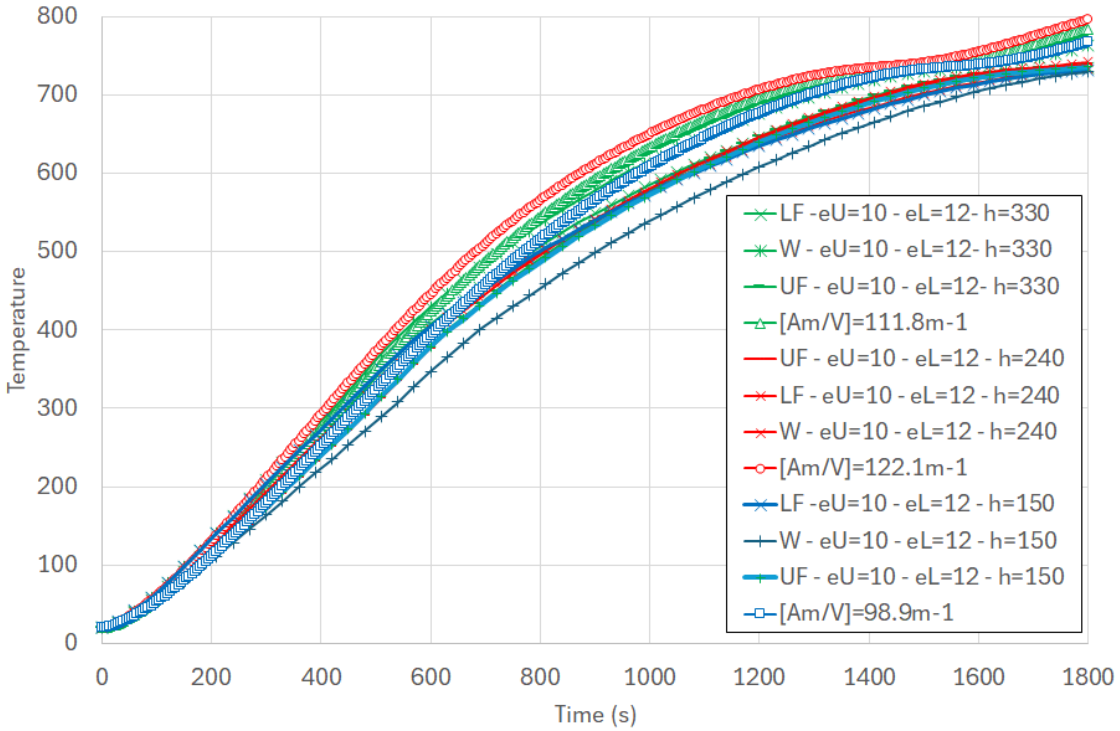

Figure 3.14: Temperature rises calculated of the U-shaped steel profile according to profile size - first fusible link solution

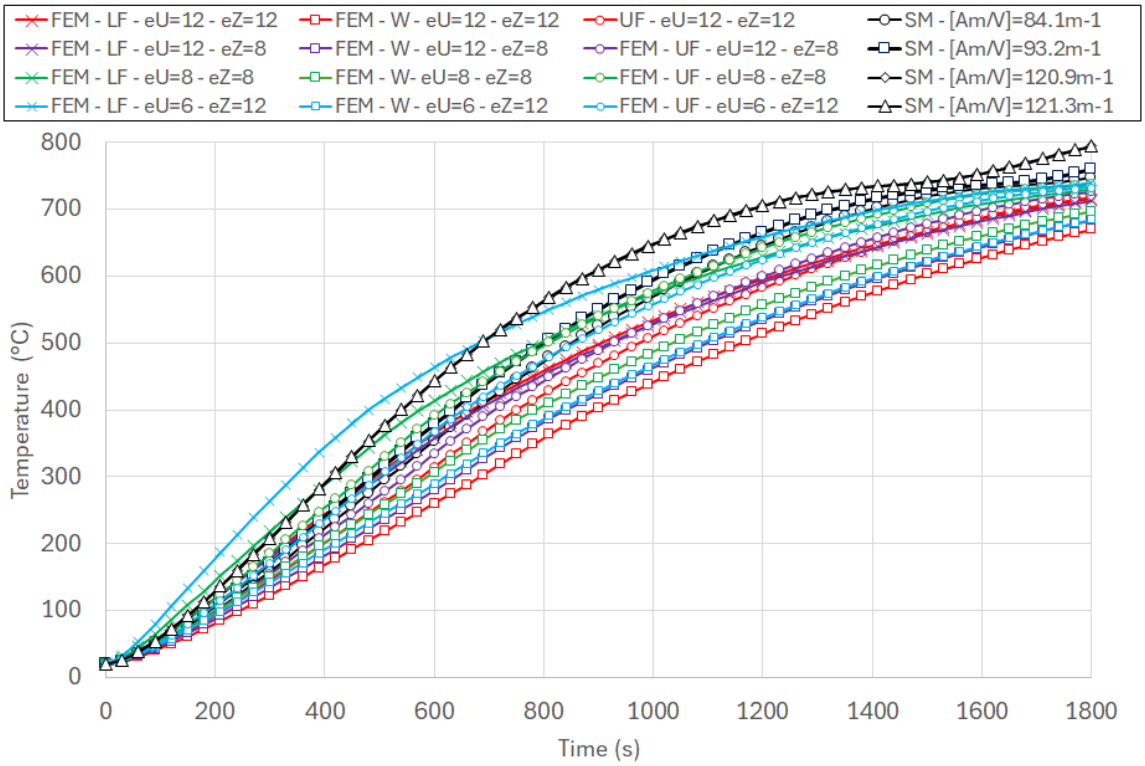

Figure 3.15: Temperature rises calculated for the U-shaped steel profiles according to the profile thicknesses – second fusible link solution

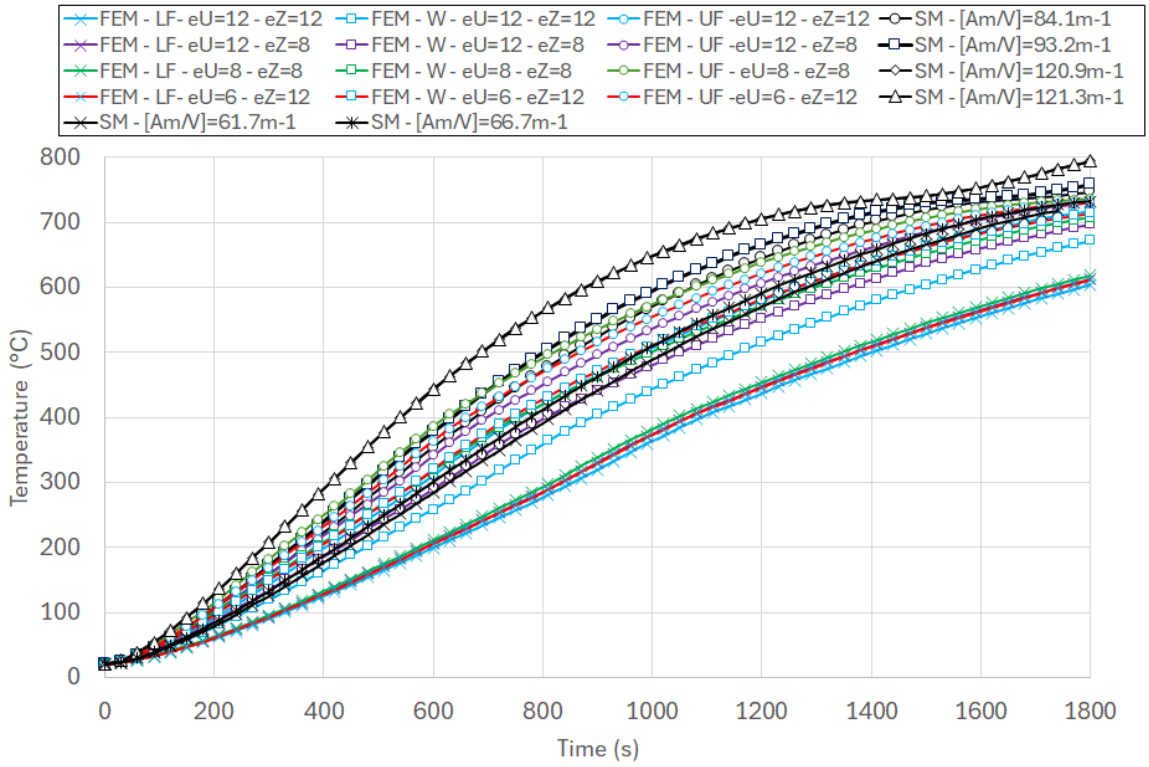

Figure 3.16: Temperature rises calculated for the Z-shaped steel profiles according to the profile thicknesses - second fusible link solution

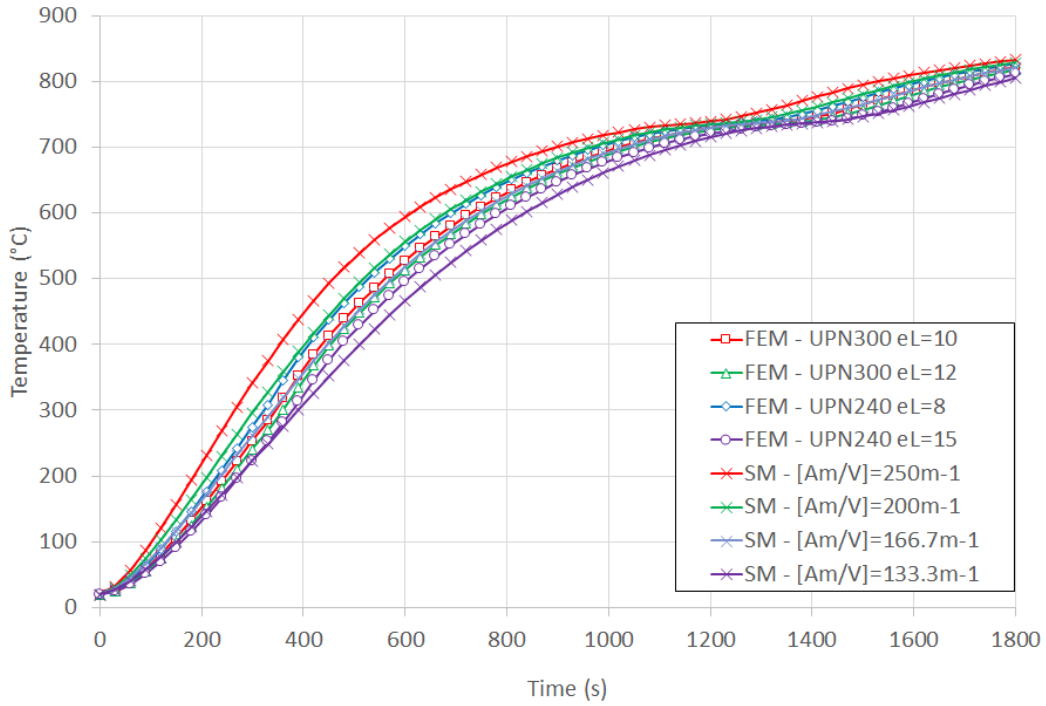

Figure 3.17: Temperature rises calculated for the L steel profile according to the profile thickness – third fusible link solution

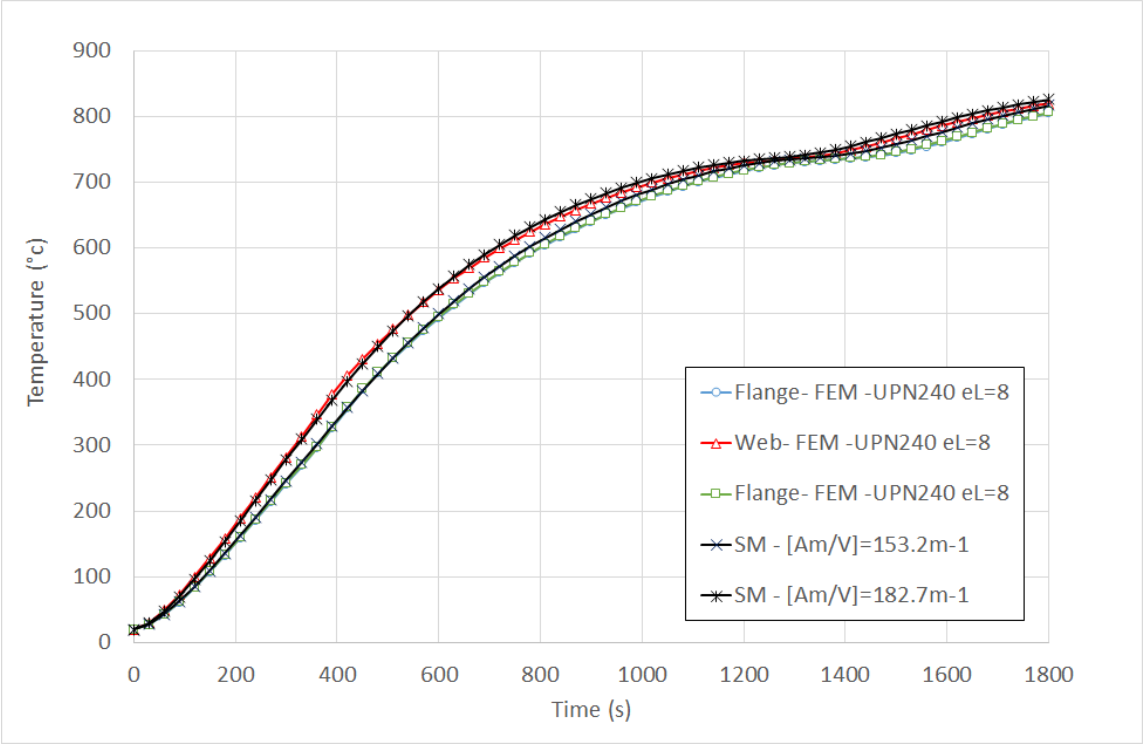

Figure 3.18: Temperature rise calculated for the UPN 240 -- third fusible link solution

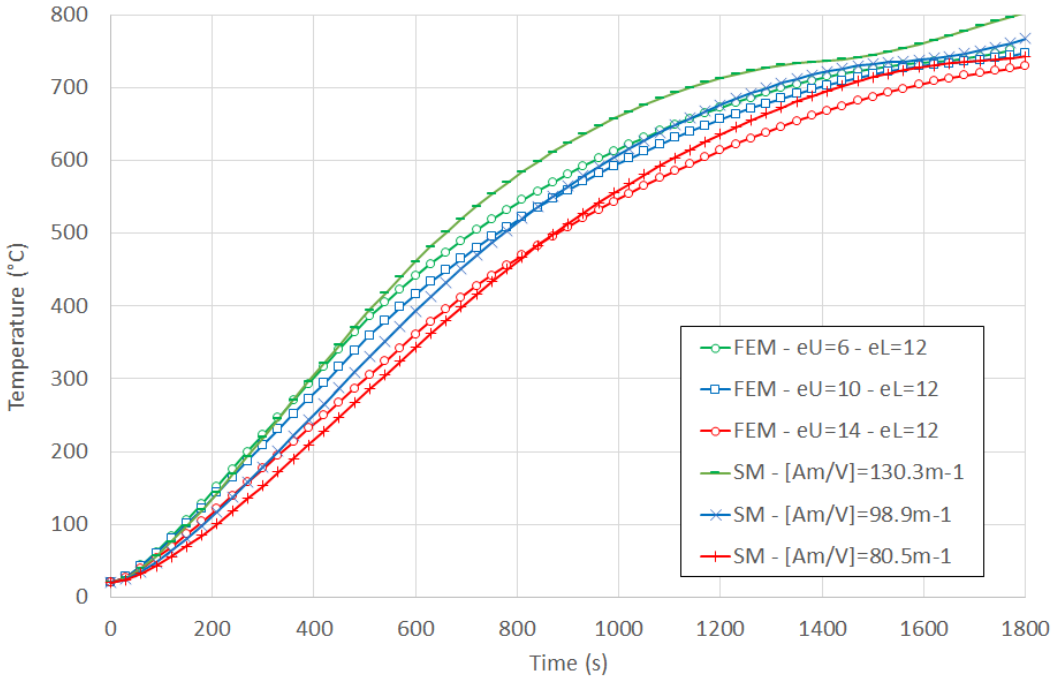

Figure 3.19: Temperature rises calculated for the stiffener of the U-shaped steel profile according to the thickness of the U profile

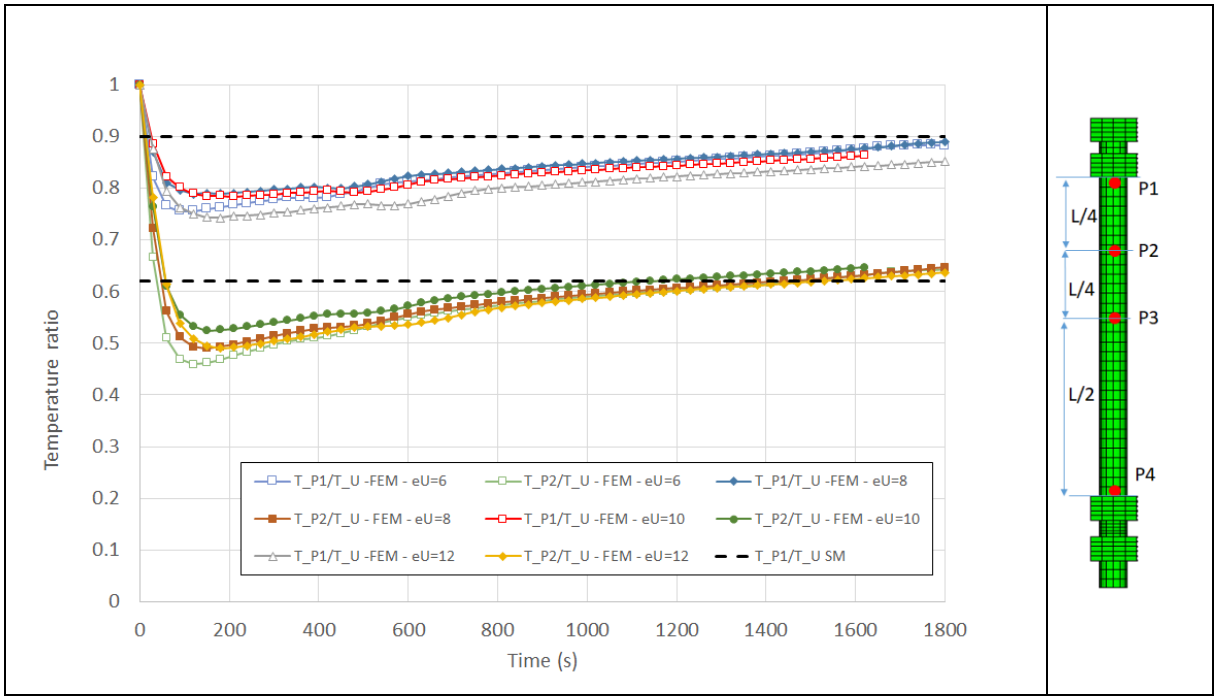

Figure 3.20: Evolution over time of the ratio between the rod temperature (at points P1 or P2) and the U-profile flange temperature, calculated from the FE models for 100 mm length rods - comparison with the proposed fixed values

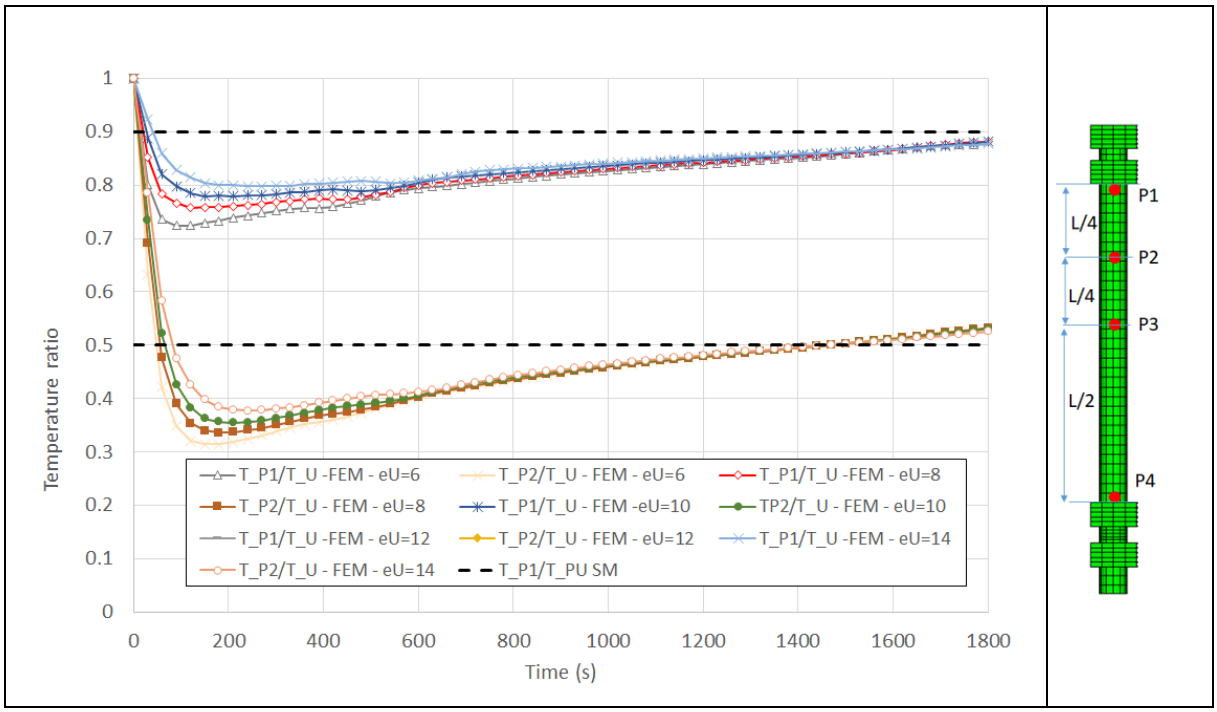

Figure 3.21: Evolution over time of the ratio between the rod temperature (at points P1 or P2) and the U-profile flange temperature, calculated from the FE models for 175 mm length rods - comparison with the proposed fixed values

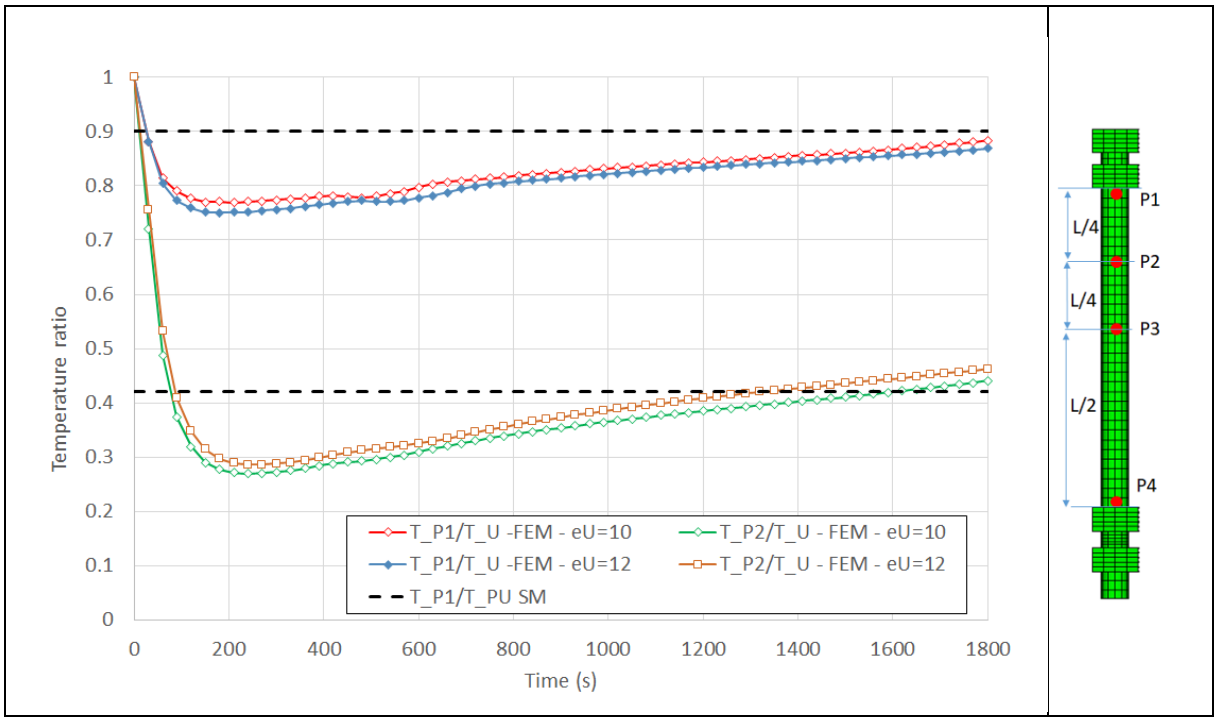

Figure 3.22: Evolution over time of the ratio between the rod temperature (at points P1 or P2) and the U-profile flange temperature, calculated from the FE models for 240 mm length rods - comparison with the proposed fixed values

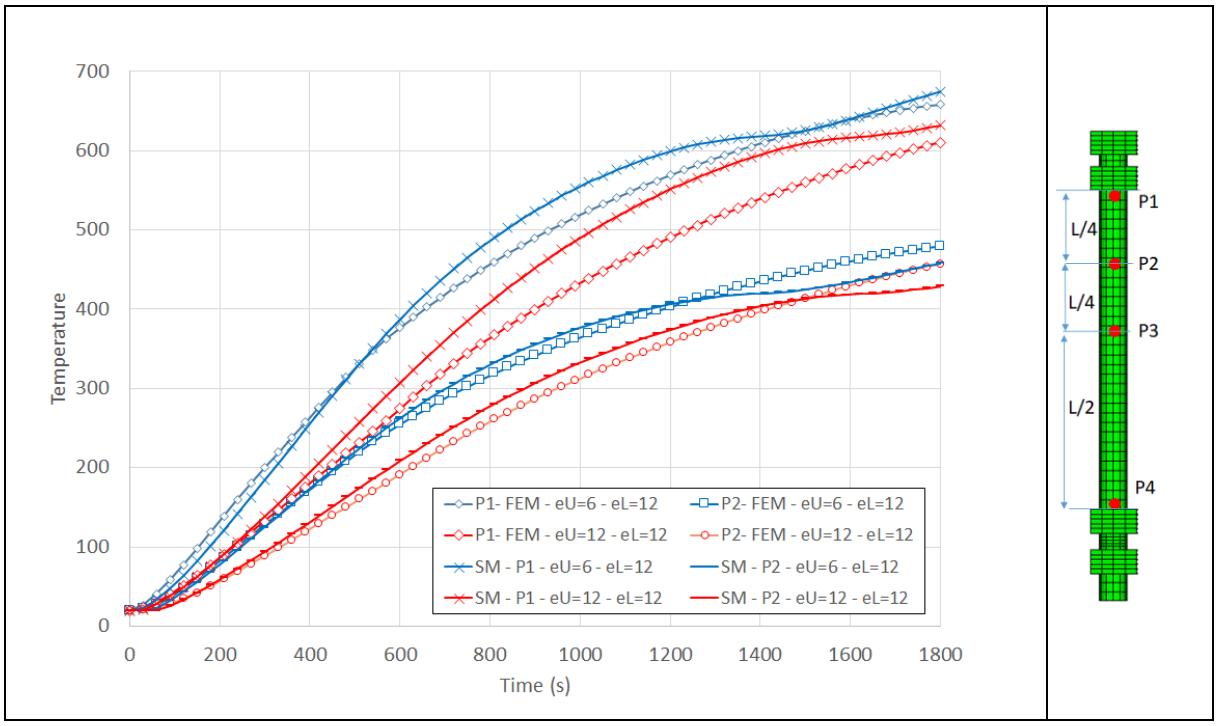

Figure 3.23: Temperature rises calculated along 100 mm length rods according to the thickness of the U profile

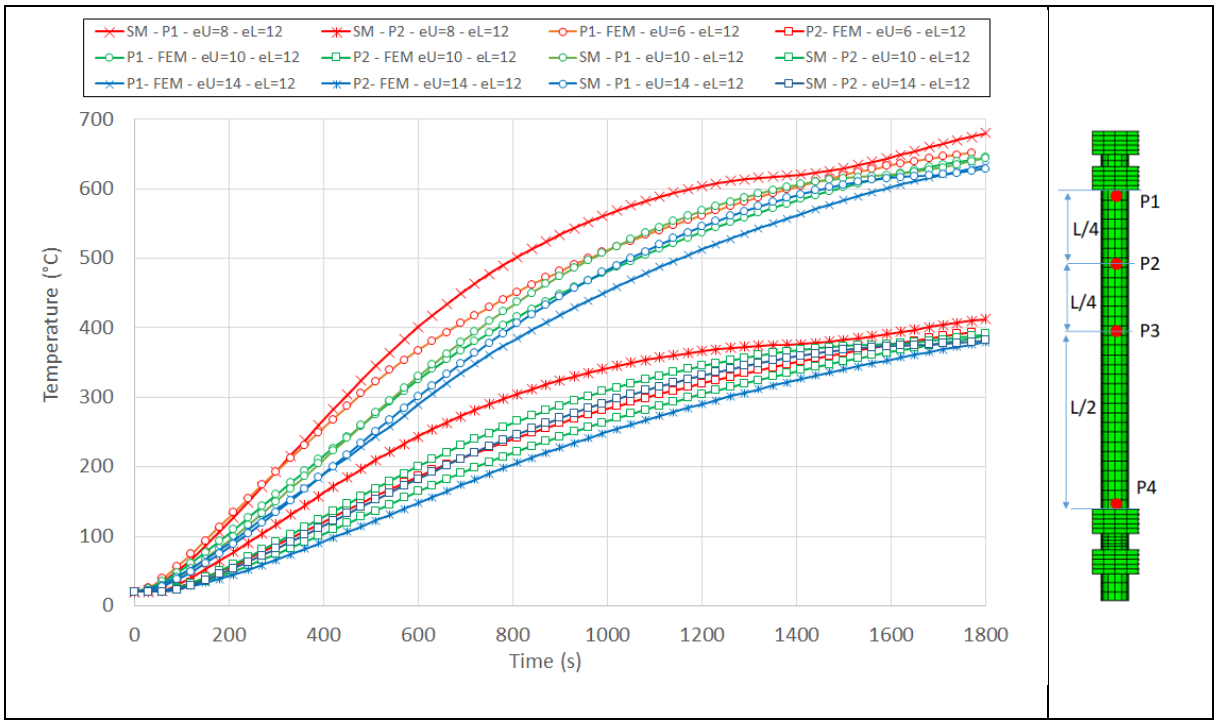

Figure 3.24: Temperature rises calculated along 175 mm length rods according to the thickness of the U profile

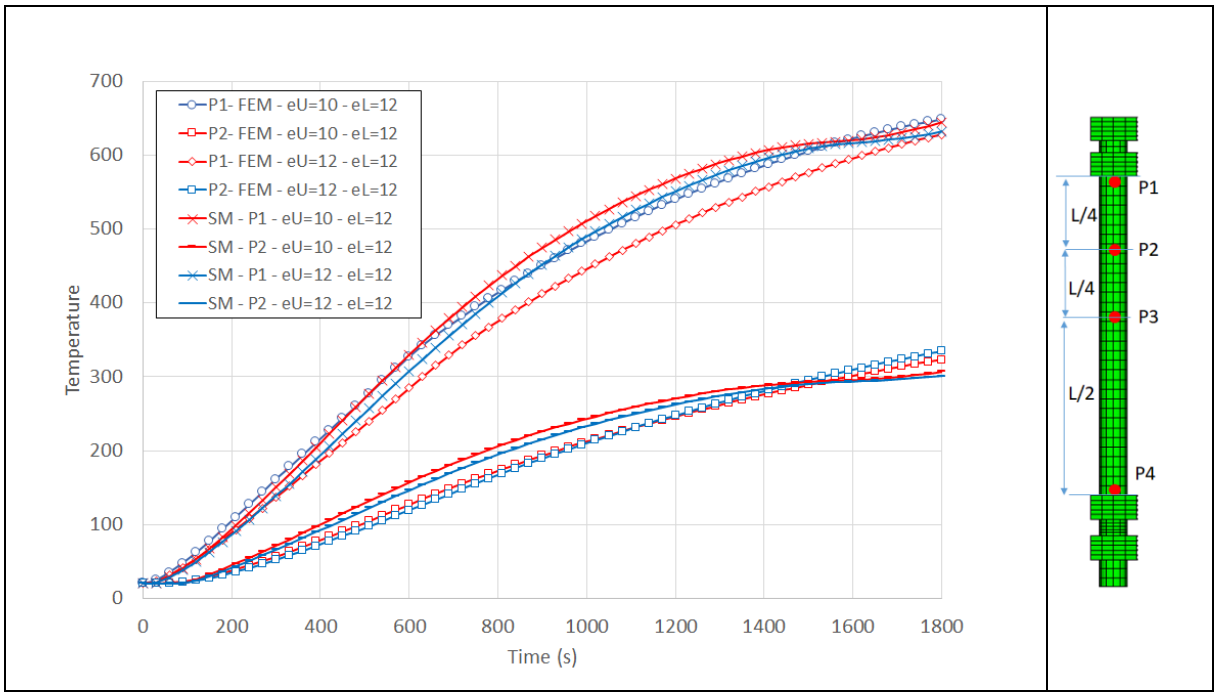

Figure 3.25: Temperature rises calculated along 240 mm length rods according to the thickness of the U profile

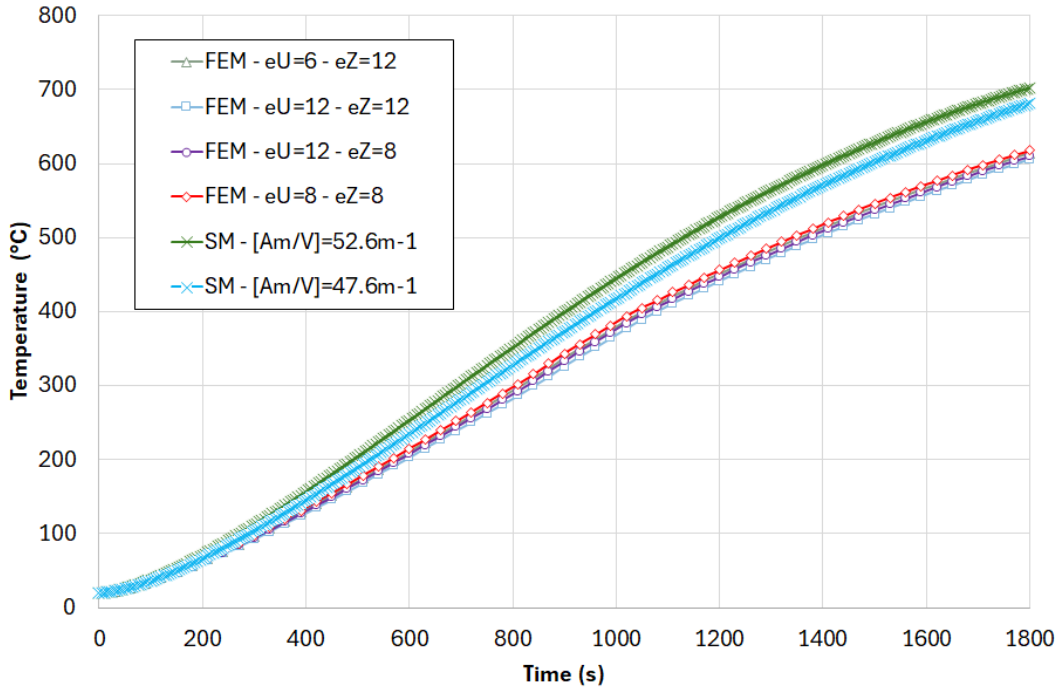

Figure 3.26: Temperature rises calculated for the steel bolts of fusible links related to the first solution, according to the profile thicknesses

3.4.2 Fire resistance calculations

The results of applying the proposed simplified rules to all the analysis cases from the parametric studies are reported hereafter, distinguishing the three investigated fusible link solutions.

3.4.2.1 First fusible link solution

To check the accuracy of the simple calculation methods described in the previous paragraph, the fire design resistance calculated using the simple calculation rules is compared to that derived from the numerical analyses for all the fusible link cases defined for the parametric studies [12]. It should be noted here that for each link the fire resistance obtained using the simplified calculation rules has been determined based on temperatures in the link corresponding to the failure time predicted by the numerical model. This fire resistance were systemically calculated using, either temperatures directly derived from the FE thermal analysis or temperatures calculated using the proposed simplified calculation methods, Moreover, the numerical fire resistance is defined as the compressive load applied in the FE modelling, with values corresponding to 30%, 50% or 70% of the normal-temperature resistance of the considered fusible link, which was initially calculated using the FE model.

The comparison results are shown in Figure 3.27 and Figure 3.28. In these figures the x-axis corresponds to the value of the numerical fire resistance $N_{fi,Rd}$ (FEM), and the y-axis to the value of the fire resistance calculated using the simplified method, $N_{fi,Rd}$ (SM). The 45° regression line represents a perfect equality between these two values. While the regression line which is slightly above represents an error of +15% of the analytical resistance as compared to the numerical value (therefore unsafe), the regression line which is slightly below the bisectrix represents, on the other hand, an error of –15% of the analytical value as compared to the numerical resistance (unsafe).

The criteria used in this work for verifying the accuracy of the developed simplified method was that approved by CEN/TC250/SC4 horizontal group fire [10] which prescribes that three criteria should be met for a calculation method to be considered accurate. Firstly, the calculation results shall not be on the unsafe side by more 15% of the reference result, secondly a maximum of 20% of individual results shall be on the unsafe side and thirdly the mean value of all percentage differences between calculation results and reference results shall be on the safe side.

The fire resistance values, as well as the failure mode, predicted by both the simplified method and the numerical model are reported and compared in Table 7 and Table 8.

All case studies reported in tables are referenced using a combination of letters: 'M' for the diameter of the steel rod, 'L' for the length of the rod, 'eU' for the thickness of the U-shaped profile, 'mx' for the distance between the rods and the web stiffener of the U-shaped profile, 'p' for the spacing between the centres of the rods in the direction of the web stiffener, and 'm' for the distance between the first rod row (closest to the web of the U-shaped profile) and the web of the U-shaped profile. Each letter is followed by the value of the corresponding parameter. The case name thus established is accompanied by the load level. The detailed dimensions of all case studies are given in deliverable D5.2 [12].
From these figures and table, it can be noted that:

- A noticeable discrepancy is observed between the simple calculation rules and the numerical models in determining the fire resistance. It appears that some points are situated on the unsafe side, but a major part of them are situated on the safe side.
- Using temperatures calculated with the proposed simple rules (see Figure 3.27) instead of the numerical ones (Figure 3.28) enhances the safety of the proposed calculation method for determining the fire resistance.
- The predicted design resistance tended to be safe while not overly conservative.
- In most cases, the simplified rules correctly identify the weakest component of the fusible links that causes failure. According to the numerical results, this component is either the bottom flange of the U-shaped steel profile or the steel rods. However, the failure mode of the steel rods is not always correctly identified (i.e. yielding or buckling). For some of the other cases, discrepancies can be explained by the very similar resistance values calculated for these components. In the other cases, it suggests that the simplified method may significantly overestimate the resistance of the weakest component. Based on the weakest component of the fusible links, as determined by numerical analysis, other comparisons were carried out between the corresponding resistances determined with the simplified calculation methods and the numerical results, when the lowest resistance of the steel rods (i.e. yielding or buckling resistance) is considered. There is still a reasonable agreement as illustrated by the green points in Figure 3.27 and Figure 3.28.

Taking all the calculation points from the parametric study results related to the first fusible link solution and calculated using temperatures calculated with the proposed simple rules (see Figure

3.28), the average error is on the safe side, with a value of 0.8 and a standard deviation of 0.13. A maximum deviation of 14% (below 15%) is observed on the unsafe side, and only 6% (below 20%) of cases lie on the unsafe side. Therefore, all the prescribed criteria are met. Conversely, the maximum deviation on the safe side is 47%. However, it should be noted that the CEN/TC250/SC4 criteria do not limit error on the safe side.

Although they have primarily been developed to calculate the fire resistance in compression of the studied fusible links, the proposed calculation methods are based on principles and methods already applied to other types of structural members or steel connections. Therefore, they should also be applicable to determining the load-bearing capacity of links at normal temperatures. Consequently, the proposed design rules have been applied at normal temperature to all the fusible link cases defined for the parametric study performed on the first fusible link solution [12]. The design resistance thus calculated, as well as the predicted failure mode are reported in Table 9. They are compared to the corresponding numerical results. It should be noted that the proposed design method produces satisfactory results when compared with numerical models. Globally, around half of the points are on the unsafe side, with the simplified rules overestimating the load-bearing capacity of links. However, the difference between the simplified method and the numerical model is not more than 15% on the unsafe side, which is fully acceptable.. Moreover, the simplified rules accurately identify the fusible link with the lowest resistance, which causes failure. However, there are some exceptions, which can be explained by the very similar resistance values calculated for these components (within a few percent).

Table 7: Comparison between the proposed simplified method (design equation) and numerical results for the first fusible link solution at elevated temperature – comparison based on the FE temperatures

Case	Time (s)	$\theta_{FB,U}$ (°C)	$\theta_{R,1}$ (°C)	$\theta_{R,2}$ (°C)	$N_{Rd,fi,r1}$	$N_{Rd,fi,r2}$	$N_{Rd,fi,U}$	$N_{Rd,fi\ (SM)}$	$N_{Rd,fi\ (FEM)}$	failure mode (FEM)	failure mode (SM)
30%_M12_L100_eU6_mx29_p70_m35	1259	678	398	596	35	66	31	31	29	bending	bending
50%_M12_L100_eU6_mx29_p70_m35	950	599	340	517	74	72	52	52	49	bending	bending
70%_M12_L100_eU6_mx29_p70_m35	760	532	293	453	98	76	75	75	68	bending	bending
70%_M12_L100_eU10_mx25_p70_m35	803	496	284	432	105	122	153	105	125	rods buckling	rods yielding
50%_M12_L100_eU10_mx25_p70_m35	1061	589	347	520	73	108	98	73	90	rods buckling	rods yielding
30%_M12_L175_eU10_mx25_p70_m35	1350	664	313	598	34	66	61	34	44	rods yielding	rods yielding
50%_M12_L175_eU10_mx25_p70_m35	1060	588	262	522	71	95	98	71	71	rods buckling	rods yielding
70%_M12_L175_eU10_mx25_p70_m35	858	518	219	455	98	102	140	98	105	rods buckling	rods yielding
30%_M12_L175_eU12_mx23_p70_m35	1453	674	322	610	31	84	84	31	48	rods buckling	rods yielding
50%_M12_L175_eU12_mx23_p70_m35	1127	593	268	528	68	100	141	68	86	rods buckling	rods yielding
70%_M12_L175_eU12_mx23_p70_m35	808	479	200	419	110	104	237	104	120	rods buckling	rods buckling
50%_M12_L175_eU14_mx21_p70_m35	1120	580	259	514	75	100	213	75	88	rods buckling	rods yielding
30%_M12_L175_eU14_mx21_p70_m35	1453	668	315	600	33	96	123	33	51	rods yielding	rods yielding
70%_M12_L175_eU14_mx21_p70_m35	730	429	173	372	122	105	376	105	123	rods buckling	rods buckling
70%_M12_L240_eU10_mx25_p70_m35	748	472	153	413	112	84	163	84	88	rods buckling	rods buckling
30%_M12_L240_eU10_mx25_p70_m35	1250	641	242	576	45	68	72	45	38	rods yielding	rods yielding
50%_M16_L175_eU6_mx29_p70_m35	916	589	250	512	143	110	56	56	67	bending	bending
30%_M16_L175_eU6_mx29_p70_m35	1220	670	305	594	67	104	34	34	40	bending	bending
70%_M16_L175_eU6_mx29_p70_m35	730	520	208	445	188	114	80	80	94	bending	bending
70%_M16_L240_eU12_mx23_p70_m35	824	486	163	402	215	196	233	196	169	rods buckling	rods buckling
30%_M16_L240_eU12_mx23_p70_m35	1608	701	297	620	55	65	66	55	73	rods yielding	rods yielding
50%_M12_L175_eU6_mx29_p70_m35	900	583	247	507	79	37	35	35	44	bending	bending
70%_M12_L175_eU6_mx29_p70_m35	630	475	182	402	115	61	56	56	62	bending	bending
50%_M12_L175_eU8_mx27_p70_m35	900	570	238	489	86	74	68	68	62	bending	bending
70%_M12_L175_eU8_mx27_p70_m35	790	515	213	448	100	91	89	89	87	bending	bending
50%_M12_L175_eU10_mx25_p50_m35	1020	576	254	510	77	95	99	77	80	rods buckling	rods yielding
70%_M12_L175_eU10_mx25_p50_m35	816	501	210	438	103	103	141	103	112	rods buckling	rods buckling
70%_M12_L175_eU10_mx25_p55_m35	760	478	196	416	111	104	146	104	105	rods buckling	rods buckling
50%_M12_L175_eU10_mx25_p55_m35	1050	585	260	519	73	90	91	73	75	rods buckling	rods yielding
30%_M12_L175_eU10_mx25_p50_m35	1350	664	313	598	34	61	58	34	48	rods yielding	rods yielding
50%_M16_L175_eU10_mx25_p70_m35	1045	584	259	518	137	136	101	101	117	bending	bending
70%_M16_L175_eU10_mx25_p70_m35	830	507	213	444	189	182	147	147	164	bending	bending
30%_M16_L175_eU10_mx25_p70_m35	1500	693	335	629	52	100	78	52	70	bending	rods yielding
30%_M12_L175_eU8_mx27_p70_m35	1370	718	321	615	30	34	25	25	38	bending	bending
50%_M12_L175_eU8_mx27_p70_m35	1067	638	271	541	62	47	46	46	63	rods buckling	bending
70%_M12_L175_eU8_mx27_p70_m35	830	536	222	464	95	85	81	81	88	rods buckling	bending
R30_M12_L175_eU8_mx27_p70_m35	900	570	238	489	86	74	68	68	84	bending	bending
30%_M14_L100_eU8_mx27_p70_m35	1220	685	398	561	71	103	53	53	51	bending	bending
50%_M14_L100_eU8_mx27_p70_m35	1015	618	357	508	107	110	85	85	85	bending	bending
70%_M14_L100_eU8_mx27_p70_m35	780	509	297	430	145	143	91	91	118	rods buckling	bending
30%_M14_L175_eU8_mx27_p70_m35	1330	711	315	607	43	60	43	43	46	bending	bending
50%_M14_L175_eU8_mx27_p70_m35	1047	631	267	535	89	63	48	48	76	rods buckling	bending
70%_M14_L175_eU8_mx27_p70_m35	830	536	222	464	129	98	81	81	108	rods buckling	bending
30%_M16_L100_eU10_mx25_p70_m35	1460	719	419	615	56	149	65	56	79	bending	rods yielding
50%_M16_L100_eU10_mx25_p70_m35	1079	615	351	525	131	169	137	131	132	bending	rods yielding
70%_M16_L100_eU10_mx25_p70_m35	813	495	287	436	194	220	153	153	185	rods yielding	bending
50%_M16_L175_eU6_mx29_p70_m35	960	602	259	525	130	109	52	52	67	bending	bending
70%_M16_L175_eU6_mx29_p70_m35	740	524	211	449	186	113	78	78	94	rods yielding	bending
50%_M16_L175_eU10_mx25_p70_m35	1151	641	279	549	109	107	72	72	117	bending	bending
70%_M16_L175_eU10_mx25_p70_m35	925	551	234	479	167	159	121	121	164	rods buckling	bending
R30_M16_L175_eU10_mx25_p70_m35	900	539	229	470	172	166	128	128	160	rods buckling	bending
R30_M16_L175_eU10_mx25_p70_m35	900	539	229	470	172	166	128	128	172	rods buckling	bending
30%_M18_L175_eU10_mx25_p70_m35	1640	736	353	652	54	136	59	54	64	bending	rods yielding
50%_M18_L175_eU10_mx25_p70_m35	1300	685	305	586	90	145	84	84	106	bending	bending
70%_M18_L175_eU10_mx25_p70_m35	1087	618	267	530	153	150	135	135	148	bending	bending
50%_M20_L100_eU12_mx23_p70_m35	1152	600	348	477	262	213	134	134	190	bending	bending
70%_M20_L100_eU12_mx23_p70_m35	887	511	283	395	340	296	214	214	266	bending	bending
70%_M20_L175_eU12_mx33_p70_m35	829	488	205	427	311	300	207	207	260	bending	bending
R30_M20_L100_eU12_mx33_p70_m35	900	516	287	400	338	277	188	188	249	bending	bending
30%_M20_L175_eU12_mx23_p70_m35	1400	663	314	598	99	210	147	99	99	rods yielding	rods yielding
50%_M20_L175_eU12_mx23_p70_m35	1250	627	290	562	150	216	187	150	165	bending	rods yielding
70%_M20_L175_eU12_mx23_p70_m35	950	535	232	472	267	286	193	193	231	bending	bending
30%_M22_L175_eU12_mx23_p70_m35	1500	683	329	619	106	283	125	106	103	rods yielding	rods yielding
50%_M22_L175_eU12_mx23_p70_m35	1200	614	281	549	209	298	202	202	172	bending	bending
70%_M22_L175_eU12_mx23_p70_m35	1000	552	243	489	310	418	285	285	240	bending	bending

Table 8 : Comparison between the proposed simplified method (design equation) and numerical results for the first fusible link solution at elevated temperature – comparison based on the analytical temperatures

Case	Time (s)	$\theta_{FB,U}$ (°C)	$\theta_{R,1}$ (°C)	$\theta_{R,2}$ (°C)	$N_{Rd,fi,r1}$	$N_{Rd,fi,r2}$	$N_{Rd,fi,U}$	$N_{Rd,fi\ (SM)}$	$N_{Rd,fi}$ (FEM)	failure mode (FEM)	failure mode (SM)
30%_M12_L100_eU6_mx29_p70_m35	1259	723	415	615	30	63	23	23	29	bending	bending
50%_M12_L100_eU6_mx29_p70_m35	950	643	369	547	59	69	43	43	49	bending	bending
70%_M12_L100_eU6_mx29_p70_m35	760	559	321	475	91	74	69	69	68	bending	bending
70%_M12_L100_eU10_mx25_p70_m35	803	516	296	439	103	121	148	103	125	rods buckling	rods yielding
50%_M12_L100_eU10_mx25_p70_m35	1061	631	362	537	64	98	80	64	90	rods buckling	rods yielding
30%_M12_L175_eU10_mx25_p70_m35	1350	712	334	606	32	42	44	32	44	rods yielding	rods yielding
50%_M12_L175_eU10_mx25_p70_m35	1060	631	296	537	64	80	80	64	71	rods buckling	rods yielding
70%_M12_L175_eU10_mx25_p70_m35	858	545	255	464	95	100	130	95	105	rods buckling	rods yielding
30%_M12_L175_eU12_mx23_p70_m35	1453	718	336	611	31	64	63	31	48	rods buckling	rods yielding
50%_M12_L175_eU12_mx23_p70_m35	1127	632	296	538	64	98	118	64	86	rods buckling	rods yielding
70%_M12_L175_eU12_mx23_p70_m35	808	491	230	418	110	102	240	102	120	rods buckling	rods buckling
50%_M12_L175_eU14_mx21_p70_m35	1120	607	285	517	74	99	190	74	88	rods buckling	rods yielding
30%_M12_L175_eU14_mx21_p70_m35	1453	705	331	600	33	87	94	33	51	rods yielding	rods yielding
70%_M12_L175_eU14_mx21_p70_m35	730	422	198	359	124	104	400	104	123	rods buckling	rods buckling
70%_M12_L240_eU10_mx25_p70_m35	748	486	191	413	112	82	164	82	88	rods buckling	rods buckling
30%_M12_L240_eU10_mx25_p70_m35	1250	690	271	587	39	44	52	39	38	rods yielding	rods yielding
50%_M16_L175_eU6_mx29_p70_m35	916	630	295	536	120	105	46	46	67	bending	bending
30%_M16_L175_eU6_mx29_p70_m35	1220	717	336	610	58	100	24	24	40	bending	bending
70%_M16_L175_eU6_mx29_p70_m35	730	543	254	462	178	109	75	75	94	bending	bending
70%_M16_L240_eU12_mx23_p70_m35	824.4	500	196	425	200	193	234	193	169	rods buckling	rods buckling
30%_M16_L240_eU12_mx23_p70_m35	1608	735	288	625	53	66	56	53	73	rods yielding	rods yielding
50%_M12_L175_eU6_mx29_p70_m35	900	624	292	531	67	35	29	29	44	bending	bending
70%_M12_L175_eU6_mx29_p70_m35	630	481	226	410	113	59	57	57	62	bending	bending
50%_M12_L175_eU8_mx27_p70_m35	900	594	278	505	80	63	62	62	62	bending	bending
70%_M12_L175_eU8_mx27_p70_m35	790	540	253	460	96	83	83	83	87	bending	bending
50%_M12_L175_eU10_mx25_p50_m35	1020	616	289	524	71	81	82	71	80	rods buckling	rods yielding
70%_M12_L175_eU10_mx25_p50_m35	816	523	245	445	101	101	134	101	112	rods buckling	rods yielding
70%_M12_L175_eU10_mx25_p55_m35	760	493	231	419	110	102	146	102	105	rods buckling	rods buckling
50%_M12_L175_eU10_mx25_p55_m35	1050	627	294	534	66	75	74	66	75	rods buckling	rods yielding
30%_M12_L175_eU10_mx25_p50_m35	1350	712	334	606	32	38	41	32	48	rods yielding	rods yielding
50%_M16_L175_eU10_mx25_p70_m35	1045	625	293	532	124	105	83	83	117	bending	bending
70%_M16_L175_eU10_mx25_p70_m35	830	531	249	451	184	169	139	139	164	bending	bending
30%_M16_L175_eU10_mx25_p70_m35	1500	733	343	623	54	99	63	54	70	bending	rods yielding
30%_M12_L175_eU8_mx27_p70_m35	1370	727	341	619	30	33	25	25	38	bending	bending
50%_M12_L175_eU8_mx27_p70_m35	1067	658	308	560	53	39	42	39	63	rods buckling	rods buckling
70%_M12_L175_eU8_mx27_p70_m35	830	561	263	477	90	76	75	75	88	rods buckling	bending
R30_M12_L175_eU8_mx27_p70_m35	900	594	278	505	80	63	62	62	84	bending	bending
30%_M14_L100_eU8_mx27_p70_m35	1220	700	402	596	48	102	48	48	51	bending	rods yielding
50%_M14_L100_eU8_mx27_p70_m35	1015	640	367	544	83	108	78	78	85	bending	bending
70%_M14_L100_eU8_mx27_p70_m35	780	535	307	455	133	135	85	85	118	rods buckling	bending
30%_M14_L175_eU8_mx27_p70_m35	1330	722	338	614	42	58	43	42	46	bending	rods yielding
50%_M14_L175_eU8_mx27_p70_m35	1047	651	305	554	76	61	44	44	76	rods buckling	bending
70%_M14_L175_eU8_mx27_p70_m35	830	561	263	477	123	85	75	75	108	rods buckling	bending
30%_M16_L100_eU10_mx25_p70_m35	1460	729	418	620	55	149	65	55	79	bending	rods yielding
50%_M16_L100_eU10_mx25_p70_m35	1079	638	366	543	114	165	125	114	132	bending	rods yielding
70%_M16_L100_eU10_mx25_p70_m35	813	522	299	444	189	213	144	144	185	rods yielding	bending
50%_M16_L175_eU6_mx29_p70_m35	960	647	303	550	107	104	42	42	67	bending	bending
70%_M16_L175_eU6_mx29_p70_m35	740	548	257	466	175	109	73	73	94	rods yielding	bending
50%_M16_L175_eU10_mx25_p70_m35	1151	662	310	563	95	103	65	65	117	bending	bending
70%_M16_L175_eU10_mx25_p70_m35	925	576	270	490	160	141	110	110	164	rods buckling	bending
R30_M16_L175_eU10_mx25_p70_m35	900	565	265	481	166	149	117	117	160	rods buckling	bending
R30_M16_L175_eU10_mx25_p70_m35	900	565	265	481	166	149	117	117	172	rods buckling	bending
30%_M18_L175_eU10_mx25_p70_m35	1640	742	348	631	62	137	59	59	64	bending	bending
50%_M18_L175_eU10_mx25_p70_m35	1300	702	329	597	78	140	75	75	106	bending	bending
70%_M18_L175_eU10_mx25_p70_m35	1087	641	300	545	137	146	123	123	148	bending	bending
50%_M20_L100_eU12_mx23_p70_m35	1152	640	300	545	175	214	180	175	190	bending	rods yielding
70%_M20_L100_eU12_mx23_p70_m35	887	532	249	452	286	287	204	204	266	bending	bending
70%_M20_L175_eU12_mx33_p70_m35	829	502	235	427	311	291	208	208	260	bending	bending
R30_M20_L100_eU12_mx33_p70_m35	900	538	252	458	281	264	178	178	249	bending	bending
30%_M20_L175_eU12_mx23_p70_m35	1400	708	332	602	95	205	106	95	99	rods yielding	rods yielding
50%_M20_L175_eU12_mx23_p70_m35	1250	671	315	571	138	210	145	138	165	bending	rods yielding
70%_M20_L175_eU12_mx23_p70_m35	950	561	263	478	323	302	285	285	231	rods yielding	bending
30%_M22_L175_eU12_mx23_p70_m35	1500	725	340	617	108	278	97	97	103	bending	bending
50%_M22_L175_eU12_mx23_p70_m35	1200	656	308	558	193	291	162	162	172	bending	bending

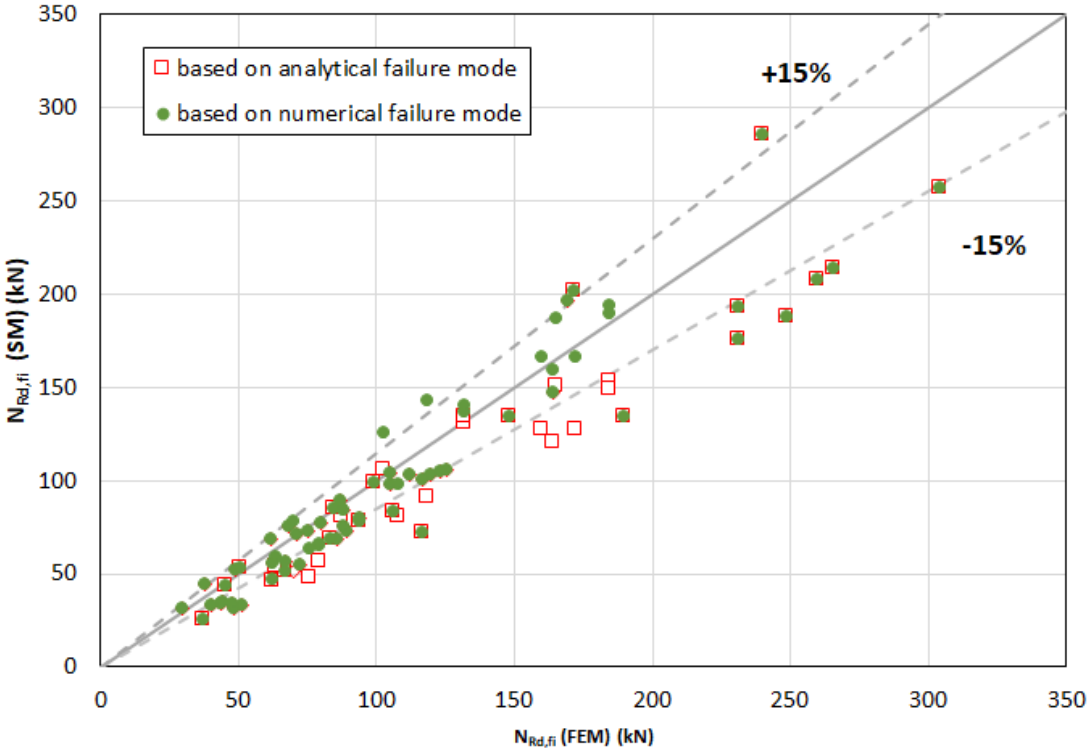

Figure 3.27: Comparison between the proposed simplified method (design equation) and numerical results for the first fusible link solution at elevated temperature – comparison based on the FE temperatures

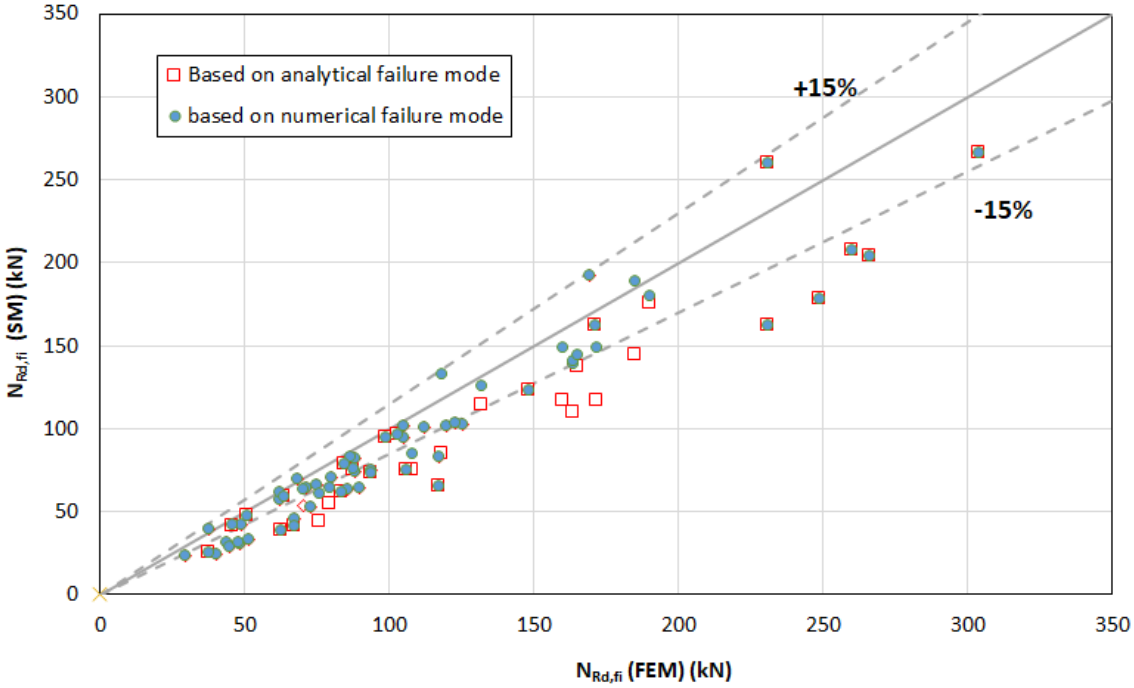

Figure 3.28: Comparison between the proposed simplified method (design equation) and numerical results for the first fusible link solution at elevated temperature - comparison based on analytical temperatures

Table 9 : Comparison between the proposed simplified method (design equation) and numerical results for the first fusible link solution at normal temperature

Case	$N_{Rd,fi,r}$	$N_{Rd,fi,U}$	$N_{Rd,fi\ (SM)}$	$N_{Rd,fi\ (FEM)}$	failure mode (FEM	failure mode (SM)
M12_L100_eU6_mx29_p55_m35	131	105	105	88	bending	bending
M12_L100_eU8_mx27_p70_m35	158	149	149	140.4	bending	bending
M12_L100_eU10_mx25_p70_m35	168	244	168	177	rods buckling	rods buckling
M12_L175_eU6_mx44_p70_m35	95	64	64	61.2	bending	bending
M12_L175_eU10_mx25_p70_m35	137	244	137	144.8	rods buckling	rods buckling
M12_L175_eU12_mx23_p70_m35	140	369	140	160.6	rods buckling	rods buckling
M12_L175_eU14_mx21_p70_m35	143	530	143	170.3	rods buckling	rods buckling
M12_L200_eU6_mx29_p70_m35	80	80	80	84	bending	rods buckling
M12_L240_eU10_mx25_p70_m35	108	244	108	125.7	rods buckling	rods buckling
M16_L175_eU10_mx25_p70_m35	267	244	244	233	bending	bending
M16_L200_eU10_mx25_p70_m35	255	244	244	230	bending	bending
M16_L220_eU9_mx26_p70_m35	211	193	193	196.8	bending	bending
M16_L240_eU12_mx30_p50_m70	226	217	217	241.8	rods buckling	bending
M16_L240_eU10_mx25_p70_m35	238	244	238	214	rods buckling	rods buckling
M12_L175_eU10_mx25_p50_m35	168	282	168	160	rods buckling	rods buckling
M12_L175_eU10_mx25_p70_m60	137	236	137	140.7	rods buckling	rods buckling
M12_L175_eU8_mx27_p70_m35	134	149	134	122.8	rods buckling	rods buckling
M12_L120_eU8_mx27_p70_m35	151	149	149	140.4	bending	bending
M12_L100_eU10_mx25_p70_m35	164	244	164	180	rods buckling	rods buckling
M12_L175_eU8_mx27_p70_m35	125	149	125	125	rods buckling	rods buckling
M12_L175_eU10_mx25_p70_m35	153	292	153	141	rods buckling	rods buckling
M16_L100_eU6_mx29_p70_m35	206	111	111	149	bending	bending
M16_L100_eU10_mx25_p70_m35	298	244	244	264	bending	bending
M16_L175_eU6_mx29_p70_m35	120	111	111	149	rods buckling	bending
M16_L175_eU10_mx25_p70_m35	257	244	244	240	bending	bending
M20_L100_eU12_mx23_p70_m35	535	462	462	425	bending	bending
M20_L175_eU12_mx33_p70_m35	388	321	321	352	bending	bending
M20_L200_eU12_mx33_p70_m35	372	321	321	340	bending	bending
M20_L240_eU12_mx33_p70_m35	348	321	321	310	rods buckling	bending
M16_L175_eU8_mx27_p70_m35	205	200	200	187	rods buckling	bending
M16_L100_eU8_mx27_p70_m35	276	200	200	202	bending	bending
M18_L175_eU6_mx29_p70_m35	200	111	111	161	bending	bending
M18_L175_eU8_mx27_p70_m35	222	200	200	200	bending	bending
M18_L175_eU10_mx25_p70_m35	324	316	316	271	bending	bending
M16_L100_eU9_mx26_p70_m35	305	254	254	233	bending	bending
M14_L175_eU8_mx27_p70_m35	174	157	157	152	bending	bending
M14_L100_eU8_mx27_p70_m35	216	200	200	170	bending	bending
M20_L100_eU10_mx25_p70_m35	476	316	316	355	bending	bending
M20_L175_eU10_mx25_p70_m35	380	316	316	326	bending	bending
M20_L100_eU8_mx27_p70_m35	436	200	200	279	bending	bending
M20_L175_eU8_mx27_p70_m35	298	200	200	257	bending	bending
M22_L100_eU12_mx29_p70_m35	647	462	462	481	bending	bending
M22_L175_eU12_mx23_p70_m35	556	462	462	440	bending	bending
M22_L100_eU12_dx45_60_m35	551	447	447	434	bending	bending
M22_L175_eU12_dx23_p60_m35	471	447	447	400	rods buckling	bending
M20_L100_eU9_mx26_p70_m35	441	254	254	318	bending	bending
M20_L175_eU9_mx26_p70_m35	315	254	254	290	bending	bending
M18_L100_eU10_mx25_p70_m35	388	316	316	296	bending	bending
M18_L175_eU9_mx26_p70_m35	279	254	254	220	bending	bending

Table 10 : Comparison between the proposed simplified method (design equation) and the numerical simulations for the first fusible link solution at normal temperature – buckling of steel rods

Case	$N_{Rd,fi\,(SM)}$	$N_{Rd,fi\,(FEM)}$
M16_L100_eU12_mx29_p70_m35	329	450
M16_L175_eU12_mx29_p70_m35	288	363
M16_L240_eU12_mx29_p70_m35	248	300
M12_L175_eU12_mx29_p70_m35	195	208
M20_L175_eU12_mx29_p70_m35	693	621
M12_L240_eU12_mx29_p70_m35	154	160
M20_L240_eU12_mx29_p70_m35	630	590
M18_L175_eU12_mx29_p70_m35	527	521
M12_L175_eU14_mx29_p70_m35	195	208
M18_L240_eU12_mx29_p70_m35	469	469
M12_L240_eU14_mx29_p70_m35	154	166

Table 11 : Comparison between the proposed simplified method (design equation) and numerical simulations for the first fusible link solution at normal temperature – transverse bending to the U profile flange

Case	$N_{Rd,fi\,(SM)}$	$N_{Rd,fi\,(FEM)}$
M12_L20_eU8_mx27_p70_m35	200	209
M12_L20_eU8_mx27_p70_m55	169	172
M12_L20_eU6_mx29_p70_m35	111	124
M12_L20_eU6_mx29_p70_m55	92	106
M12_L20_eU6_mx39_p55_m35	106	112
M20_L20_eU8_mx27_p70_m35	200	260
M20_L20_eU10_mx25_p70_m35	316	416
M16_L20_eU10_mx25_p70_m35	316	357

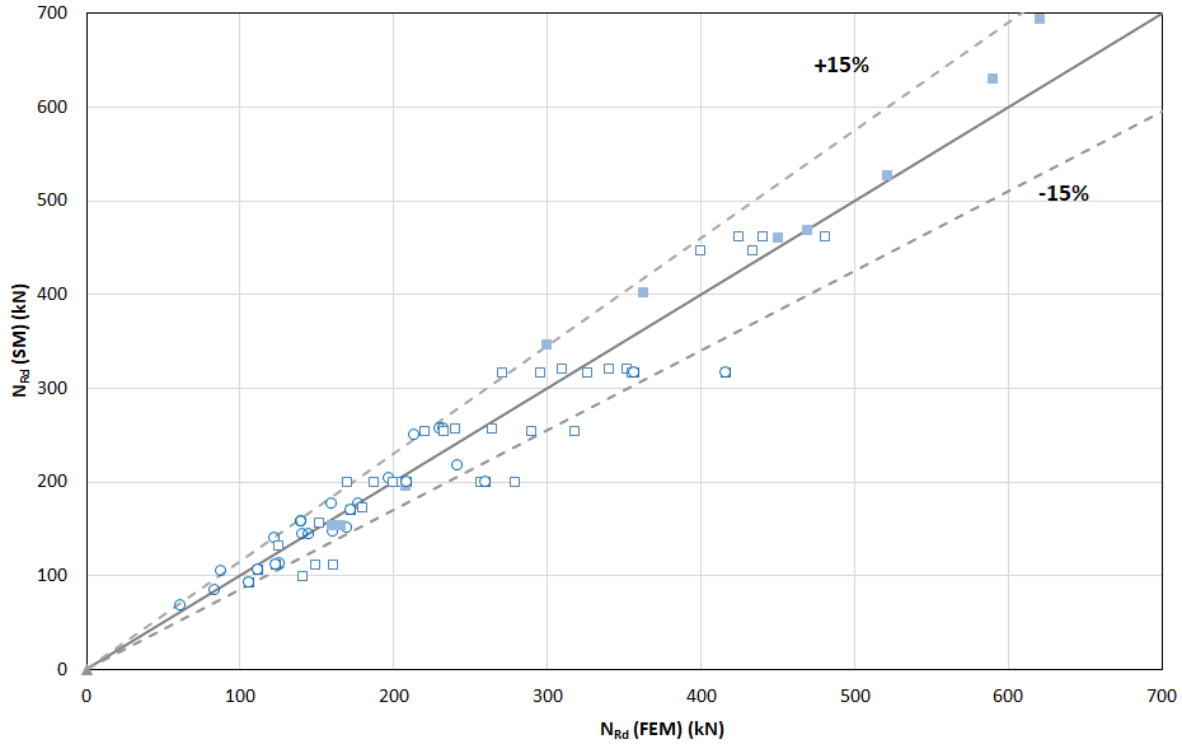

Figure 3.29: Comparison between the proposed simplified method (design equation) and numerical simulations for the first fusible link solution at normal temperature

3.4.2.2 Third fusible link solution

As with the previous fusible link solution, the fire design resistance is calculated using simple calculation rules and compared to that derived from numerical analyses for all fusible link cases related to the second solution.

The comparison results are shown in Figure 3.27 and Figure 3.28. In these figures the x-axis corresponds to the value of the numerical fire resistance $N_{fi,Rd}$ (FEM), and the y-axis to the value of the fire resistance calculated using the simplified method, $N_{fi,Rd}$ (SM). The 45° regression line represents a perfect equality between these two values. While the regression line which is slightly above represents an error of +15% of the analytical resistance as compared to the numerical value (therefore unsafe), the regression line which is slightly below the bisectrix represents, on the other hand, an error of –15% of the analytical value as compared to the numerical resistance (unsafe).

The fire resistance values, as well as the failure mode, predicted by both the simplified method and the numerical model are reported and compared in Table 12 and Table 13.

All case studies reported in tables are referenced using a combination of letters: 'M' for the diameter of the steel rod, 'L' for the length of the rod, UPN for the steel profile that extends horizontally between the columns of the building steel structure, eL for the thickness of the L-shaped profile, 'p1' for the horizontal distance between the two rod and 'DX' for the distance between the centreline of rod rows and the bolt row of the UPN connection with the column web stiffener. Each letter is followed by the value of the corresponding parameter. The case name thus established is accompanied by the load level. The detailed dimensions of all case studies are given in deliverable D5.2 [12].

Globally, the proposed simple calculation rules show satisfactory predictions, with the average error lying on the safe side. In very few cases, the failure mode of the steel rods (i.e. yielding or buckling) is not correctly identified, due to resistance values being very close. Taking all the calculation points from the parametric study results calculated using temperatures calculated with the proposed simple rules (see Figure 3.31), the average error is on the safe side, with a value of 0.91 and a standard deviation of 0.15. A maximum deviation of 14% (below 15%) is observed on the unsafe side, and 27% of cases lie on the unsafe side, which is a slightly higher than the 20% criterion. Moreover, the maximum deviation on the safe side is 47%. Therefore, all the horizontal fire group criteria are not

met. However, since the criterion relating to the number of unsafe cases is exceeded by a small margin, the method's accuracy could be considered satisfactory.

Some comparisons have been also made at normal temperature (see Figure 3.32). The design resistance thus calculated, as well as the predicted failure mode are reported in Table 13. They are compared to the corresponding numerical results. It should be noted that the proposed design method produces also satisfactory results when compared with numerical models. It is found that the resulting predicted design resistance tended to be safe while not overly conservative.

Table 12: Comparison between the proposed simplified method (design equation) and numerical results for the third fusible link solution at elevated temperature – comparison based on the FE temperatures

Case	Time (s)	θ_L (°C)	$\theta_{R,1}$ (°C)	$\theta_{R,2}$ (°C)	$N_{Rd,fi,r1}$	$N_{Rd,fi,r2}$	$N_{Rd,fi}$ (SM)	$N_{Rd,fi}$ (FEM)	failure mode (FEM)	failure mode (SM)
70%-M16_L175_UPN240_eL10_p180_DX400	380	428	146	303	113	102	102	86	rods bucklings	rods bucklings
50%-M16_L175_UPN240_eL10_p180_DX400	550	588	250	461	80	97	80	62	rods yielding	rods yielding
30%-M16_L175_UPN240_eL10_p180_DX400	881	686	334	568	41	90	41	39	rods yielding	rods yielding
70%-M16_L175_UPN240_eL10_p180_DX200	385	432	148	307	112	102	102	109	rods bucklings	rods bucklings
50%-M16_L175_UPN240_eL10_p180_DX200	550	555	226	427	90	98	90	78	rods yielding	rods yielding
70%-M20_L175_UPN240_eL10_p180_DX200	295	331	104	224	182	172	172	155	rods bucklings	rods bucklings
50%-M20_L175_UPN240_eL10_p180_DX200	620	593	254	466	123	161	123	110	rods yielding	rods yielding
30%-M20_L175_UPN300_eL10_p180_DX200	565	564	232	436	136	162	136	113	rods yielding	rods yielding
70%-M16_L175_UPN300_eL10_p180_DX200	500	524	204	396	98	99	98	112	rods yielding	rods yielding
30%-M16_L175_UPN300_eL10_p180_DX200	800	663	313	542	52	93	52	48	rods yielding	rods yielding
70%-M16_L100_UPN240_eL10_p180_DX200	430	471	245	393	98	110	98	126	rods bucklings	rods yielding
50%-M16_L100_UPN240_eL10_p180_DX200	600	583	327	499	69	104	69	91	rods yielding	rods yielding
70%-M16_L240_UPN240_eL10_p180_DX200	445	483	194	414	93	87	87	95	rods bucklings	rods bucklings
50%-M16_L240_UPN240_eL10_p180_DX200	580	572	247	491	72	84	72	68	rods yielding	rods yielding
30%-M16_L240_UPN240_eL10_p180_DX200	840	675	318	582	35	80	35	41	rods yielding	rods yielding
70%-M20_L240_UPN240_eL10_p180_DX200	450	487	197	417	144	150	144	175	rods bucklings	rods yielding
50%-M20_L240_UPN240_eL10_p180_DX200	600	583	254	500	108	146	108	125	rods yielding	rods yielding
30%-M20_L240_UPN240_eL10_p180_DX200	800	663	309	571	62	141	62	75	rods yielding	rods yielding
70%-M16_L175_UPN240_eL8_p180_DX200	366	445	322	290	114	92	92	107	rods bucklings	rods bucklings
70%-M16_L175_UPN240_eL15_p180_DX200	412	393	162	331	108	101	101	113	rods bucklings	rods bucklings
50%-M16_L175_UPN240_eL15_p180_DX200	650	566	265	481	74	96	74	80	rods bucklings	rods yielding
30%-M16_L175_UPN240_eL15_p180_DX200	860	658	329	562	44	91	44	46	rods yielding	rods yielding
70%-M16_L100_UPN240_eL10_p180_DX400	440	479	251	401	97	110	97	98	rods bucklings	rods yielding
50%-M16_L100_UPN240_eL10_p180_DX400	580	572	319	489	72	105	72	70	rods yielding	rods yielding
70%-M16_L175_UPN240_eL10_p1120_DX200	440	479	176	353	105	100	100	102	rods bucklings	rods bucklings
50%-M16_L175_UPN240_eL10_p1120_DX200	680	619	276	495	71	96	71	72	rods yielding	rods yielding
30%-M16_L175_UPN240_eL10_p1120_DX200	870	683	331	565	42	90	42	40	rods yielding	rods yielding
70%-M16_L175_UPN240_eL10_p150_DX200	433	474	172	348	106	101	101	102	rods yielding	rods bucklings
50%-M16_L175_UPN240_eL10_p150_DX200	638	601	261	475	76	96	76	73	rods yielding	rods yielding
50%-.M20_L175_UPN300_eL10_p180_DX200	600	583	246	456	127	161	127	142.2	rods yielding	rods yielding
30%-M12_L175_UPN240_eL10_p180_DX200	900	691	339	573	21	42	21	24.45	rods yielding	rods yielding
50%-M12_L175_UPN240_eL10_p180_DX200	700	628	282	504	36	44	36	35.75	rods yielding	rods yielding
70%-M12_L175_UPN240_eL10_p180_DX200	510	530	209	402	52	46	46	57.05	rods bucklings	rods bucklings
30%-M12_L175_UPN240_eL10_p180_DX400	950	702	350	587	18	41	18	19.5	rods yielding	rods yielding
50%-M12_L175_UPN240_eL10_p180_DX400	660	611	269	486	39	45	39	32.5	rods yielding	rods yielding
70%-M12_L175_UPN240_eL10_p180_DX400	500	524	204	396	53	46	46	45.5	rods bucklings	rods bucklings
30%-M16_L175_UPN300_eL10_p180_DX400	960	705	352	589	32	88	32	42.9	rods yielding	rods yielding
50%-M16_L175_UPN300_eL10_p180_DX400	670	615	272	490	72	96	72	71.5	rods yielding	rods yielding
70%-M16_L175_UPN300_eL10_p180_DX400	490	517	200	389	99	99	99	100.1	rods bucklings	rods yielding
70%-M16_L175_UPN300_eL10_p180_DX200	490	517	200	389	99	99	99	112.7	rods bucklings	rods yielding
30%-M20_L175_UPN300_eL12_p180_DX200	900	678	349	570	62	147	62	88.5	rods yielding	rods yielding
50%-M20_L175_UPN300_eL12_p180_DX200	640	578	271	476	118	160	118	147.5	rods yielding	rods yielding
70%-M20_L175_UPN300_eL12_p180_DX200	450	453	188	365	161	166	161	206.5	rods bucklings	rods yielding

Table 13 : Comparison between the proposed simplified method (design equation) and numerical results for the third fusible link solution at elevated temperature – comparison based on the analytical temperatures

Case	Time (s)	θ_L (°C)	$\theta_{R,1}$ (°C)	$\theta_{R,2}$ (°C)	$N_{Rd,fi,r1}$	$N_{Rd,fi,r2}$	$N_{Rd,fi(SM)}$	$N_{Rd,fi(FEM)}$	failure mode (FEM)	failure mode (SM)
70%-M16_L175_UPN240_eL10_p180_DX400	380	392	223	333	108	98	98	86	rods bucklings	rods bucklings
50%-M16_L175_UPN240_eL10_p180_DX400	625	581	331	494	71	90	71	62	rods yielding	rods yielding
30%-M16_L175_UPN240_eL10_p180_DX400	881	684	390	581	35	83	35	39	rods yielding	rods yielding
70%-M16_L175_UPN240_eL10_p180_DX200	385	397	226	337	107	98	98	109	rods bucklings	rods bucklings
50%-M16_L175_UPN240_eL10_p180_DX200	550	535	305	455	82	94	82	78	rods yielding	rods yielding
70%-M20_L175_UPN240_eL10_p180_DX200	295	301	172	256	180	167	167	155	rods bucklings	rods bucklings
50%-M20_L175_UPN240_eL10_p180_DX200	620	578	330	492	111	151	111	110	rods yielding	rods yielding
30%-M20_L175_UPN300_eL10_p180_DX200	565	545	311	463	124	155	124	113	rods yielding	rods yielding
70%-M16_L175_UPN300_eL10_p180_DX200	500	499	284	424	91	95	91	112	rods yielding	rods yielding
30%-M16_L175_UPN300_eL10_p180_DX200	800	659	375	560	44	85	44	48	rods yielding	rods yielding
70%-M16_L100_UPN240_eL10_p180_DX200	430	440	273	374	102	109	102	126	rods bucklings	rods yielding
50%-M16_L100_UPN240_eL10_p180_DX200	600	567	352	482	74	100	74	91	rods yielding	rods yielding
70%-M16_L240_UPN240_eL10_p180_DX200	445	453	231	385	100	85	85	95	rods bucklings	rods bucklings
50%-M16_L240_UPN240_eL10_p180_DX200	580	555	283	472	77	82	77	68	rods yielding	rods yielding
30%-M16_L240_UPN240_eL10_p180_DX200	840	672	343	571	40	77	40	41	rods yielding	rods yielding
70%-M20_L240_UPN240_eL10_p180_DX200	450	458	234	389	155	147	147	175	rods bucklings	rods bucklings
50%-M20_L240_UPN240_eL10_p180_DX200	600	567	289	482	116	143	116	125	rods yielding	rods yielding
30%-M20_L240_UPN240_eL10_p180_DX200	800	659	336	560	69	135	69	75	rods yielding	rods yielding
70%-M16_L175_UPN240_eL8_p180_DX200	366	424	242	360	104	97	97	107	rods bucklings	rods bucklings
70%-M16_L175_UPN240_eL15_p180_DX200	412	338	193	287	114	100	100	113	rods bucklings	rods bucklings
50%-M16_L175_UPN240_eL15_p180_DX200	650	520	296	442	86	95	86	80	rods bucklings	rods yielding
30%-M16_L175_UPN240_eL15_p180_DX200	880	635	362	540	53	86	53	46	rods yielding	rods yielding
70%-M16_L100_UPN240_eL10_p180_DX400	440	449	278	381	100	109	100	98	rods bucklings	rods yielding
50%-M16_L100_UPN240_eL10_p180_DX400	580	555	344	472	77	101	77	70	rods yielding	rods yielding
70%-M16_L175_UPN240_eL10_p1120_DX200	440	449	256	381	100	97	97	102	rods bucklings	rods bucklings
50%-M16_L175_UPN240_eL10_p1120_DX200	680	609	347	518	62	88	62	72	rods yielding	rods yielding
30%-M16_L175_UPN240_eL10_p1120_DX200	870	681	388	579	36	83	36	40	rods yielding	rods yielding
70%-M16_L175_UPN240_eL10_p150_DX200	433	442	252	376	101	97	97	102	rods yielding	rods bucklings
50%-M16_L175_UPN240_eL10_p150_DX200	638	588	335	500	69	90	69	73	rods yielding	rods yielding
50%-.M20_L175_UPN300_eL10_p180_DX200	600	567	323	482	116	152	116	142.2	rods yielding	rods yielding
30%-M12_L175_UPN240_eL10_p180_DX200	900	689	393	586	18	38	18	24.45	rods yielding	rods yielding
50%-M12_L175_UPN240_eL10_p180_DX200	700	619	353	526	31	41	31	35.75	rods yielding	rods yielding
70%-M12_L175_UPN240_eL10_p180_DX200	510	507	289	431	48	44	44	57.05	rods bucklings	rods bucklings
30%-M12_L175_UPN240_eL10_p180_DX400	950	701	400	596	16	38	16	19.5	rods yielding	rods yielding
50%-M12_L175_UPN240_eL10_p180_DX400	660	600	342	510	35	41	35	32.5	rods yielding	rods yielding
70%-M12_L175_UPN240_eL10_p180_DX400	500	499	284	424	49	44	44	45.5	rods bucklings	rods bucklings
30%-M16_L175_UPN300_eL10_p180_DX400	960	704	401	598	28	81	28	42.9	rods yielding	rods yielding
50%-M16_L175_UPN300_eL10_p180_DX400	670	605	345	514	63	89	63	71.5	rods yielding	rods yielding
70%-M16_L175_UPN300_eL10_p180_DX400	490	491	280	417	92	96	92	100.1	rods bucklings	rods yielding
70%-M16_L175_UPN300_eL10_p180_DX200	490	491	280	417	92	96	92	112.7	rods bucklings	rods yielding
30%-M20_L175_UPN300_eL12_p180_DX200	900	689	393	586	52	137	52	88.5	rods yielding	rods yielding
50%-M20_L175_UPN300_eL12_p180_DX200	640	589	336	501	107	150	107	147.5	rods yielding	rods yielding
70%-M20_L175_UPN300_eL12_p180_DX200	450	458	261	389	155	160	155	206.5	rods bucklings	rods yielding

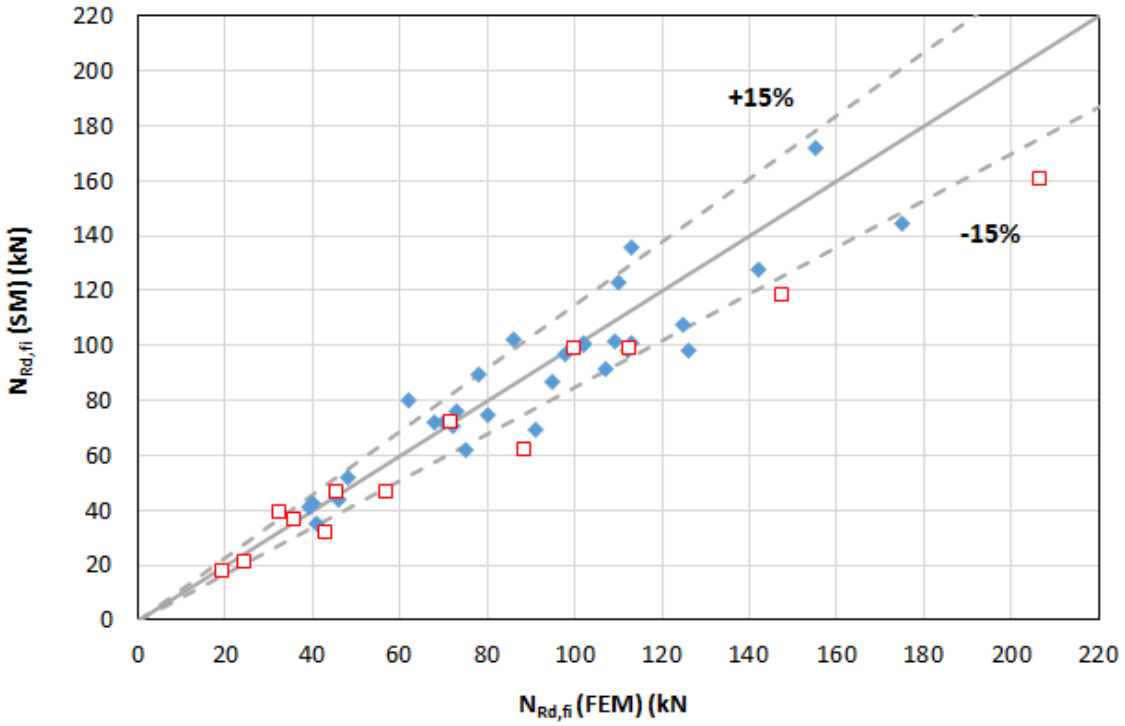

Figure 3.30: Comparison between the proposed simplified method (design equation) and numerical simulations for the third fusible link solution at elevated temperature – comparison based on the FE temperatures

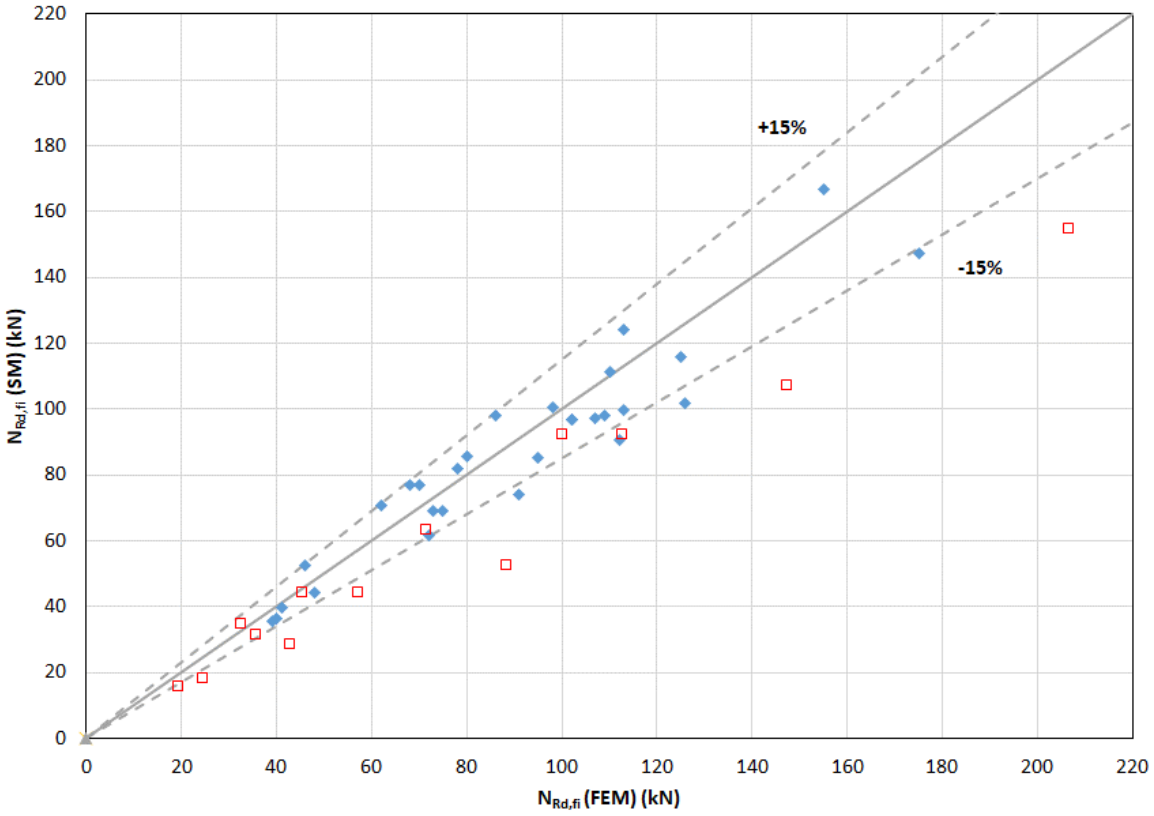

Figure 3.31: Comparison between the proposed simplified method (design equation) and numerical simulations for the third fusible link solution at elevated temperature - comparison based on analytical temperatures

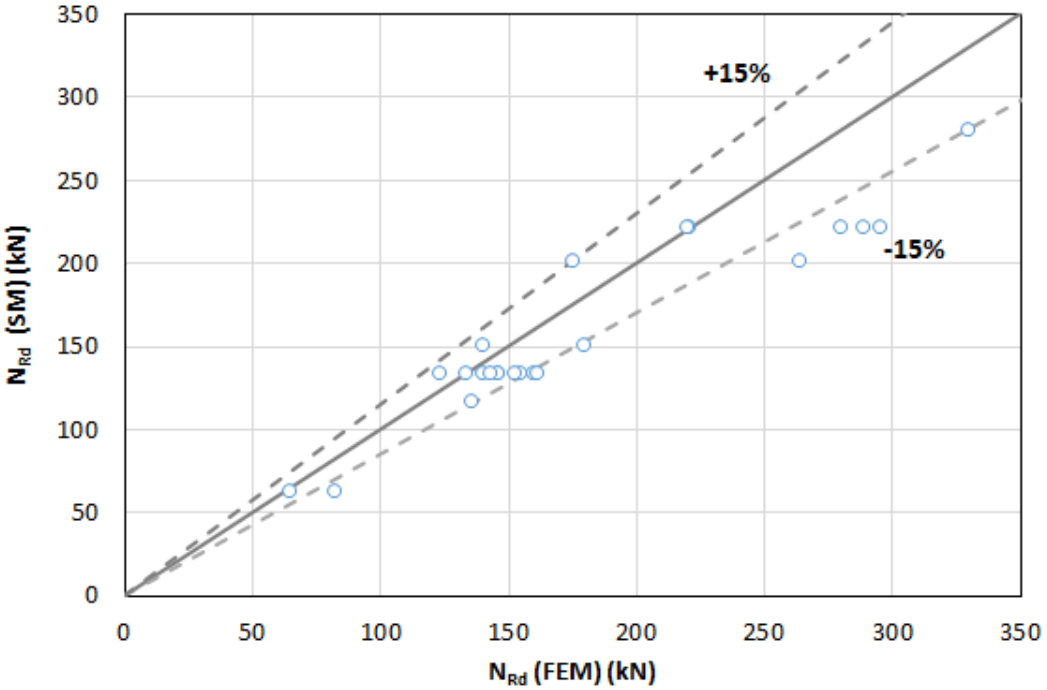

Figure 3.32: Comparison between the proposed simplified method (design equation) and numerical simulations for the third fusible link solution at normal temperature

Table 14 : Comparison between the proposed simplified method (design equation) and numerical simulations for the third fusible link solution at normal temperature

Case	$N_{Rd,fi\,(SM)}$	$N_{Rd,fi\,(FEM)}$	failure mode
M16_L175_UPN240_eL10_p180_DX400	134	123	rods buckling
M16_L175_UPN240_eL10_p180_DX200	134	155	rods buckling
M20_L175_UPN240_eL10_p180_DX200	221	221	rods buckling
M20_L175_UPN300_eL10_p180_DX200	221	289	rods buckling
M16_L175_UPN300_eL10_p180_DX200	134	160	rods buckling
M16_L100_UPN240_eL10_p180_DX200	151	180	rods buckling
M16_L240_UPN240_eL10_p180_DX200	117	136	rods buckling
M20_L240_UPN240_eL10_p180_DX200	202	175	rods buckling
M16_L175_UPN240_eL8_p180_DX200	134	153	rods buckling
M16_L175_UPN240_eL15_p180_DX200	134	161	rods buckling
M16_L100_UPN240_eL10_p180_DX400	151	140	rods buckling
M16_L175_UPN240_eL10_p1120_DX200	134	146	rods buckling
M16_L175_UPN240_eL10_p1120_DX200	134	133	rods buckling
M16_L175_UPN240_eL10_dy50_DX200	134	146	rods buckling
M16_L175_UPN240_eL10_p180_DX200	134	140	rods buckling
M12_L175_UPN240_el10_p180_DX200	63	82	rods buckling
M12_L175_UPN240_el10_p180_DX400	63	65	rods buckling
M16_L175_UPN300_eL10_p180_DX400	134	143	rods buckling
M20_L175_UPN300_eL10_p180_DX200	221	280	rods buckling
M20_L175_UPN300_eL10_p180_DX400	221	220	rods buckling
M20_L175_UPN300_eL12_p180_DX200	221	295	rods buckling
M22_L175_UPN300_eL10_p180_DX200	280	330	rods buckling
M20_L240_UPN300_eL12_p180_DX200	202	264	rods buckling

3.4.3 Second fusible link solution

The comparison of the numerical results obtained at elevated temperatures with those of the simplified design rules are shown in Figure 3.33 and Figure 3.34.

Figure 3.34. In these figures the x-axis corresponds to the value of the numerical fire resistance $N_{fi,Rd}$ (FEM), and the y-axis to the value of the fire resistance calculated using the simplified method, $N_{fi,Rd}$ (SM). The 45° regression line represents a perfect equality between these two values. While the regression line which is slightly above represents an error of +15% of the analytical resistance as compared to the numerical value (therefore unsafe), the regression line which is slightly below the bisectrix represents, on the other hand, an error of –15% of the analytical value as compared to the numerical resistance (unsafe).

The fire resistance values, as well as the failure mode, predicted by both the simplified method and the numerical model are reported and compared in Table 15 and Table 17.

All case studies reported in tables are referenced using a combination of letters: 'M' for the diameter of the steel rod, 'L' for the length of the rod, 'eU' for the thickness of the U-shaped profile, 'eZ' for the thickness of the Z-shaped profile, 'mx' for the distance between the rods and the web stiffener of the U-shaped profile, 'p' for the spacing between the centres of the rods in the direction of the web stiffener, and 'm' for the distance between the first rod row (closest to the web of the U-shaped profile) and the web of the U-shaped profile. Each letter is followed by the value of the corresponding parameter. The case name thus established is accompanied by the load level. The detailed dimensions of all case studies are given in deliverable D5.2 [12].

From these figures and table, it can be noted that:

- A noticeable discrepancy is observed between the simple calculation rules and the numerical models in determining the fire resistance. It appears that results are more dispersed than for the other two cases of fusible links. Some points are situated on the unsafe side, but a major part of them are situated on the safe side.

The design rules are more conservative when the temperatures are calculated analytically (see Figure 3.34)

- Figure 3.34) than when they are calculated numerically with the FE models (Figure 3.33). In this case, the design fire resistance predicted by the simplified method may be 45% lower than numerical failure.
- In most cases, the simplified rules correctly identify the weakest component of the fusible links that causes failure. According to the numerical results, this component is either the bottom flange of the U-shaped steel profile, bottom flange of the Z-shaped steel profile or the steel rods.

Taking all the calculation points from the parametric study results calculated using temperatures calculated with the proposed simple rules (see Figure 3.34), the average error is on the safe side, with a value of 0.78 and a standard deviation of 0.185. A maximum deviation of 13% (below 15%) is observed on the unsafe side, and 22% of cases lie on the unsafe side, which is a slightly higher than the 20% criterion. Moreover, the maximum deviation on the safe side is 50%. Therefore, all the horizontal fire group criteria are not met. However, since the criterion relating to the number of unsafe cases is exceeded by a small margin, the method's accuracy could be considered satisfactory. The proposed design method is in general conservative at elevated temperature when compared to the numerical results, with acceptable discrepancies when taking into account the complexity of the failure modes occurring for the studied links and the difficulty of predicting them in a simplified way due to the high flexibility of the Z-shaped steel profile and the lower flange of the U-shaped steel profile at elevated temperatures.

Some comparisons have also been made at room temperature (see Figure 3.35). The calculated design resistance and predicted failure mode are reported in Table 17. These are then compared to the corresponding numerical results. As with the results at elevated temperatures, it can be noted that the proposed design method generally plays it safe compared to the numerical results, with lower discrepancies.

Table 15 : Comparison between the proposed simplified method (design equation) and numerical simulations for the second fusible link solution at elevated temperature – comparison based on the FE temperatures

Case	Time (s)	$\theta_{FB,U}$ (°C)	$\theta_{R,1}$ (°C)	$\theta_{R,2}$ (°C)	$\theta_{FB,Z}$ (°C)	$N_{Rd,fi,r1}$	$N_{Rd,fi,r2}$	$N_{Rd,fi,U}$	$N_{Rd,fi\ (SM)}$	$N_{Rd,fi\ (FEM)}$	failure mode (FEM)	failure mode (SM)
70%-M16_L175_eU12_hU150_eZ8_mx23_p80_m65	750	584	319	498	429	96	152	92	92	78	Rods yielding	U bending
50%-M16_L175_eU12_hU150_eZ8_mx23_p80_m65	900	643	369	558	505	62	141	65	62	56	Rods yielding	rods yelding
30%-M16_L175_eU12_hU150_eZ8_mx23_p80_m65	1070	692	414	609	576	36	79	44	36	33.6	Rods yielding	rods yelding
70%-M16_L175_eU12_hU300_eZ12_mx23_p80_m65	683	563	265	498	354	96	158	103	96	85	Rods yielding	rods yelding
50%-M16_L175_eU12_hU300_eZ12_mx23_p80_m65	890	651	333	584	466	47	124	62	47	59	Rods yielding	rods yelding
70%-M16_L175_eU6_hU150_eZ12_mx29_p80_m65	450	518	206	439	214	119	85	71	71	65	U bending	U bending
50%-M16_L175_eU6_hU150_eZ12_mx29_p80_m65	640	635	287	560	334	61	78	38	38	46	U bending	U bending
70%-M12_L150_eU12_hU150_eZ12_mx29_p80_m65	850	634	340	570	447	30	79	69	30	45	Rods yielding	rods yelding
50%-M12_L150_eU12_hU150_eZ12_mx23_p80_m65	910	665	357	591	475	23	77	56	23	35	Rods yielding	rods yelding
30%-M12_L150_eU12_hU150_eZ12_mx23_p80_m65	1060	710	393	636	540	16	73	39	16	24	Rods yielding	rods yelding
70%-M16_L240_eU6_hU150_eZ12_mx29_p80_m65	400	460	120	357	192	144	52	38	38	56	U bending	U bending
50%-M16_L240_eU6_hU150_eZ12_mx29_p80_m65	682	626	214	517	371	86	47	40	40	40	U bending	U bending
30%-M16_L240_eU6_hU150_eZ12_mx29_p80_m65	1001	713	287	614	531	35	44	21	21	20	U bending	U bending
70%-M16_L175_eU6_hU150_eZ6_mx29_p80_m65	550	620	250	460	300	111	81	41	41	44	U bending	U bending
50%-M16_L175_eU6_hU150_eZ6_mx29_p80_m65	700	708	309	533	402	77	76	22	22	32	U bending	U bending
30%-M16_L175_eU6_hU150_eZ6_mx29_p80_m65	900	776	367	599	505	39	70	14	14	19	U bending	U bending
30%-M16_L175_eU6_hU150_eZ12_mx29_p80_m65	870	740	355	689	464	20	71	18	18	28	U bending	U bending
70%-M12_L240_eU12_hU150_eZ12_mx23_p80_m65	940	659	238	563	492	31.9	84.4	58.4	31.9	38.1	Rods yielding	rods yelding
50%-M12_L240_eU12_hU150_eZ12_mx23_p80_m65	1100	707	272	613	559	19.0	53.4	39.2	19.0	27.2	Rods yielding	rods yelding
30%-M12_L240_eU12_hU150_eZ12_mx23_p80_m65	1400	744	316	661	656	13.6	37.8	31.4	13.6	16.3	Rods yielding	rods yelding
30%-M16_L100_eU12_hU150_eZ8_mx23_p80_m65	1085	714	434	594	570	41.7	121.1	83.8	41.7	41.0	Rods yielding	rods yelding
70%-M16_L100_eU12_hU150_eZ8_mx23_p80_m65	680	605	332	468	375	107.9	149.4	81.0	81.0	95.6	Rods yielding	U bending
70%-M16_L175_eU8_hU150_eZ8_mx27_p80_m65	600	503	242	457	326	111.9	117.3	60.6	60.6	71.2	Rods yielding	U bending
50%-M16_L175_eU8_hU150_eZ8_mx27_p80_m65	750	597	302	537	421	74.0	76.2	37.7	37.7	50.9	U bending	U bending
30%-M16_L175_eU8_hU150_eZ8_mx27_p80_m65	1050	701	377	627	561	32.4	69.0	39.9	32.4	30.5	U bending	rods yelding
R30-M16_L175_eU8_hU150_eZ8_mx27_p80_m65	900	672	354	601	497	37.9	71.2	52.0	37.9	38.0	Rods yielding	rods yelding
70%-M16_L240_eU12_hU150_eZ12_mx23_p80_m65	837	664	241	568	500	56.3	74.9	56.1	56.1	76.3	Rods yielding	U bending
50%-M16_L240_eU12_hU150_eZ12_mx23_p80_m65	1000	711	276	617	566	34.5	44.1	38.4	34.5	54.5	Rods yielding	rods yelding
30%-M16_L240_eU12_hU150_eZ12_mx23_p80_m65	1315	750	320	664	665	24.7	41.7	30.2	24.7	32.7	Rods yielding	rods yelding
50%-M16_L175_eU12_hU150_eZ6_mx23_p80_m65	890	644	303	548	494	68	129	65	45	61	Z bending	Z bending
30%-M16_L175_eU12_hU150_eZ6_mx23_p80_m65	1050	698	346	604	564	37	78	42	33	36.6	Z bending	Z bending
R30-M16_L175_eU12_hU150_eZ6_mx23_p80_m65	900	666	320	571	499	55	100	55	45	62	Z bending	Z bending
70%-M12_L175_eU6_hU150_eZ12_mx29_p80_m65	570	591	260	513	287	47	26	22	22	36.9	U bending	U bending
50%-M12_L175_eU6_hU150_eZ12_mx29_p80_m65	800	677	337	607	429	20	23	13	13	18.9	U bending	U bending
30%-M12_L175_eU6_hU150_eZ12_mx29_p80_m65	900	702	362	635	478	17	22	22	17	15.3	U bending	rods yelding
70%-M20_L240_eU10_hU150_eZ10_mx25_p80_m65	700	564	207	465	384	170	122	72	72	98.7	Rods yielding	U bending
50%-M20_L240_eU10_hU150_eZ10_mx25_p80_m65	850	629	249	597	464	62	117	109	62	70.5	Rods yielding	rods yelding
30%-M20_L240_eU10_hU150_eZ10_mx25_p80_m65	1080	698	302	653	565	42	109	64	42	42.3	Rods yielding	rods yelding
30%-M16_L175_eU10_hU150_eZ10_mx25_p80_m65	1000	678	285	636	533	31	84	77	31	34.2	Rods yielding	rods yelding
50%-M16_L175_eU10_hU150_eZ10_mx25_p80_m65	845	627	248	596	462	40	88	50	40	57	Rods yielding	rods yelding
70%-M16_L175_eU10_hU150_eZ10_mx25_p80_m65	663	544	195	529	360	79	162	79	79	79.8	Rods yielding	rods yelding
30%-M16_L175_eU14_hU150_eZ14_mx21_p80_m65	1300	726	391	639	625	30	86	48	30	38.1	Rods yielding	rods yelding
30%-M16_L175_eU14_hU150_eZ14_mx21_p80_m65	1030	670	338	575	529	52	148	73	52	63.5	Rods yielding	rods yelding
30%-M16_L175_eU14_hU150_eZ14_mx21_p80_m65	900	627	306	533	471	77	155	98	77	88.9	Rods yielding	rods yelding

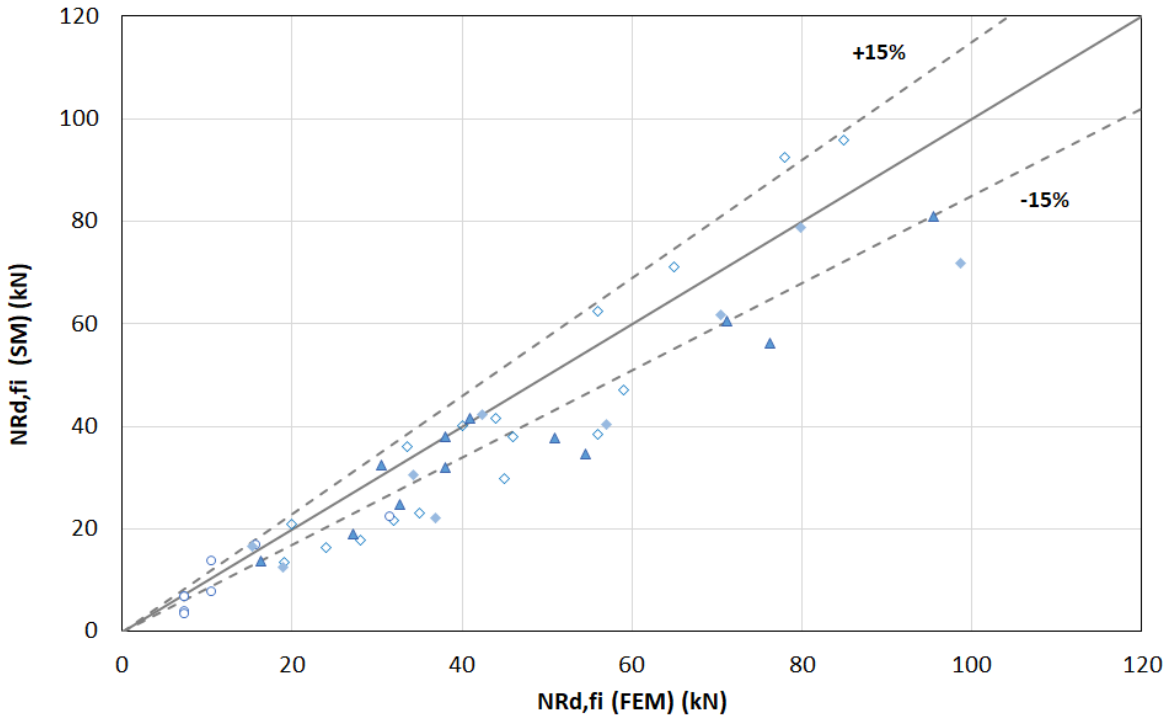

Figure 3.33: Comparison between the proposed simplified method (design equation) and numerical simulations for the second fusible link solution at elevated temperature – comparison based on the FE temperatures

Table 16 : Comparison between the proposed simplified method (design equation) and numerical simulations for the second fusible link solution at elevated temperature – comparison based on the analytical temperatures

case	Time (s)	$\theta_{FB,U}$ (°C)	$\theta_{R,1}$ (°C)	$\theta_{R,2}$ (°C)	$\theta_{FB,Z}$ (°C)	$N_{Rd,fi,r1}$	$N_{Rd,fi,r2}$	$N_{Rd,fi,U}$	$N_{Rd,fi\ (SM)}$	$N_{Rd,fi\ (FEM)}$	failure mode (FEM)	failure mode (SM)
70%-M16_L175_eU12_hU150_eZ8_mx23_p80_m65	750	616	308	555	437	63.8	154.3	76.1	63.8	78.0	Rods yielding	rods yielding
50%-M16_L175_eU12_hU150_eZ8_mx23_p80_m65	900	673	336	606	517	38.5	96.7	54.4	38.5	56.0	Rods yielding	rods yielding
30%-M16_L175_eU12_hU150_eZ8_mx23_p80_m65	1070	715	357	643	591	30.4	73.8	39.2	30.4	33.6	Rods yielding	rods yielding
70%-M16_L175_eU12_hU300_eZ12_mx23_p80_m65	683	584	292	525	370	84.1	163.4	96.1	84.1	85.0	Rods yielding	rods yielding
50%-M16_L175_eU12_hU300_eZ12_mx23_p80_m65	890	670	335	603	483	39.1	101.0	55.9	39.1	59.0	Rods yielding	rods yielding
70%-M16_L175_eU6_hU150_eZ12_mx29_p80_m65	450	551	275	496	261	99.2	80.6	61.0	61.0	65.0	U bending	U bending
50%-M16_L175_eU6_hU150_eZ12_mx29_p80_m65	640	647	324	583	386	49.3	75.9	35.0	35.0	46.0	U bending	U bending
70%-M12_L150_eU12_hU150_eZ12_mx29_p80_m65	850	656	350	591	462	24.3	81.3	61.8	24.3	45.0	Rods yielding	rods yielding
50%-M12_L150_eU12_hU150_eZ12_mx23_p80_m65	910	676	360	608	493	20.4	80.0	53.1	20.4	35.0	Rods yielding	rods yielding
30%-M12_L150_eU12_hU150_eZ12_mx23_p80_m65	1060	713	380	641	560	16.5	76.6	39.6	16.5	24.0	Rods yielding	rods yielding
70%-M16_L240_eU6_hU150_eZ12_mx29_p80_m65	400	375	158	338	228	151.7	51.7	45.4	45.4	56.0	U bending	U bending
50%-M16_L240_eU6_hU150_eZ12_mx29_p80_m65	682	583	245	525	412	83.0	46.9	23.7	23.7	40.0	U bending	U bending
30%-M16_L240_eU6_hU150_eZ12_mx29_p80_m65	1001	700	294	630	578	32.6	44.2	22.5	22.5	20.0	U bending	U bending
70%-M16_L175_eU6_hU150_eZ6_mx29_p80_m65	550	609	305	548	349	69.2	77.7	43.9	43.9	44.0	U bending	U bending
50%-M16_L175_eU6_hU150_eZ6_mx29_p80_m65	700	667	334	600	447	38.9	74.9	30.3	30.3	32.0	U bending	U bending
30%-M16_L175_eU6_hU150_eZ6_mx29_p80_m65	900	714	357	643	556	30.0	72.6	20.9	20.9	19.0	U bending	U bending
30%-M16_L175_eU6_hU150_eZ12_mx29_p80_m65	870	663	332	597	518	40.8	75.1	31.2	31.2	28.0	U bending	U bending
70%-M12_L240_eU12_hU150_eZ12_mx23_p80_m65	940	685	288	616	507	19.4	74.5	49.3	19.4	38.1	Rods yielding	rods yielding
50%-M12_L240_eU12_hU150_eZ12_mx23_p80_m65	1100	720	302	648	577	15.8	49.9	38.1	15.8	27.2	Rods yielding	rods yielding
30%-M12_L240_eU12_hU150_eZ12_mx23_p80_m65	1400	752	316	677	675	12.4	36.0	31.0	12.4	16.3	Rods yielding	rods yielding
30%-M16_L100_eU12_hU150_eZ8_mx23_p80_m65	1085	717	430	646	597	29.8	127.5	82.1	29.8	41.0	Rods yielding	rods yielding
70%-M16_L100_eU12_hU150_eZ8_mx23_p80_m65	680	582	349	524	396	85.0	151.6	97.0	85.0	95.6	Rods yielding	rods yielding
70%-M16_L175_eU8_hU150_eZ8_mx27_p80_m65	600	511	255	460	349	114.3	113.9	60.5	60.5	71.2	Rods yielding	U bending
50%-M16_L175_eU8_hU150_eZ8_mx27_p80_m65	750	586	293	527	437	82.2	79.3	41.7	41.7	50.9	U bending	U bending
30%-M16_L175_eU8_hU150_eZ8_mx27_p80_m65	1050	711	355	640	584	30.7	73.2	37.9	30.7	30.5	U bending	rods yielding
R30-M16_L175_eU8_hU150_eZ8_mx27_p80_m65	900	673	336	606	517	38.0	75.0	51.5	38.0	38.0	Rods yielding	rods yielding
70%-M16_L240_eU12_hU150_eZ12_mx23_p80_m65	837	652	274	587	456	47.7	90.6	63.9	47.7	76.3	Rods yielding	rods yielding
50%-M16_L240_eU12_hU150_eZ12_mx23_p80_m65	1000	700	294	630	535	33.2	44.9	42.5	33.2	54.5	Rods yielding	rods yielding
30%-M16_L240_eU12_hU150_eZ12_mx23_p80_m65	1315	740	311	666	651	25.4	44.0	33.6	25.4	32.7	Rods yielding	rods yielding
50%-M16_L175_eU12_hU150_eZ6_mx23_p80_m65	890	670	335	603	527	37.5	97.0	53.6	37.5	61.0	Z bending	rods yielding
30%-M16_L175_eU12_hU150_eZ6_mx23_p80_m65	1050	711	355	640	598	29.8	71.0	38.4	27.3	36.6	Z bending	Z bending
R30-M16_L175_eU12_hU150_eZ6_mx23_p80_m65	900	673	336	606	532	36.9	92.8	52.3	36.9	62.0	Z bending	rods yielding
70%-M12_L175_eU6_hU150_eZ12_mx29_p80_m65	570	619	309	557	313	33.7	22.2	18.8	18.8	36.9	U bending	U bending
50%-M12_L175_eU6_hU150_eZ12_mx29_p80_m65	800	694	347	624	434	17.8	21.2	10.9	10.9	18.9	U bending	U bending
30%-M12_L175_eU6_hU150_eZ12_mx29_p80_m65	900	714	357	643	484	15.7	20.9	9.4	9.4	15.3	U bending	U bending
70%-M20_L240_eU10_hU150_eZ10_mx25_p80_m65	700	620	260	558	380	97.1	106.1	52.0	52.0	98.7	Rods yielding	U bending
50%-M20_L240_eU10_hU150_eZ10_mx25_p80_m65	850	676	284	608	462	56.9	103.2	78.7	56.9	70.5	Rods yielding	rods yielding
30%-M20_L240_eU10_hU150_eZ10_mx25_p80_m65	1080	725	305	653	569	42.4	100.5	54.5	42.4	42.3	Rods yielding	rods yielding
30%-M16_L175_eU10_hU150_eZ10_mx25_p80_m65	1000	712	356	641	535	29.6	71.0	58.7	29.6	34.2	Rods yielding	rods yielding
50%-M16_L175_eU10_hU150_eZ10_mx25_p80_m65	845	674	337	607	460	36.7	72.8	36.0	36.0	57.0	Rods yielding	U bending
70%-M16_L175_eU10_hU150_eZ10_mx25_p80_m65	663	602	301	542	359	71.2	104.0	57.1	57.1	79.8	Rods yielding	U bending
30%-M16_L175_eU14_hU150_eZ14_mx21_p80_m65	1300	666	333	599	550	38.6	149.1	75.3	38.6	38.1	Rods yielding	rods yielding
50%-M16_L175_eU14_hU150_eZ14_mx21_p80_m65	1030	571	285	514	444	87.5	157.2	135.3	87.5	63.5	Rods yielding	rods yielding
70%-M16_L175_eU14_hU150_eZ14_mx21_p80_m65	900	512	256	461	386	110.7	158.9	179.4	110.7	88.9	Rods yielding	rods yielding

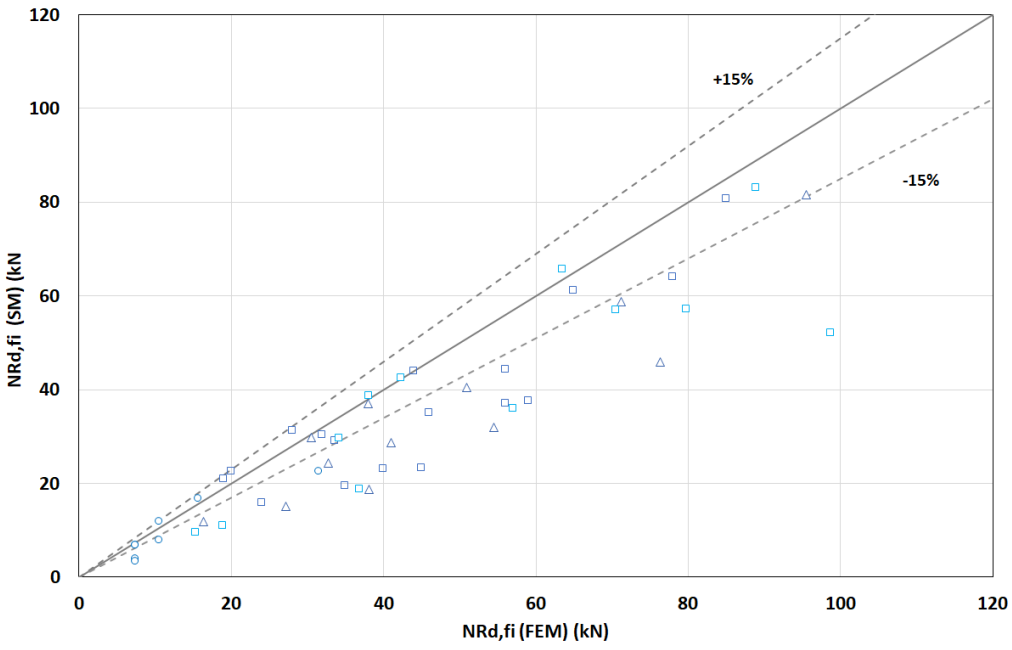

Figure 3.34: Comparison between the proposed simplified method (design equation) and numerical simulations for the second fusible link solution at elevated temperature - comparison based on analytical temperatures

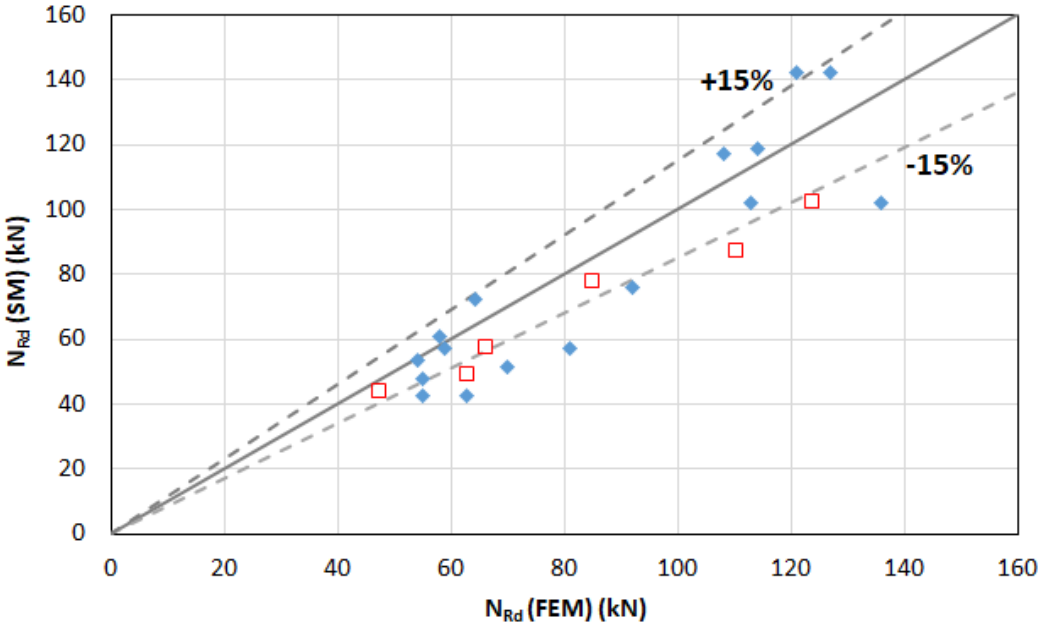

Figure 3.35: Comparison between the proposed simplified method (design equation) and numerical simulations for the second fusible link solution at normal temperature

Table 17 : Comparison between the proposed simplified method (design equation) and numerical simulations for the second fusible link solution at normal temperature

Case	$N_{Rd,fi\ (SM)}$	$N_{Rd,fi\ (FEM)}$	failure mode (FEM)	failure mode (SM)
M16_L175_eU12_hU150_eZ8_mx23_p80_m65	102	113	Z bending	Z bending
M12_L175_eU6_hU150_eZ12_mx29_p80_m65	48	55	Rods bucklings	U bending
M16_L175_eU12_hU300_eZ12_mx23_p80_m65	142	121	Rods bucklings	rods buckling
M16_L175_eU6_hU150_eZ12_mx29_p80_m65	51	70	U bending	U bending
M12_L150_eU12_hU150_eZ12_mx23_p80_m65	72	64	Rods bucklings	rods buckling
M12_L175_eU12_hU150_eZ12_mx23_60_m65	61	58	Rods bucklings	rods buckling
M16_L240_eU6_hU150_eZ12_mx29_p80_m65	43	55	Rods bucklings	U bending
M16_L175_eU10_hU150_eZ10_mx25_p80_m65	119	114	Rods bucklings	U bending
M16_L175_eU14_hU150_eZ14_mx21_p80_m65	142	127	Rods bucklings	rods buckling
M16_L175_eU6_hU150_eZ6_mx29_p80_m65	43	63	U bending	U bending
M12_L175_eU12_hU150_eZ6_mx23_p80_m65	57	59	U bending	Z bending
M12_L240_eU12_hU150_eZ12_mx23_p80_m65	53	54	Rods bucklings	rods buckling
M16_L100_eU12_hU150_eZ8_mx23_p80_m65	102	136	Z bending	Z bending
M16_L175_eU8_hU150_eZ8_mx27_p80_m65	76	92	Rods bucklings	U bending
M16_L175_eU12_hU150_eZ6_mx23_p80_m65	57	81	Z bending	Z bending
M16_L240_eU12_hU150_eZ12_mx23_p80_m65	117	108	Rods bucklings	rods buckling
M16_L175_eU12_hU150_eZ6_m30_e170	57	66	Z bending	Z bending
M16_L175_eU12_hU150_eZ6_m40_e150	49	63	Z bending	Z bending
M16_L175_eU12_hU150_eZ6_m50_e150	44	48	Z bending	Z bending
M16_L175_eU12_hU150_eZ8_m30_e170	102	124	Z bending	Z bending
M16_L175_eU12_hU150_eZ8_m40_e150	87	111	Z bending	Z bending
M16_L175_eU12_hU150_eZ8_m50_e150	78	85	Z bending	Z bending
M16_L175_eU12_hU150_eZ12_m50_e150	175	153	Z bending	Z bending
M16_L175_eU12_hU150_eZ12_m30_e170	229	215	Z bending	Z bending

3.4.3.1 Conclusion

The results of the comparison between the FE models and the simplified design method show that the proposed calculation rules are safe overall, although the level of safety varies according to the fusible link solution considered. The simplified design rules may appear overly cautious and therefore uneconomical. However, the uneconomical aspect is limited at building level since it only concerns a few connections, and underestimating the fire resistance of fusible links leads to slightly oversized link components, for example by increasing the rod diameter or profile thickness.

In conclusion, the proposed simple calculation rules are suitable for predicting the fire design resistance in compression of the studied fusible links with an acceptable level of safety.

In fact, the simple design method leads to safety level that is quite different from one dimension of section to another or from one fire duration to another.

3.5 Design in normal condition of use

Fusible links must be designed to withstand all forces associated with normal use. These Links can therefore transmit tensile and compressive forces.

These forces are particularly linked to the wind loads applied to the fire walls. There are two situations to consider:

- In cases where both buildings on either side of the wall are present, an internal wind load linked to the pressure difference between the two buildings must be considered.
- If only one of the two buildings is present (e.g. during the temporary construction phase), the wind force defined in EN 1991-1-4 §5.3 must be considered.

The design forces to be considered are usually derived from a global analysis performed to verify the stability and strength of a steel structure. These are then compared to the design resistance of the fusible links. As previously mentioned, the design resistance of the fusible links can be determined from the resistance of their components, by selecting the lowest value. The resistances to be calculated according to the chosen solution are listed in Table 18.

Table 18: Required resistance checks for fusible links

Resistance check	Steel component/part
Resistance of profile flange to transverse bending According to EN 1993-1-8 §6.2.6.5 à 6.2.6.7 and §6.3.2 According to §3.1.3.1 of this report but at normal temperature	Z-shaped steel profile U shaped steel profile L shaped steel profile Steel column of portal frame Secondary steel column supporting the wall
Resistance of unbolted profile flange to transverse bending According to EN 1993-1-1 §6.2.5 (bending) and 6.2.6 (shear) According to §3.1.3.2 of this report but at normal temperature	Z-shaped steel profile
Resistance of web profile to tension/compression according to 1993-1-1 §6.2.3 et §6.2.4	Z-shaped steel profile U shaped steel profile
Resistance of stiffener to traction According to EN 1993-1-1 § 6.2.3	U shaped steel profile
Resistance of stiffener to compression according to EN 1993-1-5 §9	U shaped steel profile

According to §3.1.3.5 of this report but at normal temperature	
Resistance of weld according to EN 1993-1-8 §4	All welds
Shear resistance of aluminium bolts according to En 1999-1-1 §8 and table 8.5	Aluminium bolts
Resistance in tension of fasteners according to 1993-1-8, table 3.4	Steel roods
Resistance in compression of fasteners According to 1993-1-1 §6.3.1 According to §3.1.3.3 of this report but at normal temperature	Steel roods
Resistance in shear of fasteners according to 1993-1-8, table 3.4	Steel bolts

3.6 Seismic Design

The developed fusible links must break adequately in the event of a fire. However, they are not considered dissipative elements in the event of an earthquake, as their resistance is mainly provided by the aluminium bolts, and they then fail in a brittle manner. Therefore, the fusible link system must be designed so that its components do not fail in a seismic situation. The seismic design should use the same rules as those for normal use conditions, as well as the rules set out in EN 1998, and consider relevant design loads.

Parametric analyses performed as part of the FISHWALL project [24] showed that the investigated fusible link systems experience low forces because they are not designed to resist lateral loads, and they have low stiffness compared to the main lateral-resisting systems of steel buildings, such as portal frames and vertical bracing systems. If the two buildings separated by the fire wall are symmetrical, the forces acting on the fusible links will be low because the buildings will have very similar dynamic properties. The fusible links are only subject to measurable forces in the event of significant differential displacement. As outlined in Deliverable 4.3 [24], which details the derivation of fragility functions, the capacity of the fusible link system can only be exceeded at high levels of seismic intensity.

It is very difficult, if not impossible, to develop simple rules for calculating the design forces required for the seismic design of fusible links, as is the case for fire design. Consequently, design loads for the link design can be determined using a global structural model representative of the single storey building in question, by performing a linear dynamic analysis with response spectrum. This method is the most common one used in design practice.

The experimental campaign conducted as part of the FISHWALL project showed that the most appropriate link configurations for seismic regions characterised by peak ground accelerations up to 0.12g are those made from U-shaped steel profiles (i.e. solutions one and three). These solutions can be used for fire walls that are either perpendicular or parallel to the portal frames. Furthermore, the constructional system that links the steel profiles of the fusible links to the steel columns that support the fire wall consists of steel rods that pass through the sandwich panels. Due to the low stiffness of the sandwich panels (which are made of rockwool and two thin steel sheets), the steel rods essentially decouple the fusible link system from the sandwich panel. Interaction between the two is expected to be limited at both low and moderate seismic levels, with possible bearing of the thin steel sheets. For this reason, the sandwich panel can be considered as mass only in the global structural model.

Modelling the steel structure of a single-storey building is not really a problem, following current practice. However, the following provisions are recommended when it comes to modelling the fusible links:

- The fusible links are modelled from elastic beam finite elements characterized by their initial elastic stiffness estimated from the laboratory tests [23]. In order to be conservative and to generalise when different elements are employed, the larger initial stiffness obtained in the tests between the positive and negative loading direction is recommended.

Table 2: Recommended initial elastic stiffness of the fusible link system

Detail	Initial stiffness (kN/mm)
First fusible link solution with M12	20
second fusible link solution with M16	117
Third fusible link solution with M16	31
Third fusible link solution with M12	21

- The steel columns that support the sandwich panels (which are connected to the fusible link systems via steel rods) are modelled using elastic beam elements.
- The sandwich panel wall is modelled using a mass element, with half of its mass concentrated at the top of the supporting columns.
- Depending on the design of the bracing system, the model can include diagonals in both tension and compression. Otherwise, only the diagonal in tension is considered and two different models must be developed to accurately represent the seismic structural behaviour in the two directions in which earthquakes occur.

4 DESIGN GUIDANCE FOR THE STEEL COLUMNS SUPPORTING THE FIRE WALLS

4.1 Design in normal condition

The resistance of the steel columns supporting the panels can be easily checked using the simplified design methods of EN 1993-1-1 [3]. The steel columns should have sufficient mechanical resistance to the design loads (calculated from the load combinations defined in EN 1990 [1]) resulting from the action of the self-weight (column itself, panels wall and encasement system) and wind. The design wind loads to be considered are the same as those considered for the panels design.

4.2 Fire design

For fire walls solidly fixed to the steel structure, there is no need to specifically check the fire resistance of steel columns supporting the fire wall encased with sandwich panels for the following reasons:

- On the one hand, the heating of the columns does not exceed 500°C if they are adequately clad with sandwich panels.
- On the other hand, steel columns remain stable if their temperature rise does not exceed 500°C (EN 1993-1-2 [4]) and if they are designed in accordance with EN1993-1-1 [3].

Indeed, the experimental results obtained from the Fishwall tests, which were performed on the fire wall incorporating large-span sandwich panels and an encased column [18], as well as on the sliding fire door system [22], showed that the temperature of the encased steel members did not exceed 500°C after two hours of standard fire exposure (the targeted fire resistance rating).

For fire walls associated with fusible links, the upper part of the columns supporting the fire wall is exposed to fire (see Figure 5.8). The fire resistance of the upper part of the columns can be assessed by considering a built-in column of a length corresponding to the column height directly exposed to the fire, design loads calculated using the relevant load combination in fire situation, considering the weight of the panels and the effects of the wind, with a column temperature of 900°C.

In addition, for both wall configurations, the columns must be designed so that the fire wall can withstand wind load, as the structure could collapse if exposed to fire. Considering that work will soon be undertaken after a disaster, the column resistance check can be carried at normal temperature out by considering the combinations of actions corresponding to the serviceability limit states. The Wind loads should be determined according to EN 1991-1-4 [6] and corresponding national annexes.

4.3 Seismic design

The supporting steel columns can be easily designed according to the relevant parts of EN 1993 and EN 1998 based on the forces obtained from numerical simulations. In particular, the supporting columns are included in the global linear dynamic analysis.

5 CONSTRUCTIONAL DETAILS AND PRACTICAL RECOMMENDATIONS

In addition to design rules, some specific construction provisions have to be satisfied to ensure the building and firewalls behave 'correctly' in fire or earthquake situations. In the event of fire, these provisions aim to prevent the building not only from collapsing outwards but also from progressive collapse. They are also aimed to avoid any damage of the fire wall due to the collapse of steel structure directly exposed to fire.

As already mentioned, two different implementations of the investigated partition fire wall solution are possible in the building. The first solution involves installing the wall between two independent steel structures and connecting it to them with fusible links. In the event of a fire, these links will enable the wall to disconnect from the structure exposed to the fire while remaining attached to unexposed steel structure. The alternative solution is to insert the fire wall directly into the steel structure of the single-storey building. Additionally, the wall can be perpendicular or parallel to main steel frames, and the fire wall can be inserted into or moved from a row of columns in the structure.

Whatever the fire wall solution used, adequate measures shall be implemented to avoid any unsafe damage of the wall because of the fire-induced movements of the steel structure exposed to fire. These measures mainly concern the fire protection of the steel structure close to fire wall, the roof system above fire wall and the bracing system.

The following sections summarise the necessary provisions. The design guide produced as part of the FISHWALL project provides more details, illustrated with drawings.

5.1 Fire protection of steel members close to fire walls

The partition fire wall can be solidly attached to the supporting steel structure of buildings, which remains continuous at the position of the wall. The requirement for there to be no fire propagation between different compartments and no progressive collapse (i.e. the fire wall must maintain its integrity and the cold parts of the structure must remain stable) means that the columns supporting the fire wall must have the same fire resistance rating as the wall itself. Additionally, the positioning of the fire wall throughout buildings means that roof structural members, such as purlins and beams, pass through the top of the wall. Consequently, any structural members that penetrate the wall must also be partially fire-protected. This protection must allow fire-induced plastic hinges to form away from the walls, thus preventing any damage of the walls due to the collapse of heated steel members.

All relevant structural members can be protected using standard fire protection systems, such as spray, boards or intumescent coatings. Alternatively, the purlins can be protected using an encasement system made from the same sandwich panels used for the walls. It should be noted that the steel portal frame beam could also be fire protected using an encasement system. However, due to the penetration of the purlins, this system could be difficult to install in practice. Several solutions can be used for the encasement system and its attachment to the steel profiles, provided they have been properly validated for the fire situation. In the case of encasement, openings at the encasement ends must be filled with mineral wool to a depth of at least 100 mm (as illustrated in Figure 5.1). In addition, it is recommended that any cavity between the panels and the steel deck should be filled with mineral wool, if the panels are not cut to size. Although the predicted and experimental displacements observed through numerical analyses [12] and fire testing [20] are more limited at wall level, it is recommended that the wall opening at purlin level is 100 mm larger than the purlin's cross-sectional dimensions. This should allow deformation of the purlins in and out of their plane to be absorbed without damaging the wall. It will also facilitate the purlin's passage through the wall and subsequent mineral wool filling of the hole. As with the fire test [20], a mineral wool strip should be placed between the wall and the encasement system. A strip at least 50 mm thick is recommended. Then, cover flashings enclosing the mineral wool strip should be fixed only to the wall panels.

Regarding the structural members crossing the fire wall, they may need to be protected on one or both sides, depending on how the wall is implemented. Fire protection should be applied to each steel beam crossing the fire wall. Where a fire wall is inserted into a column row, the protection should extend at least 500 mm beyond the wall boundary and may only be applied to the side of the wall. Conversely, if the fire wall is moved away from the column rows, fire protection should be applied to both sides of the wall, extending at least 500 mm beyond the wall boundary. It should be noted that this wall configuration requires support columns to be installed under the beams to keep

them stable. Purlins will cross the fire wall, which is implemented parallel to the steel portal frames. They must be protected on both sides of the wall. On the wall side, the purlins must be protected for a minimum distance of 500 mm beyond the wall. On the other side, the purlins has to be fully protected along the width of the portal beam.

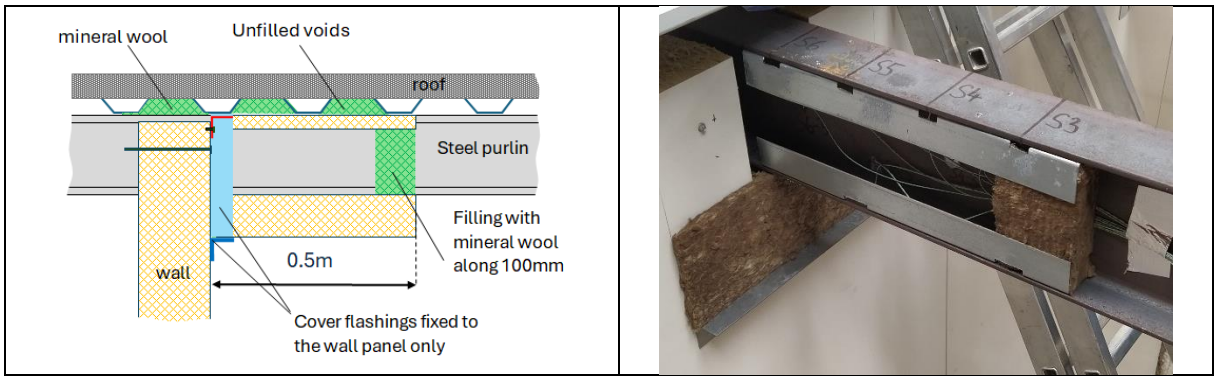

Figure 5.1: Encasement of steel purlins

For the protection of structural members, it is necessary to use products or systems which can be applied to steel structures, and which have a characterisation report (for 3 and 4 sides protection) drawn up by an approved fire resistance laboratory. The thickness of the protection to be applied to the columns can be calculated based on exposure to fire on four sides, a critical temperature of 500°C and the same degree of fire resistance as that required for the partition. Fire protection should be provided over the full height of columns.

For partially protected beams and purlins, the thickness of the fire protection material can be calculated by assuming a steel section exposed on four sides, a standard fire exposure of one hour and a critical temperature of 500°C. The required fire resistance rating can be lower than that of the wall, since the purpose of this protection is to move the fire-induced plastic hinges away from the wall.

The Figure 5.2 and Figure 5.3 illustrate some of the protection measures for structural members mentioned previously.

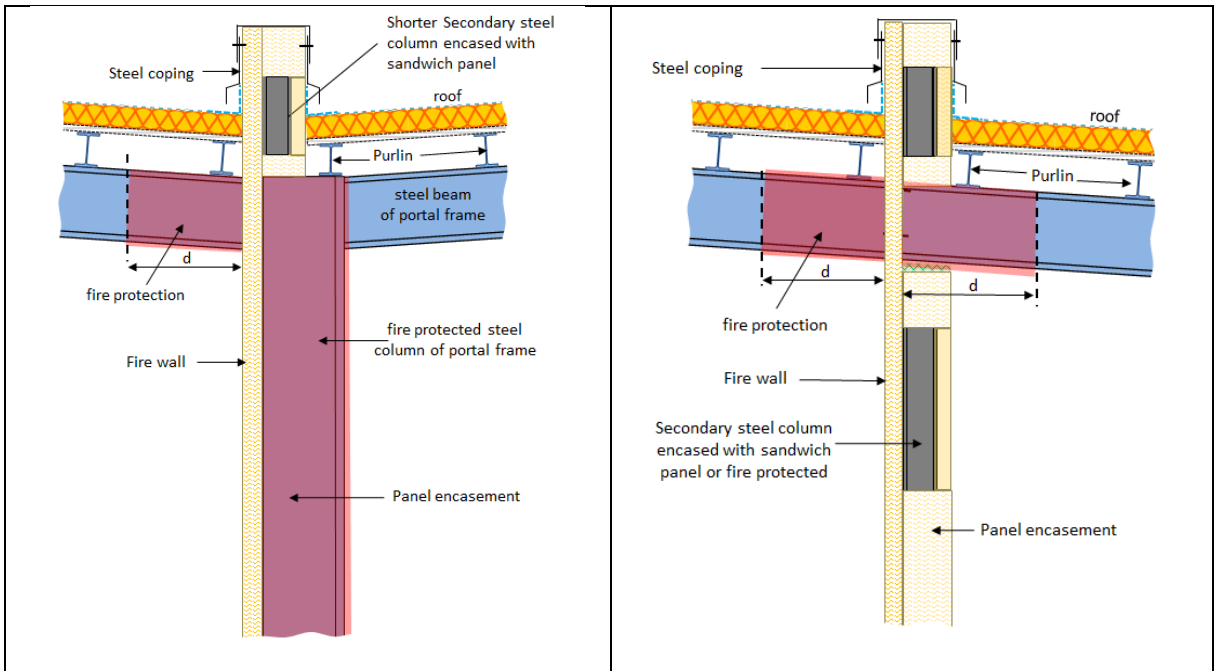

a) Beam crossing the wall – Wall inserted into a row of columns

b) Beam crossing the wall – wall inserted moved from a row of columns

Figure 5.2: Example of protection measures for structural members -

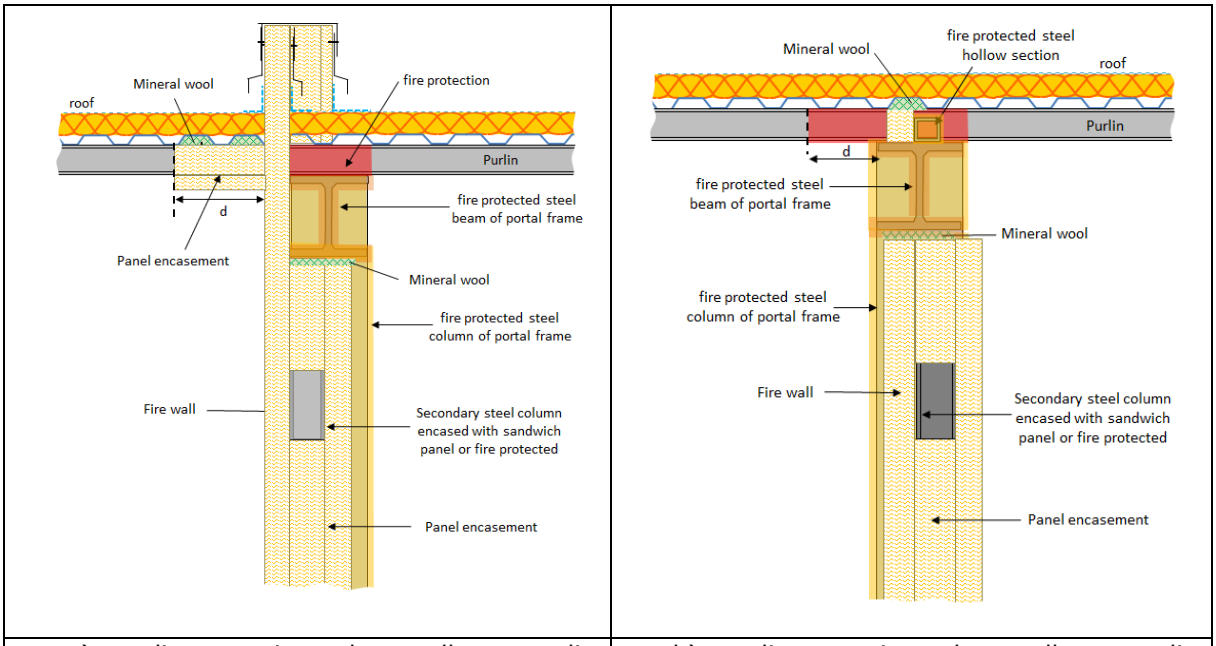

a) purlin crossing the wall – purlin protection with an encasement system

b) purlin crossing the wall – purlin protection with standard products

Figure 5.3: Example of protection measures for structural members

It should be noted that the proposed protection measures are based on the provisions set out in the design guides ([13], [15], [16]), which were developed using the results of earlier RFSC research projects. Some of the partners involved in the FISHWALL project were involved in these projects. It should also be noted that the effectiveness of the partial protection measure for structural members passing through walls has been demonstrated experimentally (see Figure 5.4 and Figure 5.5). This has been shown not only as part of the Fishwall project, which involved encasing purlins in sandwich panels [20] [14], but also in a large-scale fire test on a single-storey steel-framed building with partially fire-protected portal beams, as part of a national French research project. The test results showed that the tested protection systems around the steel members crossing the wall prevented damage to the wall; despite the collapse of the steel members exposed to fire.

a) View during the test

b) View after the test

Figure 5.4: Fire test on a fire wall crossed by steel purlins – Flumilog project

a) Test specimen before the test

b) Test specimen after the test

Figure 5.5: Fire test on a fire wall crossed by steel purlins – Fishwall project

No special protective measures are required for fire walls associated with fusible links, except for the columns supporting them. In the studied solution, this protection is provided by a sandwich panel encasement. Numerous tests carried out as part of the Fishwall project ([18], [21], [22]) have demonstrated the effectiveness of the system. The Figure 5.6shows photos of a test carried out on a partition fire wall made of large-span sandwich panels, in which a column was encased.

a) Test specimen before the test

b) Test specimen after the test

Figure 5.6: Fire test on a fire wall made with large-span sandwich panels – Fishwall project

5.2 Fire walls

The walls installation should comply with the relevant standards, technical documents, manufacturers' recommendations and fire resistance certificates.

Whatever the wall solution — whether solidly attached to the building structure or associated with fusible links — the wall must extend up to the underside of the roof. Appropriate detailing is required at the top of the wall, such as a strip of mineral wool, intumescent joints and fire-resistant sealant, to ensure its fire integrity. If the panels are not cut to size, any gaps formed between the ends of the panels and the steel decking must be filled properly with mineral wool, covering the full thickness of the panels. It is recommended that mineral wool of the same density as that used in the walls is used for this purpose. It is also recommended that the mineral wool is glued to the internal sides of the decking waves.

In addition, when securely attached to the building's structure, the fire wall can be positioned either under a portal frame beam or slightly offset to ensure continuity of the partition wall throughout its height. Whatever solution is chosen, a steel support profile must be fixed above the beam to hold the top of the wall. This support profile must be fire-protected. As it may be difficult to use an encasement system made of sandwich panels, the steel profile can be fire-protected using a standard system. The wall can be extended above the roof up to the height required by national fire safety regulations, if applicable. In this case, shorter secondary steel columns should be used to extend the portal frame columns and support the upper part of the fire wall.

If the fire wall is moved away from the column rows, a steel beam connected to all the steel columns that support the fire wall must be used. It must be fire protected and it is used to hold the purlins in place if a part of the structure fails in case of fire on one side of the fire wall. The beam should also be adequately linked to the steel purlin to stabilise the wall out of its plane. In addition, a bracing system must be installed between two consecutive steel columns to ensure the stability of the fire wall in its plane. This bracing system needs also to be fire protected. so, it is recommended that it is included in the encasement system used to fire protect the steel columns.

Regarding the firewalls associated with fusible links, an additional beam (e.g. a steel channel or hollow steel section) spanning between the secondary steel columns supporting the wall is required to support the roof and avoid any damage to the top of the wall if one of the two steel structures collapses in the event of a fire. This longitudinal beam can be fixed to the top of the columns and left unprotected.

For fire walls that are solidly fixed to the building structure, it should be noted that appropriate details must be provided at the top of the fire wall to not restrain the thermal elongation of the wall and allow the wall to absorb the vertical deflections of the steel portal frame in the event of fire. The same provisions should be made at the junction between the secondary steel columns supporting the wall and the beams to prevent the thermal expansion of these columns from being restrained when they are exposed to fire. This is usually achieved by using steel flashings with slotted holes of different widths and gap filled with mineral wool at wall end to accommodate the required expansion (as illustrated in Figure 5.7). As constructional provisions may differ between panel manufacturers and it is difficult to compile an exhaustive list (as some details are confidential), the design guide produced as part of the project only provide general recommendations. This leaves the door open to all constructional details, provided their effectiveness in a fire situation has been validated.

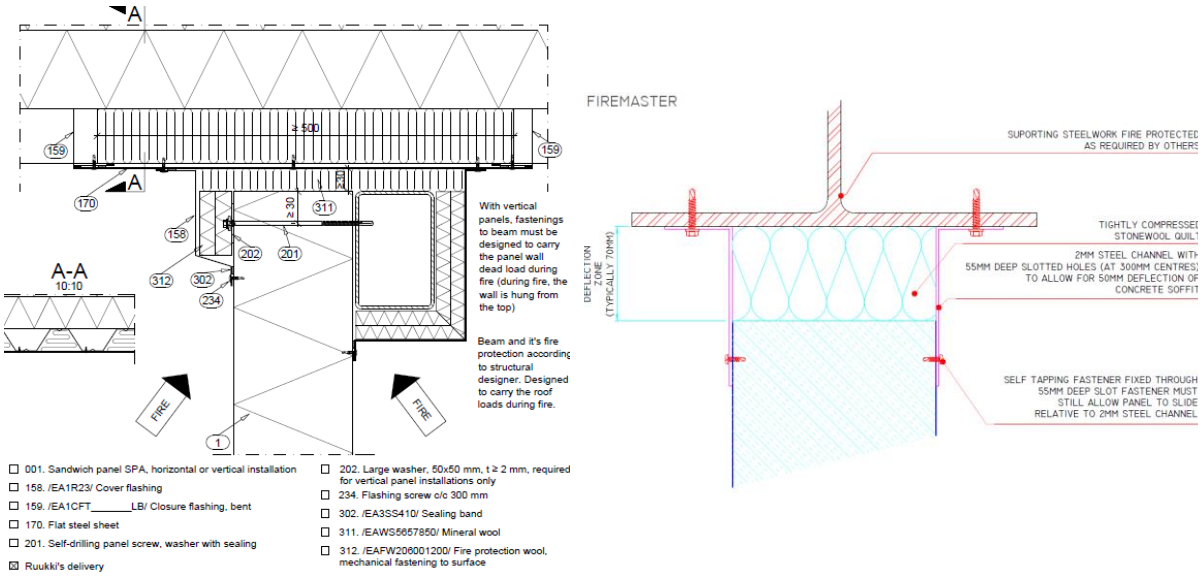

Figure 5.7: Detailing example at the wall/steel beam junction ([25], [26])

All wall openings managed at the level of structural members and steel rods must be filled with mineral wool. Mineral wool of the same density as that used in the walls is recommended.

In practice, the integrity of walls can be compromised by the passage of elements such as ducts, pipes, cables, cable trays, etc. that need to circulate within buildings. Wherever possible, these should be avoided. However, where this is not possible, special provisions must be made in the selection and installation of cable trays, ducts and other ventilation to maintain the fire performance of the walls. One solution for sealing these systems is to use fire stopping sleeves, fire stopping mortar, cable grommets or any other system with a fire resistance at least equal to that of the wall and with a classification report from an approved fire laboratory. In addition, openings are usually made in the walls to allow the passage of people or vehicles. These openings must also be closed by fire doors with a fire resistance at least equal to that of the wall. These doors and their installation must comply with the fire resistance report issued by an approved laboratory, with any extended classification.

The following figures some of the provisions mentioned previously, according to the fire wall solutions.

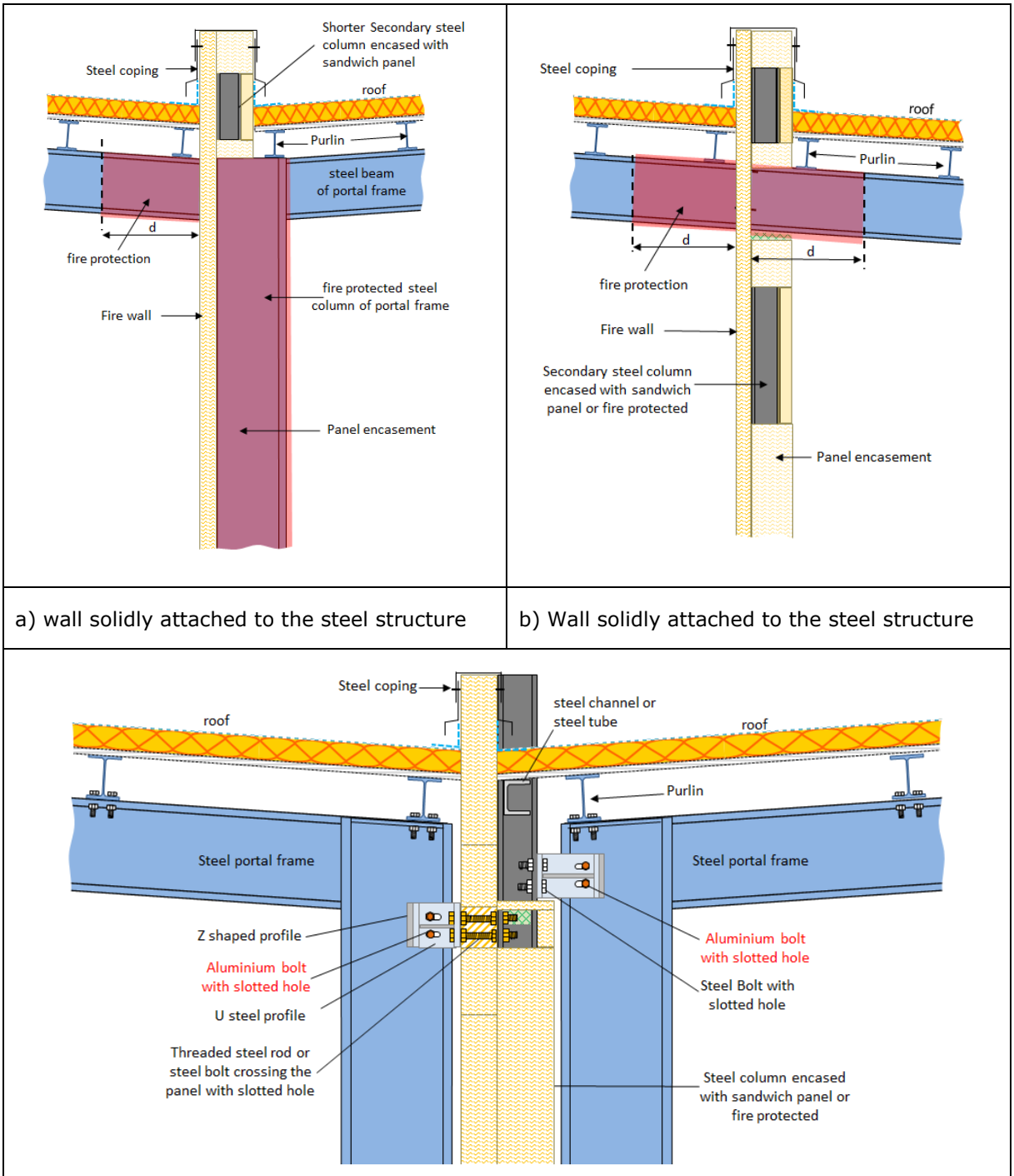

a) wall solidly attached to the steel structure

b) Wall solidly attached to the steel structure

c) wall solidly attached to the steel structure

Figure 5.8: Schematic views for a fire wall perpendicular to portal frames, inserted into a row of columns and extending beyond the roof – Portal frame columns with standard fire protection

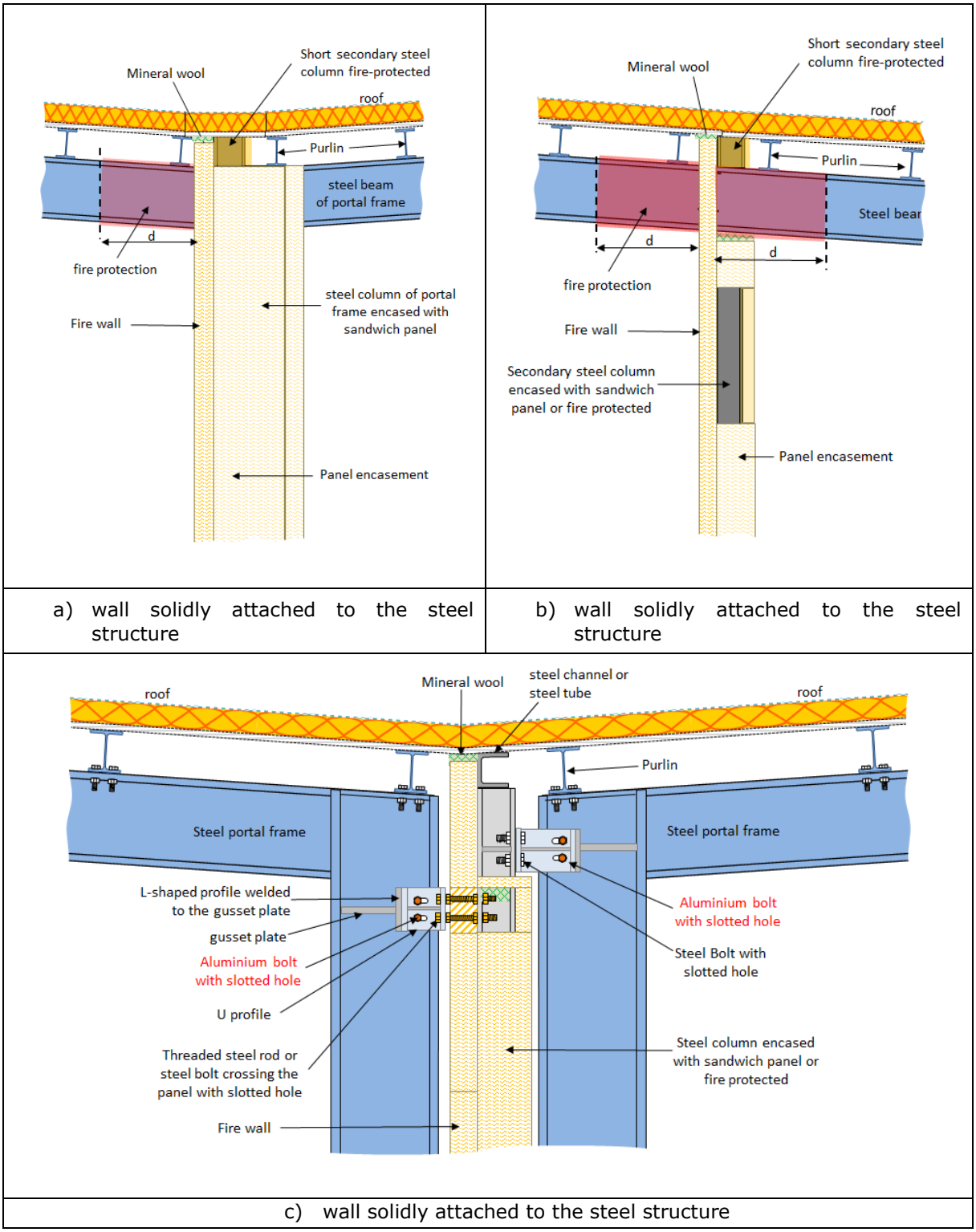

a) wall solidly attached to the steel structure

b) wall solidly attached to the steel structure

c) wall solidly attached to the steel structure

Figure 5.9: Schematic views for a fire wall perpendicular to portal frames, inserted into a row of columns and extending beyond the roof – Portal frame columns with standard fire protection

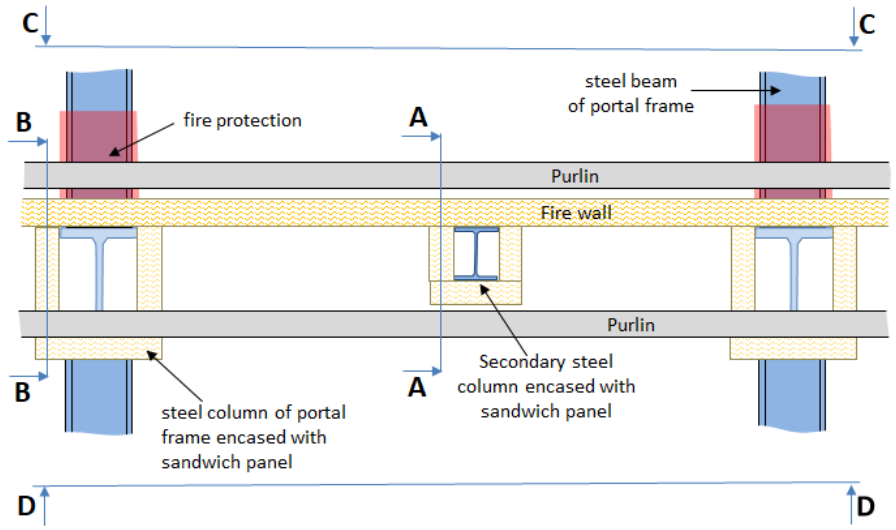

a) Top view under the roof

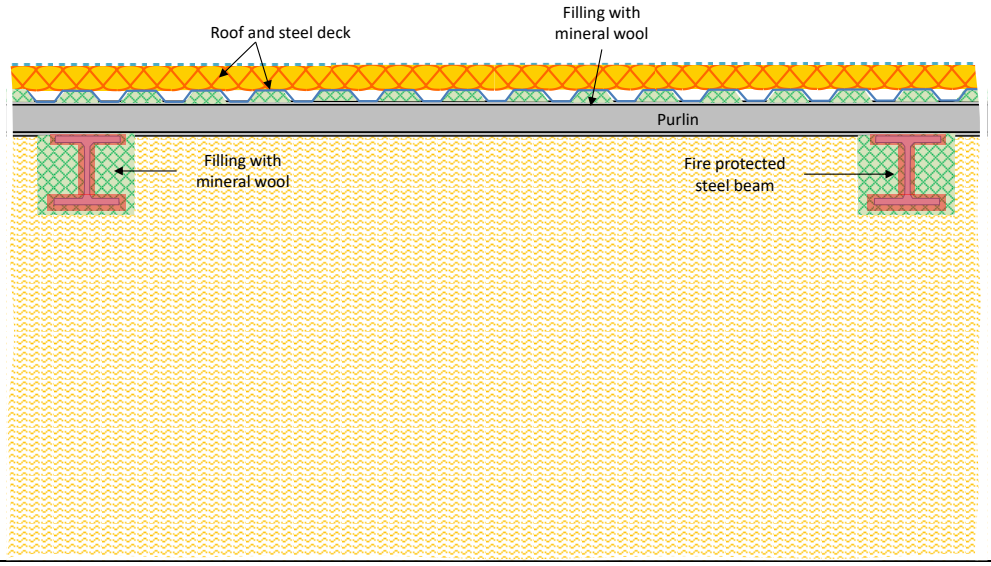

b) Front view C-C

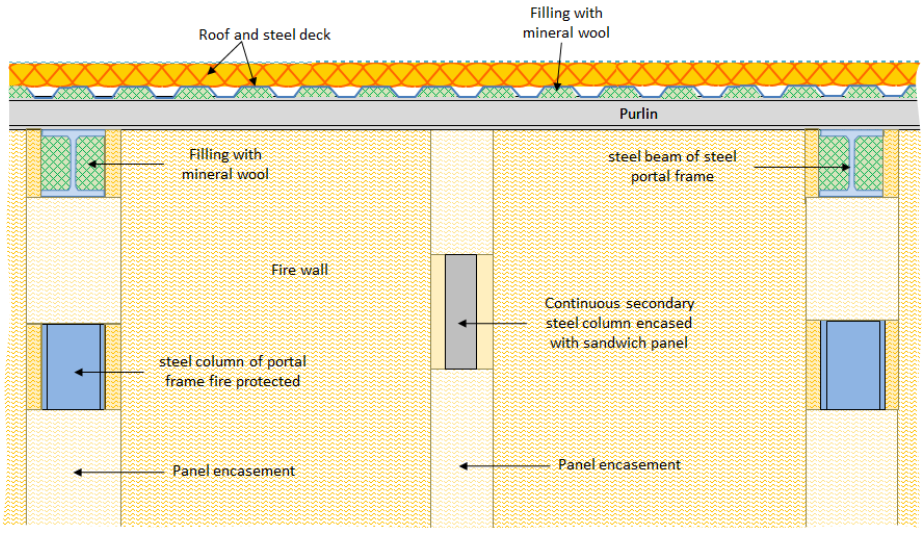

c) Front view D-D

Figure 5.10: Schematic views for a fire wall perpendicular to portal frames, inserted into a row of columns and not extending until the roof – Portal frame columns with panel encasement system

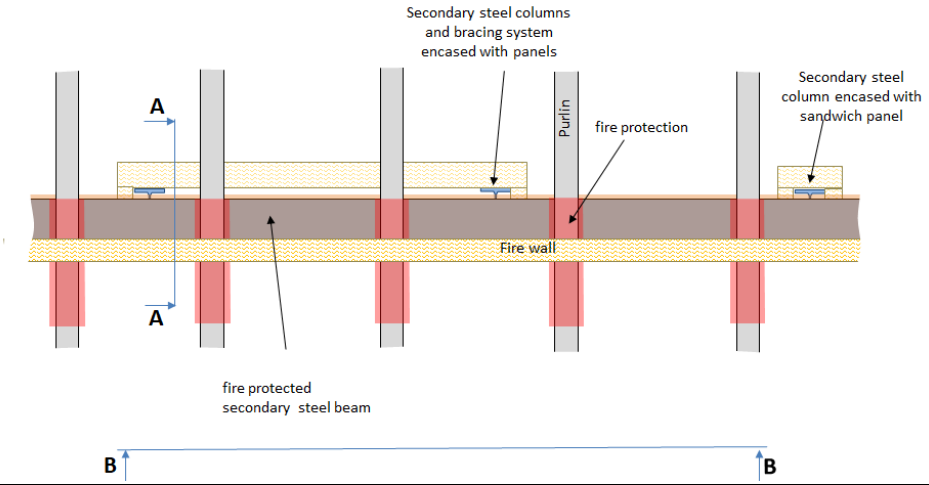

A) Top view under the roof

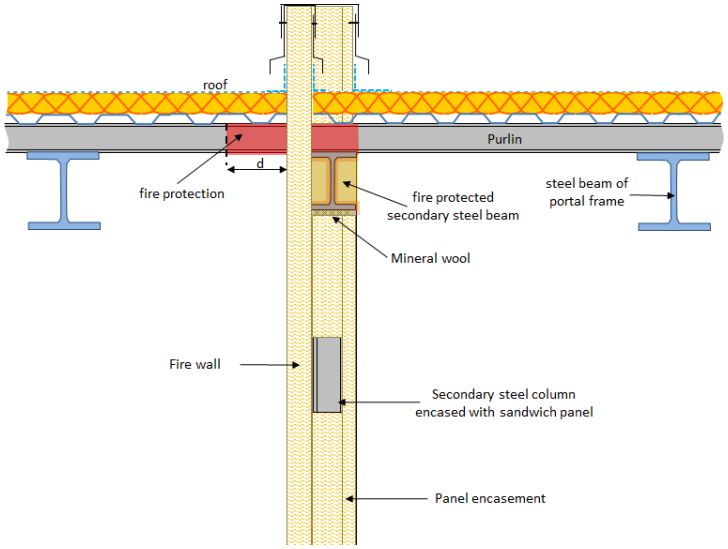

a) Side view A-A

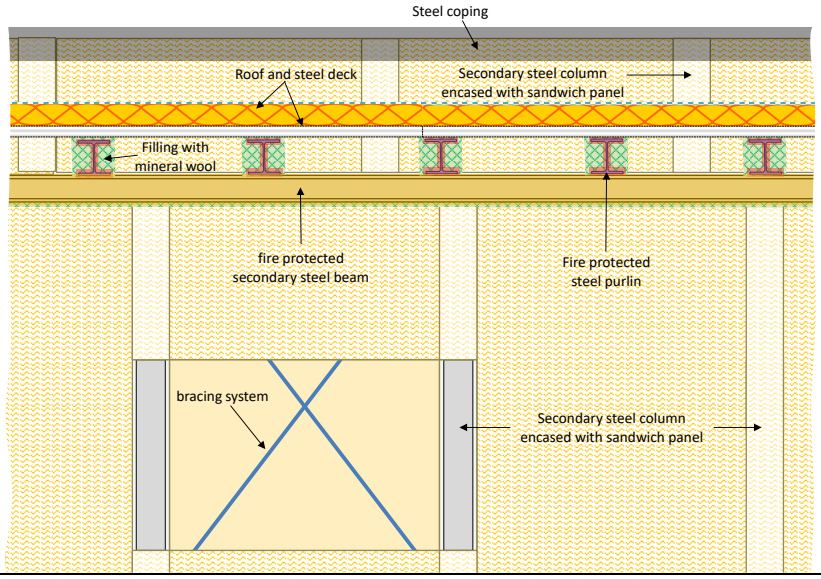

b) Front view c-c

Figure 5.11: Schematic views for a fire wall parallel to portal frames, placed between portal frames and extending beyond the roof

5.3 Fusible links and associated wall supporting columns

The fusible links has to be positioned at the top of the building's columns, as close as possible to the roof. This will ensure that they are in the hot gas layer that forms under the roof of the building in the event of a fire. Furthermore, a fusible link should be positioned symmetrically on either side of the steel columns. This prevents the steel columns from twisting during the heating process, which could occur if only one fusible link were used per column due to the combined effects of loading eccentricity and temperature rise. This also prevents the columns from meeting the sandwich panels, which cannot withstand significant compressive forces outside their plane. This could result in damage to the fire wall. Finally, it is also recommended that they are not installed at the level of a junction between sandwich panels.

The columns supporting the fire wall must be set back far enough from the steel structure columns to allow the panels to be installed. If the columns supporting the sandwich panels are individually encased for fire protection, the space between them shall be large enough to enable the encasements to be fitted correctly (see Figure 5.12). The amount of space required will depend on the thickness of the panels and the tools used for their connections. To reduce the minimum spacing between the two columns supporting the wall, they can be encased together, as shown in Figure 5.13. Some recommendations are included in the Fishwall guide.

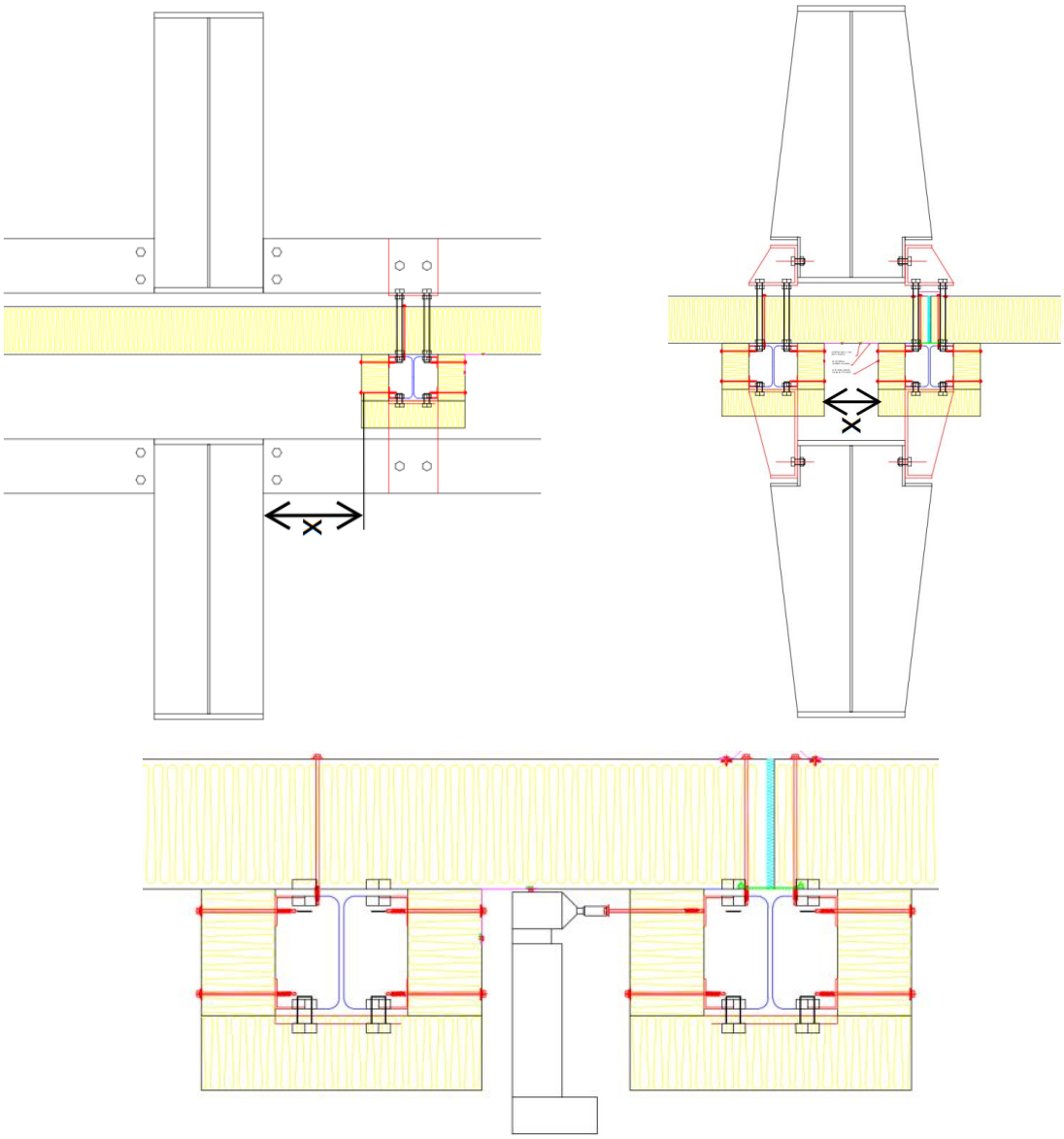

Figure 5.12: Spacing between the columns of the steel structure and the column encasement system of the wall

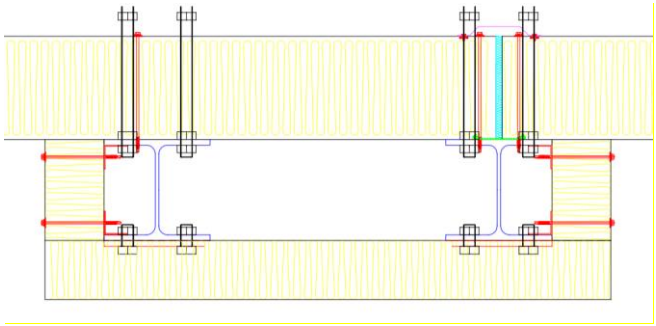

Figure 5.13: Encasement of the two columns together

When designing and detailing the links, the following provisions must be followed:

- For fusible links consisting of an L-or T shaped steel profile assembled with aluminium bolts to steel channels bolted at its ends to the columns of the steel structure slotted holes must be accommodated at joints to allow the free longitudinal thermal expansion of the steel channels (see Figure 5.14). Considering slotted holes at each profile end, the length of slotted holes can be taken equal to 0.0055×L, where L is the span of the steel profile. The distance between the ends of the steel channel and the web of the column must be of at least the same order of magnitude. In addition, a steel plate must be installed between the head of the steel rods and the adjacent flange of the steel channel. Finally, a web stiffener should be welded between the flanges of the steel channel in the centre plane of the rods (as illustrated in Figure 5.15).
- Particular attention must be paid to the installation of threaded rods to ensure they are correctly bolted and not damaged during installation (e.g. panels and other structural parts).
- There must be a minimum of four steel rods. The steel rods must be at least M12.
- Class 4 cross-section according to EN 1993-1-2 should be avoided.
- The U-shaped steel profile shall be at least 6 mm thick.
- The L-shaped steel section shall be at least 10 mm thick.
- Web stiffeners must be placed in the centre plane of steel rods and bolts for the steel column supporting the wall.
- The bolt and rod holes must fulfil the requirements with respect to minimum and maximum spacing between the holes, end distances and edge distances given in EN 1993-1-8.
- The steel grade of the stiffeners is not lower than that of the steel profiles.
- The thickness of the stiffeners is not smaller than the thickness of the profile flange.
- Only steel bolts and steel rods of at least class 8.8 may be used.

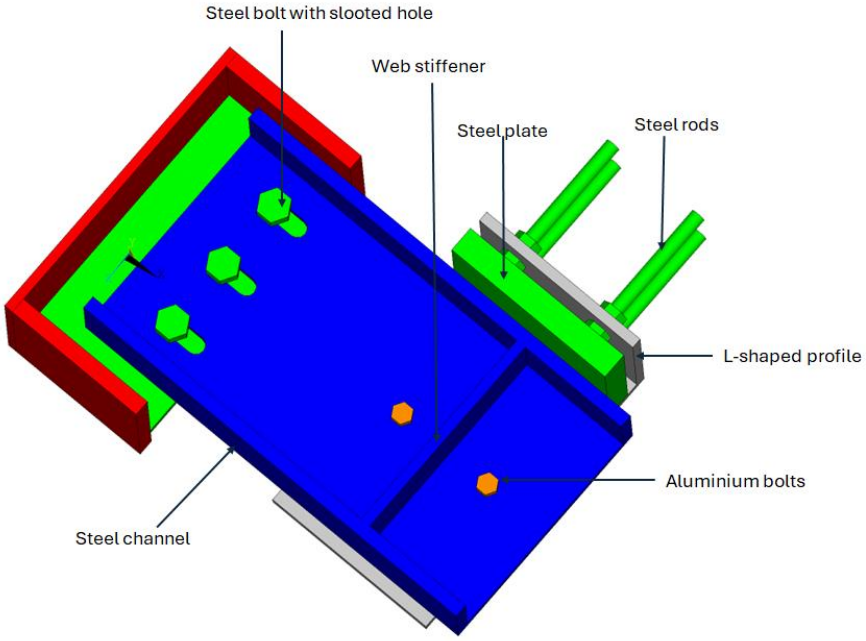

Figure 5.14: Details accommodated for the third fusible link solution

Based on results gained from tests and parametric numerical studies ([23], [24]), for seismic-prone regions, the following constructional details are recommended:

- Details with larger size and low number of aluminium bolts are preferable, M16 instead of M12, because the low number of aluminium bolts reduces the imperfections and misalignments observed during the test [23], and leads more easily to the necessary loadbearing capacity of the fusible links.
- As an alternative to a single U-profile, a double U-profile configuration coupled with a T-shaped steel profile can be used to reduce the number of aluminium bolts required, as shown in Figure 5.15).

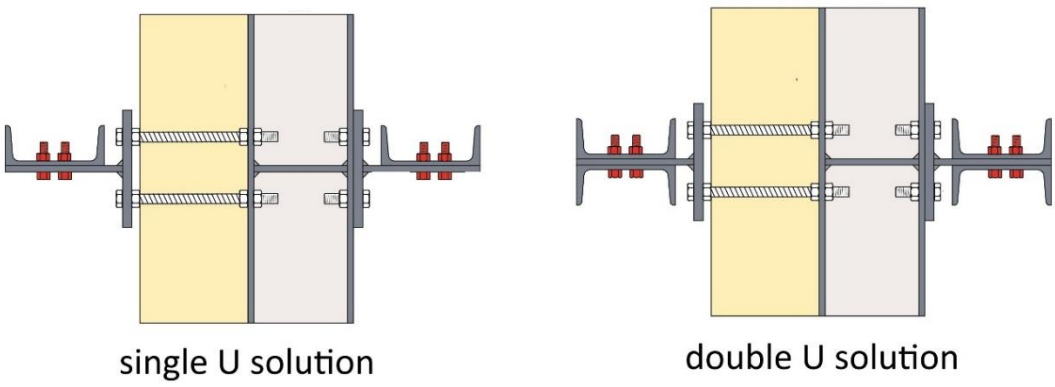

Figure 5.15: Fusible link detail with single U profile and Tee solution for seismic-prone regions

5.4 Purlin systems

Where purlins penetrate a wall, continuity of the purlins (with possible splicing) must be ensured at wall level.

5.5 Sliding fire doors

As alternative to a rigid frame (like concrete frame), large sliding fire door can be installed in walls made with sandwich panels. Unless door manufacturers can provide other tests evidence, installation of such door in a sandwich panel wall can be done using a steel portal frame fire-protected with sandwich panels. It is recommended that the same sandwich panels that form the wall are used to make the encasement system. Several solutions can be used for the encasement system and its attachment to the steel profiles, if they have been properly validated for the fire situation. Alternatively, standard fire protection systems, such as spray, boards or intumescent coatings could also be used.

The vertical part of this frame can be made from the supporting steel columns of the fire wall. The column spacing shall be adapted locally to the width of the fire door. The steel frame provides also supports for the upper rail system and the fire seals which are fixed to the frame through the panels.

An example of the design concept of a fire door mounted in a partition fire wall made of sandwich panels is shown in Figure 5.16 and Figure 5.17.

The fire resistance of the steel frame supporting the fire doors can be checked in the same way as the resistance of the steel columns supporting the walls (see §4).

When designing the steel frame, it is recommended that slotted holes are included at the beam-column connection to allow for the steel beam's free longitudinal thermal expansion. If slotted holes are only present at one end of the beam, their length can be taken as 0.01×L, where L is the span of the steel beam. The distance between the ends of the beam and the column web must be at least the same order of magnitude.

It should be noted that even if the tested specimen did not achieve the desired EI 120 fire resistance performance, the fire tests performed on the sliding steel door system demonstrated the effectiveness of using a supporting steel frame.

In any case, the doors and their installation must comply with the fire resistance classification report done according to EN 13501-2 and issued by an official laboratory.

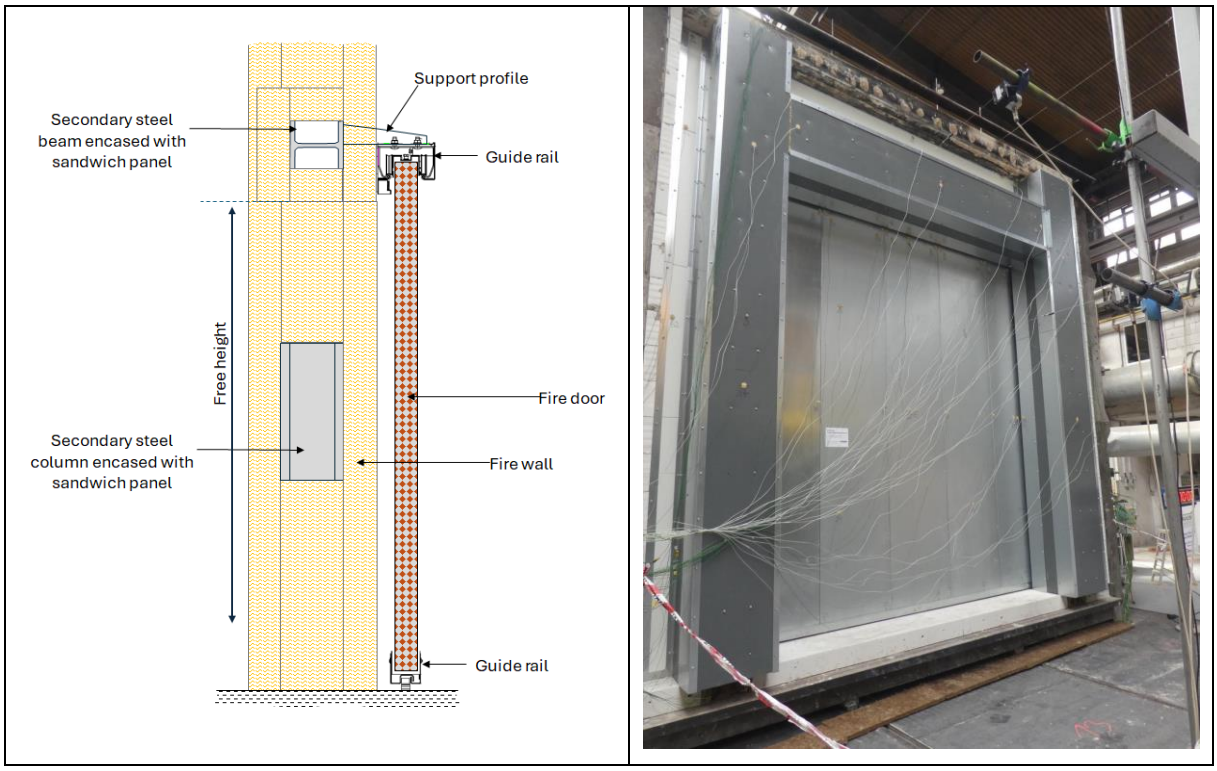

Figure 5.16: Schematic views of a fire door mounted in a partition fire wall made of sandwich panels - side view

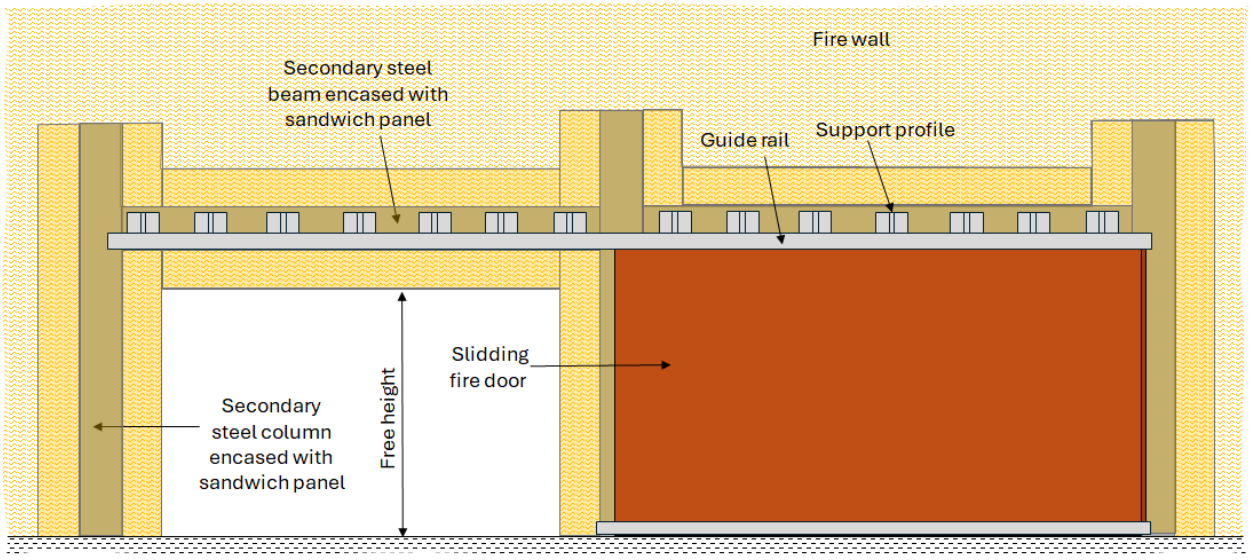

Figure 5.17: Schematic views of a fire door mounted in a partition fire wall made of sandwich panels - front view

5.6 Bracing systems

Appropriate bracing systems can prevent progressive collapse of the building. Each fire compartment should have its own bracing system.

The recommendations given below are mainly based on common sense and the provisions already set out in the literature ([13], [15], [16]). They apply primarily to firewalls that are solidly fixed to the steel structure of a building. These recommendations are automatically met in designs for normal conditions involving walls with fusible links, since each steel structure is usually designed independently.

5.6.1 Fire wall perpendicular to the portal frames

Figure 5.18 illustrates the situation where the fire wall is perpendicular to the steel frame. The following provisions must be taken with this solution:

- Use additional vertical bracing systems at both ends of fire wall, to ensure integrity of wall. These bracing systems should be designed to support a lateral load due to normal wind actions (calculated according to the combination of actions for the fire situation), calculated for a gable area that is limited to the width between gable columns.
- Provide double vertical bracing systems (i.e. have bracing systems on both sides of fire walls) or fire-protect the bracing system.
- The bracing systems must be arranged in a way that they will not cause problems for normal temperature design, for example by compromising movement of an expansion joint.

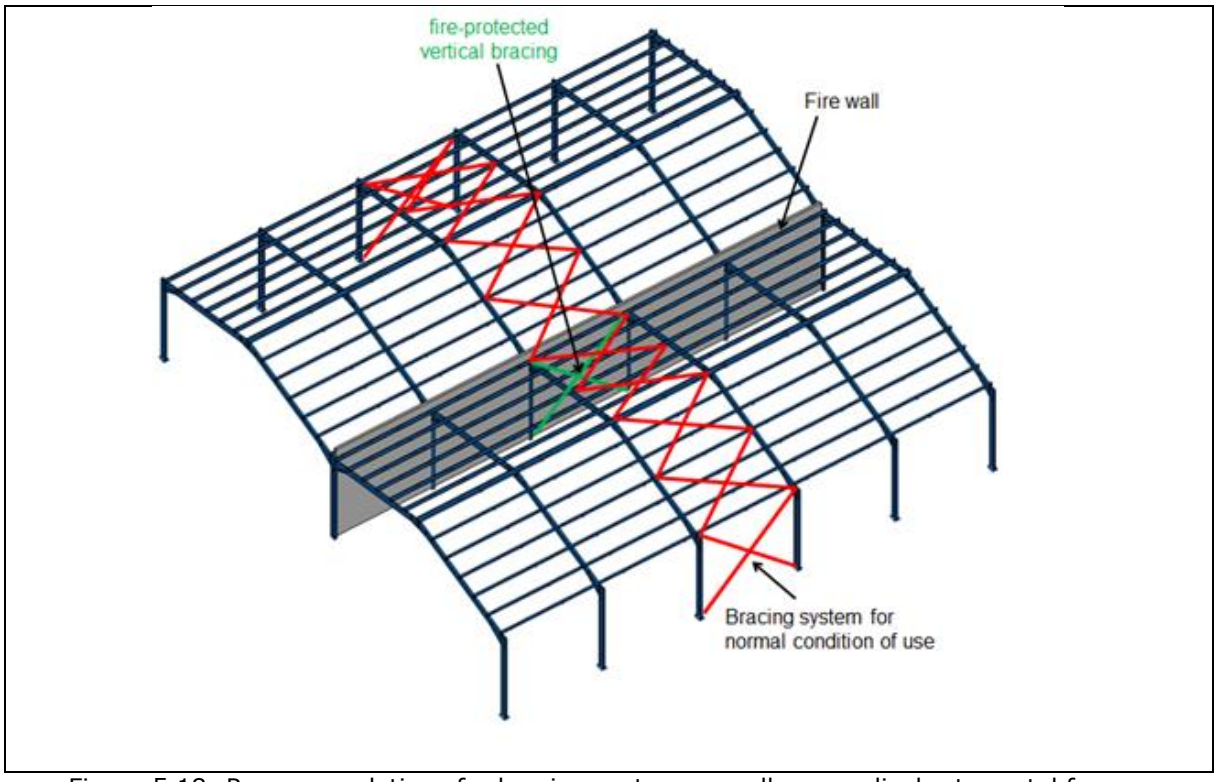

Figure 5.18: Recommendations for bracing systems – wall perpendicular to portal frames

It should be noted that the literature recommends the use of additional vertical bracing systems at both ends of the fire wall to ensure its integrity.

However, a large-scale fire test carried out on a single-storey steel-framed building with partially fire-protected portal beams as part of a French national research project [14] indicated that this provision is unnecessary. Therefore, it was not selected.

a) View during the test | b) View after the test

Figure 5.19: Large-scale fire test on a single-storey steel-framed building – Flumilog project

5.6.2 Fire wall parallel to the portal frames

Figure 5.20 illustrates the situation where the fire wall is parallel to the steel frame. For this situation:

- Install bracing systems (vertical bracing and horizontal bracing on roof) in each fire compartment. This solution may lead to additional bracing systems for normal conditions.
- Design each bracing system to provide adequate stability in normal condition and to support in fire condition a horizontal uniform load [N/m] taken as $F = 1{,}19 \times (G + \psi \times S_n) \times l_f$, where l_f is the spacing between steel frames, G is the permanent action including service overloads, S_n is the snow load and ψ ($\Psi_{1,1}$ or $\Psi_{2,1}$) is the load factor according to load combination coefficients defined in EN 1990 and corresponding national annexes.

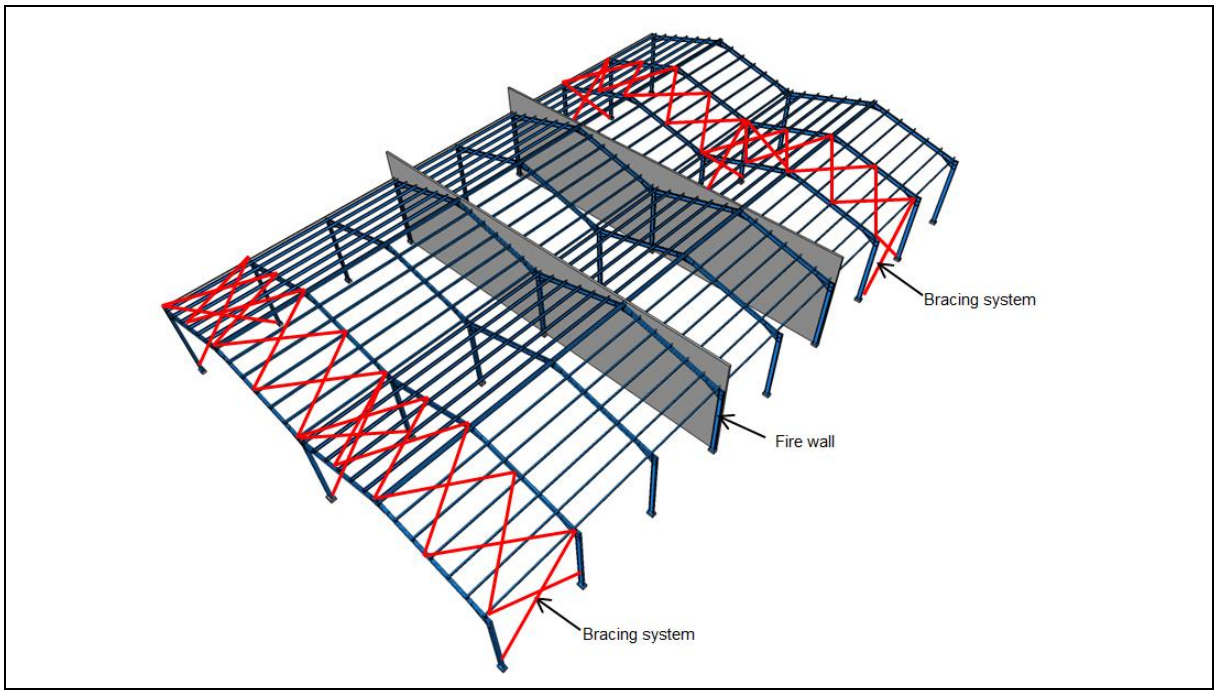

Figure 5.20: Recommendations for bracing systems – wall parallel to portal frames

5.7 Roof systems near the separation fire walls

Whatever the fire-wall solutions, the roof should be independent of each fire compartment by adopting the following recommendations:

- Purlins or other additional supports should be provided on both sides of fire walls perpendicular to steel portal frames.
- The roof should be stopped on both sides of the fire wall.

It is recommended avoiding any fastenings between the building's roof and the fire wall, including the supporting columns.

For information purposes, such recommendations are illustrated in the following figure for a fire partition fire wall that is solidly attached to the steel structure.

In addition to the extension of the wall above the roof, national fire codes may specify special requirements for the building roof in the vicinity of fire walls (fire protection measures for an appropriate length on each side of the wall).

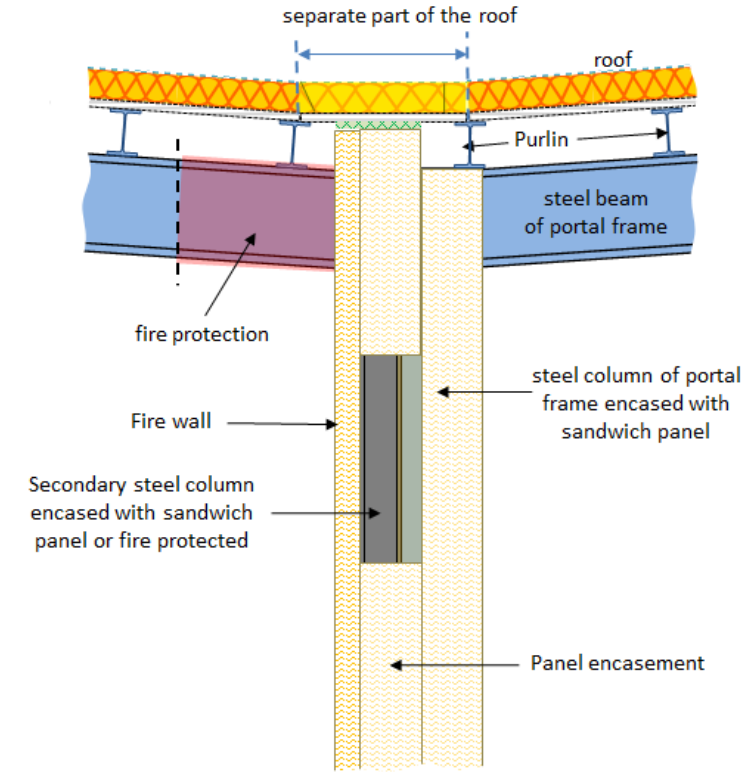

a) Wall perpendicular to steel frame

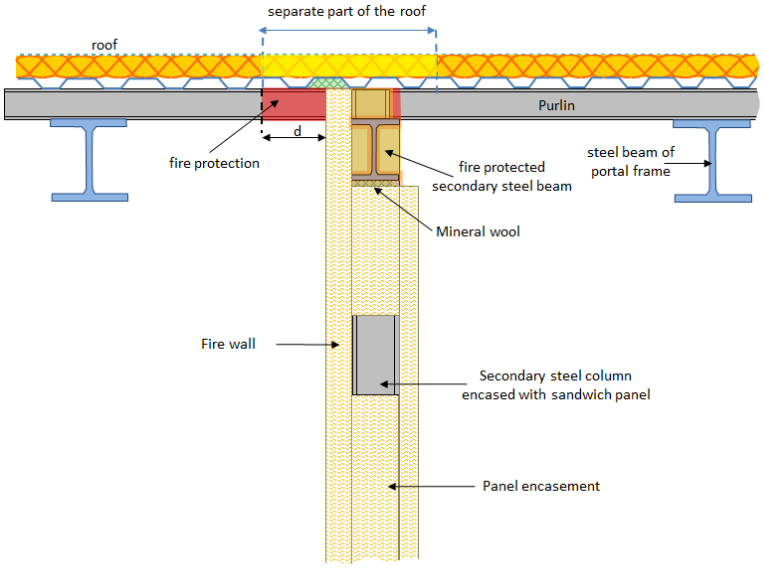

b) Wall parallel to steel frame

Figure 5.21: Roof system near the partition fire walls

5.8 Support of façade elements

To prevent the external collapse of façade elements due to excessive movement of the steel structure in the event of a fire or earthquake, it is essential to ensure that the façade elements remain fixed to the building's structure.

In the case of steel façades (steel cladding systems, sandwich panels, etc.), the risk of external collapse is easily avoided by complying with the current rules of good practice for their design in normal conditions and for their installation (as illustrated in Figure 3.1 for the fire situation).

Figure 5.22: Steel façade collapsing with the building steel structure.

6 CONCLUSION

The aim of this document was to briefly present the design rules and details proposed in the Fishwall project, to ensure adequate performance of the investigated fire wall solution made of sandwich panels, as well as the developed fusible link systems in single-storey steel buildings with unprotected steel structures, in the event of a fire or seismic activity.

All the information presented here formed the basis for the design guide produced as part of the Fishwall project.

7 REFERENCES

[1] EN 1990: Eurocode – Basis of structure design, Brussels, Belgium, CEN, 2003.

[2] EN 1991-1-2: Eurocode 1: Actions on structures - Part 1-2: General actions - Actions on structures exposed to fire, Brussels, Belgium, CEN, 2002.

[3] EN 1993-1-1: Eurocode 3: Design of steel structures. Part 1-1: General rules and rules for buildings, CEN, 2005.

[4] EN 1993-1-2: Eurocode 3: Design of steel structures – Part 1-2: General rules – Structural fire design, Brussels, Belgium, CEN, 2005.

[5] EN 1999-1-2, Eurocode 9: Design of aluminium structures - Part 1-2: Calculation of fire behaviour, Brussels, Belgium, CEN, 2007.EN 1998-1-1: Design of structures for earthquake resistance. Part 1-1: General rules, seismic actions and rules for building, CEN, Brussels, 2005.

[6] EN 1991-1-4: Actions on structures - Part 1-4: General actions - Wind actions, , Brussels, Belgium, CEN, 2005.

[7] EN 1999-1-2, Eurocode 9 - Design of aluminium structures - Part 1-2: Calculation of fire behaviour, CEN, Brussels, 2007.

[8] EN 1998-1-1: Design of structures for earthquake resistance. Part 1-1: General rules, seismic actions and rules for building, CEN, Brussels, 2005.

[9] EN 1993-1-8: Design of steel structures – Part 1-8: Design of joints, Brussels, Belgium, CEN, 2005.

[10] CTICM, Eurocodes – fire parts: Proposal for a methodology to check the accuracy of assessment methods, technical report MZE-99/83-JK/IM, 2014.

[11] Renaud C., FISHWALL project, RFSC-2020, GAN 101034083, Work Package 3, Deliverable 3.4, Development and validation of FE numerical models, 2025.

[12] Renaud C., FISHWALL project, RFSC-2020, GAN 101034083, Work Package 3, Deliverable 3.5, Parametric studies on the mechanical response of steel structures associated with fire walls using "fusible" links, 2025.

[13] RFCS PR378, Fire safety of industrial halls and low-rise buildings, Realistic fire design, active safety measures, post-local failure simulation and performance-based requirements, Final report, 2007.

[14] Flumilog, Description de la méthode de calcul des effets thermiques produits par un feu d'entrepôt – Partie A, DRA-09-90977-14553A Version 2, août 2011.

[15] Fire safety of industrial hall, Design Guide, RFCS research project, Luxembourg, 2007.

[16] Single-Storey Steel Buildings Part 7: Fire Engineering, design guide, European project "Facilitating the market development for sections in industrial halls and low-rise buildings (SECHALO) RFS2-CT-2008-0030".

[17] Vaněk J., FISHWALL project, RFSC-2020, GAN 101034083, Work Package 3, Deliverable 3.3, Fire test report on fire wall connected to an unprotected steel structure by means of fusible links, 2023.

[18] Vaněk J., FISHWALL project, RFSC-2020, GAN 101034083, Work Package 2, Deliverable 2.1, Fire test reports on partition fire walls made of sandwich panels with large spans, 2023

[19] Vijayakumar M., Kozich M. and Wald F. FISHWALL project, RFSC-2020, GAN 101034083, Work Package 3, Deliverable 3.1, Experimental analysis of mechanical behaviour of aluminium bolts at ambient and elevated temperature, 2022

[20] Vaněk J., FISHWALL project, RFSC-2020, GAN 101034083, Work Package 3, Deliverable 3.2, Fire test report on a fire wall solidly attached to an unprotected steel structure and penetrated by steel purlins, 2024.

[21] Vaněk J., FISHWALL project, RFSC-2020, GAN 101034083, Work Package 2, Deliverable 2.3, Fire tests on steel members protected by sandwich panels, 2023.

[22] Vaněk J., FISHWALL project, RFSC-2020, GAN 101034083, Work Package 2, Deliverable 2.2, Fire test report on a sliding steel framed door system built into a lightweight sandwich wall panel,2025.

[23] S. Pasquali, N. Tondini, G. Zanon, FISHWALL project, RFSC-2020, GAN 101034083, Work Package 4, Deliverable 4.1, Full seismic test report including all detailed experimental data gathered during the seismic tests, 2024.

[24] S. Pasquali, N. Tondini, G. Zanon, FISHWALL project, RFSC-2020, GAN 101034083, Work Package 4, Deliverable 4.3, Parametric numerical analyses, 2025.

[25] Rikki, sandwich panels, compartment details, "spa-fire-wall-details_en_30062023.pdf"

[26] Eurobond, "147110_Eurobond Firemaster Install Manual.pdf", "Firemaster Vertical Details (Collated).pdf"